

# **Transport of Natural Lead and Cadmium in Rivers: Global Flux Implications**

Thesis by  
Yigal Erel

In Partial Fulfillment of the Requirements  
for the Degree of  
Doctor of Philosophy

California Institute of Technology

Pasadena, California

1991

(Submitted May 31, 1990)

This work is dedicated with love to:

Alin and David;

Eran and Gabriel;

Osnat and Tamar-Kiki.

## XXV

*And this delightful Herb whose living Green  
Fledges the River's Lip on which we lean -  
Ah, lean upon it lightly! for who knows  
From what once lovely Lip it springs unseen!*

*Rubaiyat  
of  
Omar Khayyam*

## **Acknowledgments**

I thank my mentors, Professor Clair C. Patterson for his endless efforts to educate me about careful analytical work and his attempts to convert me into a real scientist, and Professor Jim J. Morgan for his guidance and the unlimited knowledge he was always willing to share.

I also would like to thank Professors Sam Epstein and Norman H. Brooks from Caltech, Professor Karl K. Turekian from Yale and Professor Phil M. Gschwend from MIT for long and fruitful discussions.

I thank Mike Wolf, Susan Kornreich Wolf, Mike Scott, Simon Wdowinsky, Sieger van der Laan, Jennifer Blank, Mark Fahnestock, Bernhard Wehrli, and Osnat who were willing to hike several miles in the wilderness with heavy loads on their backs and return home with only a few bottles of water.

Mike Scott, Mark Schlautman, Jeff Collett and Bruce Daube helped me with parts of the analytical work and tried to show me different ways of tackling aquatic chemistry problems. I also would like to thank Professor Mike Hoffmann for the Friday group meetings; they were among the best parts of my education at Caltech.

Professor L.T. Silver dedicated a lot of his time to make sure that I would not lose my geological roots during the process of turning into an aquatic chemist. He also provided the mineral separates for the leaching experiments, and was deeply involved in planning both the field and the laboratory experiments.

Dorothy Settle and Hal Maring directed my first steps in the clean laboratory and taught me many of the techniques I used in my work.

David Marrett, Bob Graham and Jerry Ervin from the Department of Soil and Environmental Sciences UCR, Riverside, let me use their laboratories, and assist me with the soil analyses.

I would like to thank my friends from the Division of Geological and Planetary Sciences: Mike Wolf and Diane Knott (the perfect office mates), Mark Fahnstock, Charlie Rubin, David Bell, Joel Blum, the secretaries Priscila Piano, Fran Barnard, Meg Garstang, Kerry Etheridge, and the librarians Jim O'Donnel, (Geology) and Rayma Harrison (Environmental Engineering) that have helped me in endless ways during the last five long years.

This work would not be finished without the great help from Bernhard, Mike, Susan and my wife, Osnat, who pushed forward till the very last minute.

## **Abstract**

Lead and cadmium concentrations in marine and terrestrial ecosystems, in surfaces of soils, and in the atmosphere have been highly elevated on a global scale due to industrial pollution. In order to ascertain the natural (rock-derived) levels of lead and cadmium in streams, pristine mountain watersheds in the Sierra Nevada, California were studied for their lead and cadmium contents, and the transport of lead and cadmium was related to metal relatively uninfluenced by pollution that share similar transport patterns. In addition, rock and unpolluted water samples from granodiorite, basalt and carbonate terrains were analyzed for the concentrations of lead, iron and other elements. Whole-rock samples as well as biotite and feldspar mineral separates were used for laboratory leaching and adsorption-desorption experiments to investigate the relationship between lead and iron chemistry under controlled conditions.

The concentrations of lead and cadmium in the late-summer drainage are shown to be close to the natural levels that are controlled by the weathering of bedrock and soil. This is demonstrated by measurements of 1) lead isotopic composition, and Fe/Pb ratios in stream water, ground water, soil and bedrock, and 2) the removal rate of excess atmospheric lead and cadmium from the water as it flows downstream.

After the spring snow-melt runoff, most of the lead in alpine streams originates from ground water, and has isotopic ratios that are consistent with values expected from bedrock and soil sources, indicating that this lead is not anthropogenic in origin. The lead found in unpolluted ground waters is more radiogenic than the lead in the bedrock drained by these waters. A preferential release of radiogenic lead into waters and leached phases of rock and soil can be explained by the preferential weathering of radiogenic accessory minerals and to a lesser extent by a preferential release of U and Th decay products due to the recoil effect.

The lead uptake mechanism is proposed to be adsorption on oxy-hydroxide surfaces. In contrast, the uptake of cadmium in the stream water is erratic and cannot be explained by the same mechanism. Adsorption-desorption experiments suggest that lead coprecipitates and is adsorbed on particle surfaces, mainly ferric iron hydroxides. Due to a similar transport mechanism and comparable rate of release from common rock and soil minerals, the ratio between natural (rock-derived) lead and iron in rivers should be similar to their average upper continental crustal molar ratio of 1:6,500.

Experiments and speciation models indicate that complexation of lead by man-made organic compounds decreases the fraction of lead bound to surface sites. Such an indirect pollution effect mobilizes lead and decreases the Fe/Pb ratio in rivers regardless of any direct addition of anthropogenic lead.

Many trace metals maintain their average upper continental crustal ratio with iron in unpolluted river water, river sediments and soils; However, large excesses of most trace metals relative to iron are found in deep-ocean water. At the transition from fresh water to saline ocean water, two processes take place: 1) rapid removal of iron (and other particle-forming elements) from the water column due to coagulation and settling; and 2) partial desorption of trace metals from particle surfaces. While more than 99% of the riverborne iron settles to the sediment within the continental shelf, some of the trace metals are released to solution as dissolved chloro-complexes and are further transported to the open sea. In addition, some of the trace metals attached to airborne and recycled sea-floor particles may desorb when these particles are in contact with sea water.

The adsorption/desorption process in sea water account for the relative abundances of many trace metals in deep-sea water (not including REE). Furthermore, it is suggested that the observed concentrations of these trace metals in deep-ocean water are relatively unaffected by pollution and are largely determined by natural processes.

**Table of Contents**

	<u>page #</u>
Dedication.....	ii
Acknowledgments.....	iv
Abstract.....	vi
List of Figures.....	xii
List of Tables.....	xiv
 Chapter 1 Introduction.....	 1
1.1 The research objectives of the thesis.....	1
1.2 Justification.....	2
1.3 Lead and cadmium in the lithosphere, hydrosphere and atmosphere.....	2
1.3.1 Lead and cadmium distribution in minerals and rocks.....	2
1.3.2 Lead and cadmium in rivers.....	5
1.3.3 Lead and cadmium in estuary and coastal environments.....	9
1.3.4 Lead and cadmium in the ocean.....	10
1.3.5 Lead and cadmium in the atmosphere.....	12
1.4 Aquatic chemistry of lead, cadmium, zinc and copper.....	13
1.4.1 Chemical and physical properties of lead, cadmium, zinc and copper.....	13
1.4.2 Grouping of elements in the aquatic environment.....	13
1.4.3 Speciation of lead, cadmium, zinc and copper in fresh and sea water.....	16
1.4.4 Surface chemistry of lead, cadmium, zinc and copper.....	19
1.4.5 Modeling of lead, cadmium, zinc and copper speciation in water including $\text{Fe}(\text{OH})_3(\text{s})$ surfaces.....	26
1.4.6 Kinetic consideration.....	27
1.5 Human use of lead and cadmium.....	28
1.6 Isotopic composition of lead: Systematics of changes during weathering of rocks and minerals.....	31

Chapter 2	Experimental methods.....	38
2.1	Sampling.....	38
2.1.1	Preparation and precleaning procedures.....	38
2.1.2	Collection sites.....	40
2.1.2.1	Granodioritic site.....	40
2.1.2.2	Granitic site.....	40
2.1.2.3	Basaltic site.....	41
2.1.2.4	Carbonate site.....	41
2.1.2.5	Minerals.....	42
2.1.3	Collection methods.....	42
2.1.3.1	Lake water.....	43
2.1.3.2	Stream water.....	43
2.1.3.3	Ground water.....	44
2.1.3.4	Soil, rock and stream-bed samples.....	44
2.1.3.5	Atmospheric deposition.....	44
2.2	Sample preparation and experimental procedures.....	45
2.2.1	Stream and ground water.....	46
2.2.2	Soil, stream-bed and rock samples.....	47
2.2.3	Leaching experiments.....	48
2.2.4	Adsorption experiment.....	49
2.2.5	Desorption experiment.....	50
2.3	Analysis.....	50
2.3.1	Water, rock and soil samples.....	50
2.3.2	Water samples.....	51
2.3.3	Soil, stream-bed and rock samples.....	52
Appendix 2.1	Precleaning of field and laboratory ware.....	56
Appendix 2.2	Dialysis membrane calibration.....	62

Appendix 2.3	Digestion, extraction and separation techniques.....	64
Appendix 2.4	Calibration of a multicollector VG-Sector solid-source mass spectrometer.....	66
Appendix 2.5	Experimental methods used in Thompson Canyon.....	70
Chapter 3	Field study.....	73
3.1	Transport of industrial lead in snow through soil to stream water and ground water.....	74
3.1.1	Introduction.....	74
3.1.1.1	Industrial lead and the hydrological cycle.....	74
3.1.1.2	Study area.....	75
3.1.2	Character of data.....	76
3.1.2.1	Rock lead: $^{206}\text{Pb}/^{207}\text{Pb}$ ratio and storage in the nonlabile reservoir.....	76
3.1.2.2	Rock lead: $^{206}\text{Pb}/^{207}\text{Pb}$ ratio and storage in the labile reservoir.....	76
3.1.2.3	Industrial lead: $^{206}\text{Pb}/^{207}\text{Pb}$ ratio and storage in the abile reservoir.....	77
3.1.3	Results.....	78
3.1.3.1	Meltwater-soil relationships.....	78
3.1.3.2	Soil-stream water and ground water relationships....	79
3.1.4	Conclusions.....	80
3.2	Natural levels of lead and cadmium in remote mountain streams.....	89
3.2.1	Introduction.....	89
3.2.2	Study area.....	89
3.2.3	Results.....	90
3.2.4	Discussion.....	92
3.2.4.1	Anthropogenic input of lead and cadmium to Moraine Creek.....	92
3.2.4.2	Changes of the isotopic composition of rock- derived lead during weathering.....	94

	3.2.4.3	The chemical composition of Moraine Creek water..	95
	3.2.4.4	Transport of lead and cadmium in Moraine Creek....	98
	3.2.4.5	Iron, lead and cadmium relationships in Moraine Creek.....	102
	3.2.5	Conclusions.....	104
Chapter 4		Transport of natural lead in rivers: Global flux implications.....	120
	4.1	Introduction.....	120
	4.2	Results.....	123
	4.3	Discussion.....	124
	4.3.1	The release of lead and iron from rocks and soil.....	124
	4.3.2	Adsorption of lead on iron particles.....	128
	4.3.3	Desorption of lead from iron particles.....	130
	4.3.3.1	Effect of man-made organic chelators.....	130
	4.3.3.2	Effect of sea water: A new model for the speciation of trace metals in aquatic systems.....	131
	4.4	Conclusions.....	137
References.....			151

## List of Figures

	<u>page #</u>
<b>Figure 1.1:</b> Variability and trend of lead measurements in rivers, the effect of analytical capabilities. ....	7
<b>Figure 1.2:</b> Summary of major processes and mechanisms in the interactions between dissolved and solid metals species in surface waters.....	8
<b>Figure 1.3:</b> Complexation field diagram for the cationic elements.....	15
<b>Figure 1.4:</b> Coordination phenomena at oxide-water interface.....	20
<b>Figure 1.5:</b> Fractional adsorption of metals on various substrates.....	22
<b>Figure 1.6:</b> Cadmium uptake by bacteria surfaces as a function of pH.....	28
<b>Figure 1.7:</b> Production of lead during the last 5000 years, and its relation to major historical events.....	30
<b>Figure 1.8:</b> Amounts of lead in snow strata and in pond sediments relative to current levels.....	30
<b>Figure 1.9:</b> Systematic of changes in the isotopic composition of lead during rock leaching and weathering.....	37
<b>Figure 2.1:</b> A map of Moraine Creek drainage area and the location of the sampling stations.....	54
<b>Figure 2.2:</b> Schematic description of the adsorption experiment.....	55
<b>Figure 2.3:</b> Rate of lead and cadmium transfer through a 1000 MWCO dialysis membrane.....	63
<b>Figure 2.2:</b> Fractionation of the mass spectrometer as a function of temperature.....	68
<b>Figure 3.1.1:</b> The relations between concentraion of lead lead incorporated by organic matter and the concentration of organic matter in soil.....	86
<b>Figure 3.1.2:</b> $^{206}\text{Pb}/^{207}\text{Pb}$ ratios in the labile reservoir, in non - labile reservoir, in stream water, soil moisture and in ground water as a function of depth.....	87
<b>Figure 3.1.3:</b> The general composition of stream water and ground water in Thompson Canyon, spring 1986.....	88
<b>Figure 3.2.1:</b> Isotopic composition of lead in atmospheric precipitations and in stream water in Moraine Creek.....	113
<b>Figure 3.2.2:</b> Change of $^{206}\text{Pb}/^{207}\text{Pb}$ ratios in stream water, during the fall as a function of the distance from the lake in Moraine Creek.....	114
<b>Figure 3.2.3:</b> $^{206}\text{Pb}/^{207}\text{Pb}$ vs. $^{206}\text{Pb}/^{204}\text{Pb}$ and $^{206}\text{Pb}/^{208}\text{Pb}$ vs. $^{206}\text{Pb}/^{207}\text{Pb}$ of total lead in rocks, rock leached phase and natural stream waters.....	115

<b>Figure 3.2.4:</b> The various forms of lead and cadmium in stream water compared with the adsorption model of Dzombak (1986).....	116
<b>Figure 3.2.5:</b> Mass balance of various elements in Moraine Creek.....	117
<b>Figure 3.2.6:</b> Ferrous iron concentration in the stream water as a function of distance.....	118
<b>Figure 3.2.7:</b> Lead-iron relations in rock, rock and soil leach, stream and ground waters.....	119
<b>Figure 4.1:</b> Concentrations of lead and iron in rock, rock leach, mineral and mineral leach samples.....	142-144
<b>Figure 4.2:</b> Concentrations of lead and iron in granodiorite, in the leached phase and in stream and ground waters draining the bedrock.....	145
<b>Figure 4.3:</b> Lead adsorption on iron rich particles in the presence of high magnesium concentrations as a function of pH.....	146
<b>Figure 4.4:</b> Desorption of lead from $\text{Fe}(\text{OH})_3$ surfaces due to complexation by EDTA.....	147
<b>Figure 4.5:</b> Complexation field diagram of cations present in natural water.....	148
<b>Figure 4.6:</b> The effect of Cl vs. OH complexation on the relative abundances of trace metals in deep-sea water.....	149
<b>Figure 4.7:</b> The effect of Cl vs. surface complexation on the relative abundances of trace metals in deep-sea water.....	149
<b>Figure 4.8:</b> The effect of Cl vs. OH complexation on the relative abundances of REE in deep-sea water.....	150

## List of Tables

	<u>page #</u>
<b>Table 1.1:</b> Lead and cadmium in rock forming minerals, crustal units and upper magma.....	4-5
<b>Table 1.2:</b> Concentrations of lead, cadmium, zinc, copper, and iron in uncontaminated sediments and soils, and in river and deep sea water.....	7
<b>Table 1.3:</b> Emission of lead, cadmium and manganese from natural sources.....	12
<b>Table 1.4:</b> Some physical and chemical properties of lead, cadmium, zinc and copper.....	14
<b>Table 1.5:</b> Model speciation of cadmium, copper, lead and zinc in fresh and sea water.....	17
<b>Table 1.6:</b> Equilibrium model: effect of organic complex formation on distribution of metals in aerobic waters.....	18
<b>Table 1.7:</b> Surface properties of common particles.....	24
<b>Table 1.8:</b> Model speciation of metal cations with major anions and iron hydroxide surfaces.....	27
<b>Table 1.9:</b> Emission to the atmosphere of lead, cadmium, zinc, copper and manganese; natural versus anthropogenic sources.....	29
<b>Table 1.10:</b> $^{206}\text{Pb}/^{204}\text{Pb}$ , $^{207}\text{Pb}/^{204}\text{Pb}$ , and $^{208}\text{Pb}/^{204}\text{Pb}$ ratios in rock forming minerals and common rock types.....	34-36
<b>Table 1.11:</b> $^{206}\text{Pb}/^{207}\text{Pb}$ ratios in selected major lead bearing ores.....	37
<b>Table 2.1:</b> Blanks of reagent, ware and procedures.....	39
<b>Table 2.2:</b> Isotopic composition of lead in NBS standards measured by the VG MS and other MS from CIT laboratories.....	69
<b>Table 3.1.1:</b> A comparison between bedrock and soil at the south drainage, Thompson Canyon.....	83
<b>Table 3.1.2:</b> Lead concentration and $^{206}\text{Pb}/^{207}\text{Pb}$ ratios in the labile reservoir and in the nonlabile reservoir at various depths in meadow soil.....	84
<b>Table 3.1.3:</b> Concentrations of water, organic matter and labile reservoir in meadow soil at various depths.....	84
<b>Table 3.1.4:</b> Concentrations of lead and $^{206}\text{Pb}/^{207}\text{Pb}$ ratios in snow, stream water, ground water and soil moisture.....	85
<b>Table 3.1.5:</b> Ca/Pb ratio in the hydrological cycle.....	85
<b>Table 3.2.1:</b> Chemical composition of bedrock and soil in Moraine Creek.....	106

<b>Table 3.2.2:</b> Particle size distribution, organic carbon, pH and water saturation percent of Moraine Creek soil.....	107
<b>Table 3.2.3:</b> Exchangeable cations at the pH of the soil.....	107
<b>Table 3.2.4:</b> Free (secondary) iron, aluminum and manganese oxides and hydroxides in Moraine Creek soil.....	107-108
<b>Table 3.2.5:</b> Stream water, ground waters and atmospheric deposition composition in Moraine Creek.....	108-111
<b>Table 3.2.6:</b> A comparison between measured and calculated IC based on mass balance consideration.....	112
<b>Table 4.1:</b> Composition of the solution leached from Jossi Spring biotite.....	139
<b>Table 4.2:</b> Concentration of major cation of the adsorption experiment solution as a function of pH.....	140
<b>Table 4.3:</b> Concentrations of lead and iron in uncontaminated sediments and soils....	141

## Chapter 1: Introduction

This chapter starts with a statement about the thesis objectives and their justifications. The distribution of lead and cadmium in rocks and common crustal minerals is described in the subsequent section. A major part of the chapter deals with the occurrence of lead and cadmium in rivers, marine waters and in the atmosphere. The thermodynamic and kinetic properties which determine the behavior of lead and cadmium in the aquatic environment are discussed in the subsequent sections. In order to get a more general view, lead and cadmium are compared to zinc and copper, two trace metals which have somewhat similar properties to those of lead and cadmium. The fifth part of the chapter deals with the large anthropogenic impact on the global cycle of lead, cadmium and other metals. The last part concentrates on the isotopic characteristics of lead release from rocks and minerals, since lead isotopes provide a powerful tool for tracing lead migration and differentiating between natural (rock-derived) and industrial lead sources.

The conventional wisdom about the fate of lead, cadmium and other trace metals in rivers is summarized by Turekian (1977); "Thus we see that all the processes of transfer of materials from the continents to the oceans are constrained by the removal of reactive elements onto particles." It is important to note that using a 0.45  $\mu\text{m}$  pore size filter is an arbitrary, operation-dependent distinction between solution and particulate matter (Laxen and Chandler, 1982; Salomons and Förstner, 1984; Morel and Gschwend, 1987). A large fraction of the oxide, organic and biological particles does pass through the 0.45  $\mu\text{m}$  pores.

### 1.1. The research objectives of the thesis

1) To detect natural (rock-derived) lead and cadmium in remote mountain streams in spite of worldwide pollution, and to distinguish between natural and anthropogenic sources using isotopic tracers.

- 2) To study the physicochemical speciation of natural lead and cadmium in those streams.
- 3) To determine the characteristics of lead and cadmium transport in rock, soil, ground water, and stream water systems, and to find other elements unaffected by global pollution which are transported in a similar way.
- 4) To combine field and laboratory studies in order to generalize the results obtained in remote mountain streams to larger and more contaminated rivers.
- 5) To re-examine the global flux of lead and cadmium to the oceans in light of new estimated levels in rivers.

## **1.2. Justification**

Lead and cadmium are among the elements most affected by human activity (Salomons and Förstner, 1984; Patterson and Settle, 1987; Wong, 1987; Nriagu, 1989), and the aquatic behavior of  $Pb^{2+}$  and  $Cd^{2+}$  is similar to a large group of toxic and essential elements like  $Ni^{2+}$ ,  $Zn^{2+}$ ,  $Cu^{2+}$ ,  $Mn^{2+}$ , and  $Fe^{2+}$ . Lead has two oxidation states ( $Pb^{2+}/Pb^{4+}$ ), but  $Pb^{2+}$  is by far more abundant in most natural environments. In addition, lead has four stable isotopes whose ratios are highly affected by rock and soil weathering; therefore, lead can be used as a tracer to study erosion processes both in the present and in the geological past. Nevertheless, any anthropogenic effect should be minimal in order to detect these isotopic changes.

## **1.3. Lead and cadmium in the lithosphere, hydrosphere and atmosphere**

### **1.3.1. Lead and cadmium distribution in minerals and rocks**

Lead and cadmium are present in the lithosphere in trace amounts. The estimated average concentrations in the continental crust are: 15 ppm lead and 100 ppb cadmium (Heinrichs et al., 1980).

**Ore minerals:** Both metals appear as major constituents in opaque (ore-forming) minerals and in accessory rock-forming minerals (Dana and Ford, 1932). Lead minerals are common in ore bodies, while cadmium minerals are much less abundant. Both lead and cadmium minerals are rare in common terrestrial rocks. The major **lead** minerals are: **galena** (PbS), **cerussite** (PbCO<sub>3</sub>), and **anglesite** (PbSO<sub>4</sub>). The major **cadmium** minerals are: **greenockite** (CdS), **cadmiumoxide** (CdO), **otavite** (CdCO<sub>3</sub>), and **sphalerite** (ZnS) where cadmium replaces zinc.

**Rock-forming minerals:** Lead and cadmium are found in trace amounts in rock-forming minerals. Lead has an affinity for 8-12 coordination sites in mica, K-feldspar and plagioclase. Cadmium, on the other hand, is mainly found in ferromagnesian minerals in magmatic rocks and in Ca minerals in carbonate rocks (Table 1.1a).

**Magmatic rocks:** Lead is much more abundant in granitic and granodioritic rocks than in any other type of magmatic rock, while cadmium distribution is very uniform in ultra mafic to granitic rocks, except for very low values in peridotitic inclusions. Therefore, there is much more variation in lead than in cadmium concentrations within the crust (Fleischer, 1976; Heinrichs et al., 1980; Table 1.1b).

**Sedimentary rocks:** Lead has higher concentrations in shale and other rocks with high clay content than in other sedimentary rocks. Cadmium concentrations are higher both in shale and in some carbonate rocks than in other sedimentary rock types. In general, cadmium distribution in sedimentary rock is more uniform than lead (Heinrichs et al., 1980; Table 1.1b). The uniformity presented by cadmium over such a wide range of rock types might be partly an analytical artifact caused by its low concentration in most rocks.

**Table 1.1:** Lead and cadmium a) in rock-forming minerals; and b) in crustal units and upper mantle, calculated from lead and cadmium distribution in different rock types. All values are in ppm, from Heinrichs et al. (1980).

**a) rock-forming minerals:**

1 = basalt (tot. Cd: .05-.09, tot. Pb: 2.7-5)

2 = granite/gneiss/migmatite (tot. Cd: .03-.28, tot. Pb: 15-47)

3 = granite (tot. Cd: .06-.07, tot. Pb: 75-76)

4 = sedimentary rock, clastic and carbonate (tot. Cd: .04-.21, tot. Pb: 5-22)

in brackets, relative proportions in minerals as fraction of total rock.

mineral	Cd	Pb	rock
plagioclase	.04 (29)	4 (70)	1
plagioclase	.05 (36)	5 (50)	1
plagioclase	.03 (12)	10 (81)	1
pyroxene	.06 (20)	1 (13)	1
pyroxene	.10 (42)	2 (13)	1
pyroxene	.08 (46)	3 (24)	1
magnetite	.23 (16)	2 (4)	1
magnetite	.31 (46)	4 (8)	1
magnetite	.23 (35)	3 (8)	1
olivine	.05 (17)	2 (12)	1
biotite	.06 (12)	18 (4.6)	2
biotite	.21 (96)	9 (9.6)	2
biotite	.64 (100)	54 (19)	2
biotite	.32 (12)	35 (2)	2
biotite	.14 (15)	22 (3.4)	2
biotite	.09 (4.5)	12 (2)	2
biotite	.84 (79)	36 (27)	2
biotite	.08 (15)	24 (5.8)	2
biotite	.41 (100)	6 (4.7)	2
K-feldspar	.05 (28)	23 (32)	3
K-feldspar	.05 (26)	26 (28)	3
total clay	.22	39	4
illite	-	55	4
chlorite	1.0	-	4
carbonate	0-1.0	0-70	4

**Table 1.1 cont.**

**b) crustal units and upper mantle:**  
In brackets, range of concentrations.

	<u>Cd</u>	<u>Pb</u>
Sedimentary rocks	.12(.09-.14)	17 (15-18)
Magmatic rocks, upper continental crust	.09	28
Metamorphic rocks, upper continental crust	.10	15
Upper continental crust	.10	21
Lower continental crust	.10	8.5
Continental crust	.10	15
Upper mantle	.04	.2

### 1.3.2. Lead and cadmium in rivers

The extremely low concentrations of trace metals like lead and cadmium in river water make them hard to analyze and increase the probability of contamination during sampling and handling. Moreover, the global pollution of both lead and cadmium in the environment tends to mask their natural concentrations (Murozumi et al., 1969; Meybeck and Helmer, 1989). The "natural" concentrations of lead and cadmium in rivers, as a function of sampling date, are continuously decreasing, probably due to improvements in sampling and analytical techniques (Fig. 1.1).

The major processes affecting metal speciation in surface waters in general, and in river waters in particular, are summarized in Figure 1.2. Based on laboratory experiments and field studies it seems that in most fresh surface waters, a substantial fraction of trace metals (including lead and cadmium) is adsorbed on organic and metal oxide surfaces (see section 1.4.4; Gibbs, 1973; Benninger et al., 1975; Hem, 1976; Getz et al., 1977; Lewis, 1976, 1977; Turekian, 1977; Vuceta and Morgan, 1978;

Mouvet and Bourg, 1983; Laxen, 1985; Benes et al., 1985; Trefry et al., 1985; Buffle and Altmann, 1987; Sigg, 1987). While the adsorption process is relatively fast (minutes to hours), desorption of both lead and cadmium from sediments is usually a slower process (Lion et al., 1982). Humic materials present in most natural fresh waters have different effects on the adsorption of various trace metals on oxide surfaces. It seems that the adsorption of lead and cadmium on oxide particles is either enhanced or unaffected by the presence of humic material while the adsorption of copper decreases (Laxen, 1985). In addition, trace metals are accumulated by microorganisms in natural waters by a variety of processes (see section 1.4.4; Coombs, 1979; Nelson et al., 1981; Baudo, 1982).

Since anthropogenic input of lead and cadmium tend to mask their natural concentrations in rivers, it is extremely hard to estimate their natural river load. Levels of both lead and cadmium in rivers reported as background concentrations are probably affected by pollution (Martin and Whitfield, 1983; Salomons and Förstner, 1984; Taylor and McLennan, 1985). By comparing lead, cadmium, zinc and copper concentrations in rivers with unpolluted elements that have similar transport properties, one can estimate the degree of lead, cadmium, zinc and copper pollution in rivers.

River sediments are less affected by pollution, since the background concentrations of both lead and cadmium are initially high. Based on metal concentrations in unpolluted sediments summarized by Salomons and Förstner (1984) it seems that lead, copper, and zinc in river, coastal sediments, and soils maintain their average upper continental crust ratios with iron, while cadmium is enriched compared with iron (Table 1.2). This observation fits well with calculations of equilibrium speciation. While both lead and zinc can follow iron through adsorption, cadmium, which is adsorbed only at higher pH values (where major cations like magnesium and calcium compete on surface sites more effectively), may stay in solution. A large excess of lead, cadmium, zinc and copper relative to iron is found in contemporary

rivers compared with soils and sediments (Table 1.2). The relative increase of lead, cadmium, zinc and copper concentrations in rivers compared with iron will be discussed in chapter 4.

**Table 1.2:** Concentrations of lead, cadmium, zinc, copper, and iron in uncontaminated sediments, soils, river water, and deep ocean water. Sediment and rock values except for iron are in ppm, river and ocean values in ppb. (1) Turekian and Wedepohl (1961); (2) Förstner and Müller (1974); (3) Förstner (1978); (4) Ure and Berrow (1982); (5) Taylor and McLennan (1985); (6) Yeats and Bewers (1982); (7) Kennedy and Sebetich (1976); (8) Boyle (1978); (9) Trefry and Presley (1976); (10) Schell and Nevissi (1977); (11) Martin et al. (1989).

metal	shale & clays (1)	sub-recent Rhine sediment (2)	lacustrine sediments (3)	soils (4)	up. cont crust (5)	BG rivers	deep ocean(11)
Fe (%)	4.72	3.23	4.34	3.2	3.5	55(6)	0.036
Zn	95	115	118	60	71	0.5(7)	0.62
Cu	45	51	45	26	25	1(8)	0.16
Pb	20	30	34	29	20	0.2(9)	0.0007
Cd	0.2	0.3	0.4	0.6	0.1	0.02(10)	0.095
Fe/Zn	500	300	400	500	500	110	0.06
Fe/Cu	1000	650	1000	1200	1400	55	0.23
Fe/Pb	2400	1100	1300	1100	1750	275	50
Fe/Cd	250,000	110,000	110,000	55,000	350,000	2750	0.4

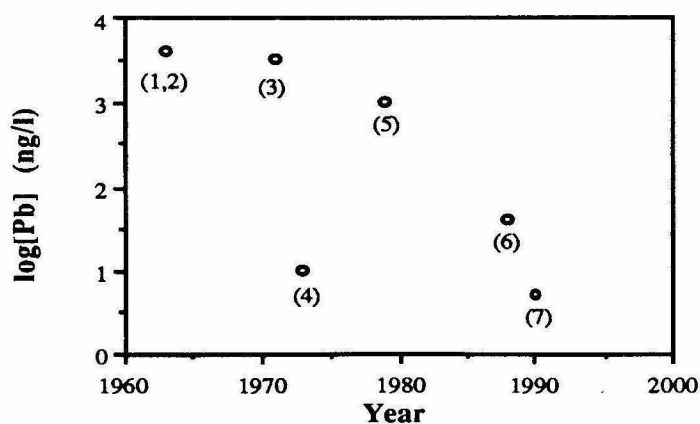


**Figure 1.1:** Variability and trend of lead measurements in rivers, the effect of analytical capabilities, after Meybeck and Helmer (1989). (1) Durum and Haffty (1961); (2) Livingstone (1963); (3) Turekian (1971); (4) Patterson et al. (1973); (5) Martin and Meybeck (1979); (6) Elbaz-Poulichet (1988); (7) this work.

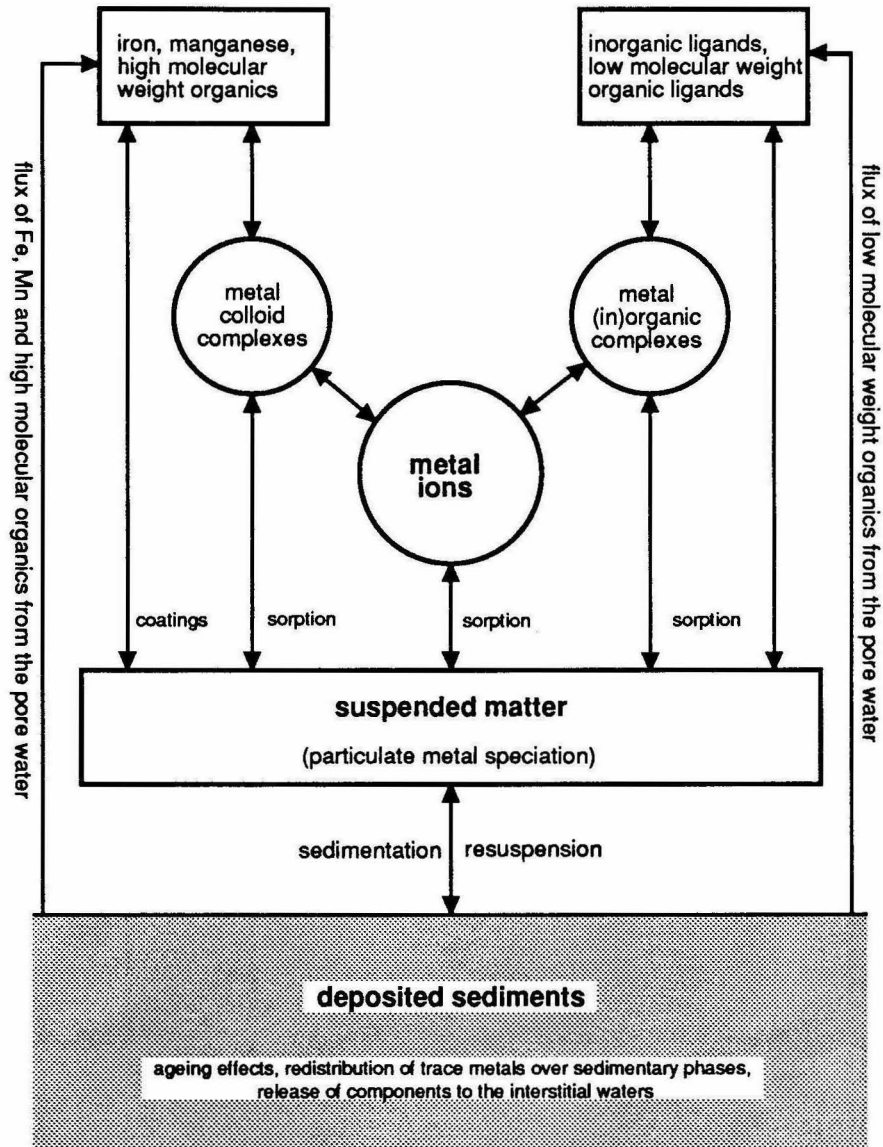


**Figure 1.2:** Summary of major processes and mechanisms in the interactions between dissolved and solid metal species in surface waters. (From Salomons and Förstner, 1984.)

### 1.3.3. Lead and cadmium in estuary and coastal environments

The transition zone between continental fresh water and marine water is a very dynamic environment where many physical and chemical processes take place at various time scales. Some of these processes have a large effect on trace metal transport. Suspended particles in river water start to coagulate upon flowing into the higher ionic strength saline water due to the compression of the electrical double layer, and sink to the sediment. Presumably, this process reduces the concentration of some dissolved elements by more than 90%. These elements include iron and manganese which form particles, and trace metals like lead and cadmium, which are adsorbed onto particles (Turekian, 1977; Martin and Whitfield, 1983). However, it has been pointed out that remobilization of trace metals in the estuary environment does occur (Salomons and Förstner, 1984; Elbaz-Poulichet et al., 1984, Boyle et al., 1982; Gobeil et al., 1987). There are researchers who interpret the apparent remobilization as a simple mixing between polluted river water and relatively clean sea water (Förstner and Müller, 1974), while others suggest nonconservative behavior of trace metals within the estuary system (Groot and Allersma, 1975). Field studies which involve isotopic analysis of lead (Elbaz-Poulichet et al., 1984) and laboratory studies (Kharkar, 1968; Salomons, 1980) indicate that partial desorption of trace metals takes place with increasing chlorinity. A recent study by Pucci et al. (1989) correlates elevated lead and cadmium concentrations in ground water with intrusion of saline water, which causes a substantial release of both metals from particles.

To what degree is the estuarine trace metal cycle self-contained? According to Turekian (1977) almost all the riverborne trace metals are trapped within the estuary and do not reach the open ocean environment. Other researchers point out that a substantial fraction of trace metals like lead and cadmium does leave the estuary system (Jouanneau, 1982; Kerdijk and Salomons, 1981). A study by Yeats and Bewers (1982) suggests that while 99.8% of the iron is retained in the coastal zone, only 69%

of the cadmium, 54% of the zinc, and 66% of the copper are scavenged there. In a different study, it was found that only 70% of the lead was scavenged by particles within the estuary (Paulson et al., 1988). Such a difference between iron (mostly particulate) and trace metals suggests a partial release of trace metals.

The time scale of major processes controlling the transport of trace metals (adsorption, desorption, dissolution, precipitation and coagulation) compared with the residence time of the water in the coastal zone, and the rate of sedimentation (and burial) determine the relative significance of each process. Therefore, there is an expected variation in the observed behavior of trace metals in different estuaries depending on the particular physical properties of each system.

Based on equilibrium speciation, it is likely that lead and cadmium will be complexed by chloride more than zinc, and therefore will be released in larger amounts from oxide surfaces (Smith and Martell, 1976). The fact that the observed remobilization of all three metals is more or less the same suggests that kinetic and transport processes determine the remobilization of metals in the estuary.

#### **1.3.4. Lead and cadmium in the ocean**

Lead and cadmium have different profiles in ocean water. Cadmium has a nutrient-like profile with a very low concentration at the surface which increases with depth, reaching a maximum at approximately one kilometer, and then decreasing slowly all the way down to the sea floor at five kilometers (Bruland, 1980). High correlation between cadmium and phosphate was reported by Bruland et al.(1978), Bruland and Franks (1983), and Boyle (1988). Such a similarity between cadmium and phosphate suggests that cadmium is removed rapidly from surface sea water by organisms and is released to solution as a result of partial dissolution of biogenic particles at depth (Morel and Hudson, 1987; Whitfield and Turner, 1987).

The profile of lead in sea water is almost the opposite of that of cadmium; lead concentrations are high in surface waters down to 200-300 meters and then they decrease, reaching a constant value at approximately 2.5 kilometers (Schaule and Patterson, 1981). The profile of lead in the ocean is different from that of phosphate (Schaule and Patterson, 1981; Bruland, 1980), manganese (Schaule and Patterson, 1981) and iron (both smaller and larger than  $0.4 \mu\text{m}$ ; Martin et al., 1989), suggesting no significant uptake of lead by organisms. The lead profile indicates a large atmospheric input, and a relatively slow removal from surface waters. It is interesting to note that both lead and cadmium in sea water are found in "solution" (Schaule and Patterson, 1981; Stukas and Wong, 1983), although, a distinction between "dissolved" and "particulate" matter is operation dependent (see sections 1.0, 3.2, 4.4). Based on its concentration profile, Schaule and Patterson (1981) suggested that the residence time of lead in the Pacific surface water is 20 years, and 80 years in the deep Pacific water. Other estimates of residence time of lead in deep ocean water range from 45 to 1100 years! The large difference between various estimates is the result of large uncertainties regarding lead concentrations in ocean water, lead flux to the ocean from the atmosphere and from rivers, and the magnitude of its removal to deep sea sediments. Whitfield (1981) showed that for most elements the ocean is at steady state, based on the correlation between the residence time of these elements in the ocean and their partitioning function, defined as the ratio between their concentration in sea water and their concentration in crustal rocks. However, lead, zinc, and copper (cadmium is not mentioned) as well as a few other elements (e.g., mercury and selenium) fall away from the correlation line, having an excess of concentration in sea water. Whitfield (1981) used a residence time of approximately 1100 years for lead in the ocean, much larger than the one calculated by Schaule and Patterson (1981). If one uses the residence time of lead given by the latter, lead plots even further away from the line, suggesting that it is either in a transient state in the ocean (according to Schaule and

Patterson, 1981), or that there is a large excess of lead in sea water coming from sources other than crust weathering.

### 1.3.5. lead and cadmium in the atmosphere

The emission of lead and cadmium to the atmosphere from natural sources is given in Table 1.3 (Ng and Patterson, 1981; Nriagu, 1989). The wide range of values reported for lead demonstrate the uncertainty associated with estimates of global emissions of metals whose anthropogenic sources are a few orders of magnitude larger than their natural ones.

Atmospheric input is probably the main source for many metals in mid-ocean environments. According to Crecelius (1982), 96% of the lead, 50% of the cadmium, 79% of the zinc and 30% of the copper in mid-ocean surface waters come from atmospheric sources. Schaule and Patterson (1981) also claim that most of the lead in surface sea water comes from the atmosphere, the majority of which is anthropogenic, and Martin et al. (1989) suggest that most of the iron in mid-ocean surface waters comes from natural sources via the atmosphere.

**Table 1.3:** Emission of lead, cadmium and manganese from natural sources. All values in  $10^9$  g/yr. (1) Nriagu (1989); (2) Ng and Patterson (1981).

source	Cd	Mn	Pb
soil (1)	0.21	221	3.9
sea spray (1)	0.06	0.86	1.4
volcanoes (1)	0.82	42	3.3
forest fire (1)	0.11	23	1.9
biogenic			
continental (1)	0.19	28	1.5
marine (1)	0.05	1.5	0.24
total emission (1)	1.3	317	12
total emission (2)	-	-	4

## 1.4. Aquatic chemistry of lead, cadmium, zinc and copper

### 1.4.1 Chemical and physical properties of lead, cadmium, zinc and copper

The physical and chemical properties of lead, cadmium, zinc and copper (Table 1.4) determine their fate in aquatic systems. The electronic configurations and the ionic radii are probably the most important parameters since they determine the tendency of an element to form ionic versus covalent bonds.

### 1.4.2. Grouping of elements in the aquatic environment

Voluminous literature describes the tendencies of various cations to form complexes with organic and inorganic ligands in water (Stumm and Morgan, 1981; Morel, 1983; Salomons and Förstner, 1984). Many attempts have been made to divide cations present in natural waters into subgroups. Turner et al. (1981) combined the field strength,  $Z^2/r$ , the overall hydrolysis coefficient,  $\alpha_{M,OH}$  ( $\alpha_{M,OH} = 1 + \sum_j \beta_{M,OH}[OH]^j$ ), and  $\Delta\beta$  ( $\Delta\beta = \log[\beta_{MF}^0] - \log[\beta_{MCl}^0]$ ) = a measure of the difference between a-type and b-type metals, Ahrlund et al., 1958) in order to form groups of metals and cations with similar aquatic properties. Based on their electrostatic ( $Z^2/r$ ) and covalent ( $\Delta\beta$ ) measures,  $Pb^{2+}$ ,  $Fe^{2+}$ ,  $Mn^{2+}$ ,  $Zn^{2+}$ ,  $Cu^{2+}$ ,  $Ni^{2+}$  fall into one group, while  $Cd^{2+}$ , which is more strongly complexed by chloride, falls into an adjacent group (Fig. 1.3). As a consequence, one would expect a similar but not identical aquatic behavior of all these cations, with cadmium being more sensitive to changes in chloride concentrations. Similar attempts to subdivide elements based on their electrostatic and covalent properties, with more or less the same results, have been made by Baes and Mesmer (1976), by Nieboer and Richardson (1980) and many others (see section 4.4.3).

**Table 1.4:** Some physical and chemical properties of lead, cadmium, zinc and copper, from: (1) Weast (1986); (2) Turner et al. (1981); (3) Smith and Martell (1976); (4)  $\log K_{s1}^{int} = 1^{st}$  adsorption constant on am-Fe(OH)<sub>3</sub>, Dzombak (1986); (5)  $\log k =$  characteristic rate constant for H<sub>2</sub>O substitution in inner coordination sphere of metal ions, Basolo and Pearson (1967).

	Pb	Cd	Zn	Cu
atomic weight (1)	207.19	112.41	65.38	63.55
atomic number (1)	82	48	30	29
melting point (°K,1)	600.6	594.2	692.7	1357.6
boiling point (°K,1)	2023	1040	1180	2836
density (gr/cm <sup>3</sup> ,1)	11.4	8.65	7.14	8.96
charge (1)	2,4	2	2	2,1
atomic radius (Å,1)	1.81	1.71	1.53	1.57
electronic configuration	[Xe]4f <sup>14</sup> 5d <sup>10</sup> 6s <sup>2</sup> p <sup>2</sup>	[Kr]4d <sup>10</sup> 5s <sup>2</sup>	[Ar]3d <sup>10</sup> 4s <sup>2</sup>	[Ar]3d <sup>10</sup> 4s <sup>1</sup>
electronegativity (1)	2.33	1.69	1.65	1.90
	Pb <sup>2±</sup>	Cd <sup>2±</sup>	Zn <sup>2±</sup>	Cu <sup>2±</sup>
ionic radius (Å,1)	1.20	0.97	0.74	0.72
field strength (Z <sup>2</sup> /ion rad,1)	3.33	4.12	5.41	5.56
$\log \beta_{F^-}^{\circ}$ (2)	2.06	1.08	1.15	1.52
$\log \beta_{Cl^-}^{\circ}$ (2)	1.58	1.97	0.49	0.40
$\log \beta_{OH^-}^{\circ}$ (2)	6.29	3.92	5.14	6.00
$\log \beta_{CO_3^{2-}}^{\circ}$ (2)	7.00	4.35	4.75	6.75
$\log \beta_{SO_4^{2-}}^{\circ}$ (2)	2.75	2.45	2.36	2.36
$\log K_{soS^{2-}}$ (3)	-27.5	-27.0	-24.7(α)	-36.1
$\log K_{s1}^{int}$ (4)	4.71	0.43	0.97	2.85
$\log k$ (S <sup>-1</sup> ,5)	-	8.4	7.5	8.5

	a $\Delta\beta > 2$	a' $2 > \Delta\beta > 0$	b' $0 > \Delta\beta > -2$	b $\Delta\beta < -2$
<b>I</b> $Z^2/r < 2.5$	Li, Na, K Rb, Cs  < 0.1		Cu(I), Tl(I)  < 0.1 (FW) 0.3-5.2 (SW)	Ag, Au  0.2-6.1 (FW) 5.3-12.9 (SW)
<b>II</b> $2.5 < Z^2/r < 7$	Mg, Ca Sr, Ba  < 0.2	Co, Ni, Zn, Pb Mn(II), Fe(II) Cu(II)  < 0.1 (FW, pH 6) 0.2-1.5 (SW) 0.2-2.7 (FW, pH 9)	Cd  < 0.1 (FW, pH 6) 1.6 (SW) 0.3 (FW, pH 9)	Hg  6.9 (FW, pH 6) 14.2 (SW) 11.8 (FW, pH 9)
<b>III</b> $7 < Z^2/r < 11$	Ln, Y  0.1-0.2 (FW, pH 6) 0.4-1.3 (SW) 1.8-4.2 (FW, pH 9)		Bi  9.1 (FW, pH 6) 14.8 (SW) 18.0 (FW, pH 9)	Tl(III)  14.6 (FW, pH 6) 20.5 (SW) 23.6 (FW, pH 9)
<b>IV</b> $11 < Z^2/r < 23$	Be, Al, Sc, Ga Cr(III), Fe(III) Zr, Hf, Th U(IV)  0.8-14.3 (FW, pH 6) 2.7-24.0 (SW) 4.5-28.8 (FW, pH 9)	In  5.5 (FW, pH 6) 11.5 (SW) 14.6 (FW, pH 9)		

**Figure 1.3:** Complexation field diagram for the cationic elements. The symbol Ln represents the lanthanide series. The cations are divided into four groups both on the horizontal axis ( $\Delta\beta$ ) and on the vertical axis ( $Z^2/r$ ). The values below each group of elements show the range of  $\log \alpha$  values calculated for model sea water and fresh waters ( $\alpha$  = overall hydrolysis coefficient). Ia and IIa are very weakly complexed cations. Ib' and Ib are chloro-dominated cations, while IIb' and IIb are partially complexed by chloride. IVa and IVa' are hydrolysis-dominated cations. (From Turner et al., 1981.)

### 1.4.3. Speciation of lead, cadmium, zinc and copper in fresh and sea water

The inorganic speciation of lead, cadmium, zinc and copper in fresh water at pH 6.0 and 9.0 and in sea water at pH 8.2 were calculated by Turner et al. (1981) with no consideration of organic ligands and surface sites (Table 1.5). In fresh water at pH 6.0, all four elements are mainly present as free cations. However, at pH 9.0 both lead and copper form mainly carbonate species, while almost half of the cadmium is free and the other half is complexed by carbonate, and zinc is mostly hydrolyzed. In sea water, almost all the cadmium forms chloro complexes, while most of the copper is still complexed to bicarbonate. Lead is mainly bound both to chloride and to carbonate, while half of the zinc is still free and about a third of the zinc is complexed by chloride.

The relative tendencies of these metals to form complexes with organic ligands is summarized by Stumm and Morgan (1981) using a mixture of organic ligands, sulfate, bicarbonate, carbonate and chloride (Table 1.6). In fresh water, there is a minimal effect by organic ligands on the speciation of lead, cadmium and zinc. Only copper is substantially affected by the addition of citrate (100% of copper is complexed by citrate). At the same time, approximately 90% of the citrate in the fresh water sample complexes calcium. In sea water, high concentrations of  $\text{Cl}^-$  and  $\text{HCO}_3^-$  further suppress the effect of organic ligands on the speciation of all of the metals compared with fresh water. Only copper is substantially affected by the addition of organic ligands, mainly by citrate (100% is complexed by citrate). It is important to note that most of the citrate is consumed by magnesium which is more abundant than copper by five orders of magnitude.

**Table 1.5:** Model speciation of cadmium, copper, lead and zinc in fresh and sea water. a) Total concentration of major components in fresh and sea water; b) Speciation of metals in fresh water at pH 6.0; c) fresh water, pH 9.0; and d) sea water, pH 8.2. Speciation of metals in percent of total. alkalinity =  $[\text{HCO}_3^-] + 2[\text{CO}_3^{2-}]$ . (From Turner et al., 1981.)

**a) total concentrations (-log(mol/l))**

	<u>sea water</u>	<u>fresh water</u>
alkalinity	2.65	3.68
B	3.37	6.05
Br	3.07	6.70
C	2.71	3.19
Ca	1.98	3.47
Cl	0.25	3.66
F	4.16	5.30
K	1.98	4.23
Mg	1.27	3.77
Na	0.32	3.56
S	1.54	3.93
Sr	4.05	6.10

cation	free	OH <sup>-</sup>	F <sup>-</sup>	Cl <sup>-</sup>	SO <sub>4</sub> <sup>2-</sup>	CO <sub>3</sub> <sup>2-</sup>
--------	------	-----------------	----------------	-----------------	-------------------------------	-------------------------------

**b) model fresh water, pH=6.0**

Cd <sup>2+</sup>	96	<1	<1	2	2	<1
Cu <sup>2+</sup>	93	1	<1	<1	2	4
Pb <sup>2+</sup>	86	2	<1	1	4	7
Zn <sup>2+</sup>	98	<1	<1	<1	2	<1

**c) model fresh water, pH=9.0**

Cd <sup>2+</sup>	47	4	<1	1	1	47
Cu <sup>2+</sup>	<1	3	<1	<1	<1	96
Pb <sup>2+</sup>	<1	5	<1	<1	<1	95
Zn <sup>2+</sup>	6	78	<1	<1	<1	16

**d) model sea water, pH=8.2**

Cd <sup>2+</sup>	3	<1	<1	97	<1	<1
Cu <sup>2+</sup>	9	8	<1	3	1	79
Pb <sup>2+</sup>	3	9	<1	47	1	41
Zn <sup>2+</sup>	46	12		35	4	3

**Table 1.6:** Equilibrium model: effect of organic complex formation on distribution of metals in aerobic waters. a) fresh water; b) sea water. All concentrations are given as  $-\log(\text{mol/l})$ . Charge of species are omitted. (From Stumm and Morgan, 1981.)

**a) fresh water**

inorganic fresh water plus  $10^{-5.15}$  mol/l of each of the indicated organic ligands corresponding to 2.3 mg/l of soluble organic carbon; pH=7.0, 25°C, pSO<sub>4</sub>=3.4, pHCO<sub>3</sub>=3.1, pCO<sub>3</sub>=6.1, pCl=3.3

	Cd	Cu	Pb	Zn
M <sub>tot</sub>	7.7	7.0	7.0	6.7
free	7.76	9.93	8.04	6.72
major inorg. species	CdSO <sub>4</sub> ,9.2	CuCO <sub>3</sub> ,9.7	PbCO <sub>3</sub> ,7.1	ZnSO <sub>4</sub> ,8.2
Acetate	11.5	13.1	11.0	10.3
Citrate	9.2	7.0	8.9	10.5
Tartrate	9.6	11.3	8.8	8.9
Glycinate	11.5	9.4	10.1	9.6
Glutamate	9.7	9.4	-	8.6
Phthalate	9.7	11.4	9.2	9.1

**b) sea water**

inorganic sea water plus  $10^{-5.15}$  mol/l of each of the indicated organic ligands corresponding to 2.3 mg/l of soluble organic carbon; pH=8.0, 25°C, pSO<sub>4</sub>=1.95, pHCO<sub>3</sub>=2.76, pCO<sub>3</sub>=4.86, pCl=0.25

	Cd	Cu	Pb	Zn
M <sub>tot</sub>	8.5	7.7	8.2	7.2
free	10.9	10.8	9.9	7.8
major inorg. species	CdCl <sub>2</sub> ,8.7 CdCl,8.7	CuCO <sub>3</sub> ,9.4 Cu(CO <sub>3</sub> ) <sub>2</sub> ,10.5	PbCO <sub>3</sub> ,8.6 PbOH,8.7	ZnOH,7.4 ZnCl,8.0
Acetate	15.1	14.3	13.2	11.7
Citrate	13.1	7.7	11.3	11.3
Tartrate	13.5	16.7	11.5	10.9
Glycinate	13.6	9.6	11.8	8.8
Glutamate	13.4	10.6	-	9.7
Phthalate	13.6	13.0	11.7	10.9

#### 1.4.4. Surface chemistry of lead, cadmium, zinc and copper

In addition to complexation by dissolved compounds in water, trace metals are likely to be attached to surface sites of organic and inorganic particles (Vuceta and Morgan, 1978; Stumm and Morgan, 1981; Buffle and Altmann, 1987). In the last two decades, many investigators have studied the adsorption of various cations and anions on oxide surfaces (Hohl and Stumm, 1976; Schindler et al., 1976; Hohl et al., 1978; Davis, 1977; Benjamin and Leckie, 1982; Hayes and Leckie, 1985; Dzombak, 1986; Dzombak and Morel, 1990).

**The adsorption model:** The oxide surface behaves like a diprotic acid whose dissociation constants are affected by changes of the surface charge, caused by exchange of a proton with a cation from solution, or hydroxide with anion (Schindler, 1981; Fig. 1.4). The interaction of a cation with a surface site is a combination of specific (chemical) and non-specific (electrostatic) interaction (Dzombak, 1986; Schindler and Stumm, 1987). The importance of the specific interaction is best demonstrated by the fact that  $\delta\text{-Al}_2\text{O}_3$  and  $\text{Fe}(\text{OH})_3(\text{s})$  strongly adsorb cations at pH values below their zero point of charge (ZPC), in spite of a positive surface charge. In addition, changes in ionic strength have no effect on the adsorption edge of lead on goethite in spite of a large effect on the electrical double layer (Hayes and Leckie, 1985). The charge-potential relationship at the oxide surface and the distribution of the electrical charge as a function of distance from the surface have not been determined experimentally, as no one has been able to produce an oxide electrode. At least four different models attempt to describe the charge distribution near the surface. The constant capacitance model (Schindler and Stumm, 1987), the Stern model (Fokkink et al., 1990), the diffuse layer model (Gouy-Chapman model, Stumm et al., 1970; Dzombak, 1986) and the triple layer model (Yates, 1975; Hayes and Leckie, 1985). As shown by Westall and Hohl (1980) and Morel et al. (1981), all models can fit adsorption data, nevertheless, certain models explain electrokinetic data better than others. Observed zeta potentials coincide with the

Gouy-Chapman calculated potential at the diffuse layer in low potential and low ionic strength systems. At high ionic strength, the constant capacitance model probably gives

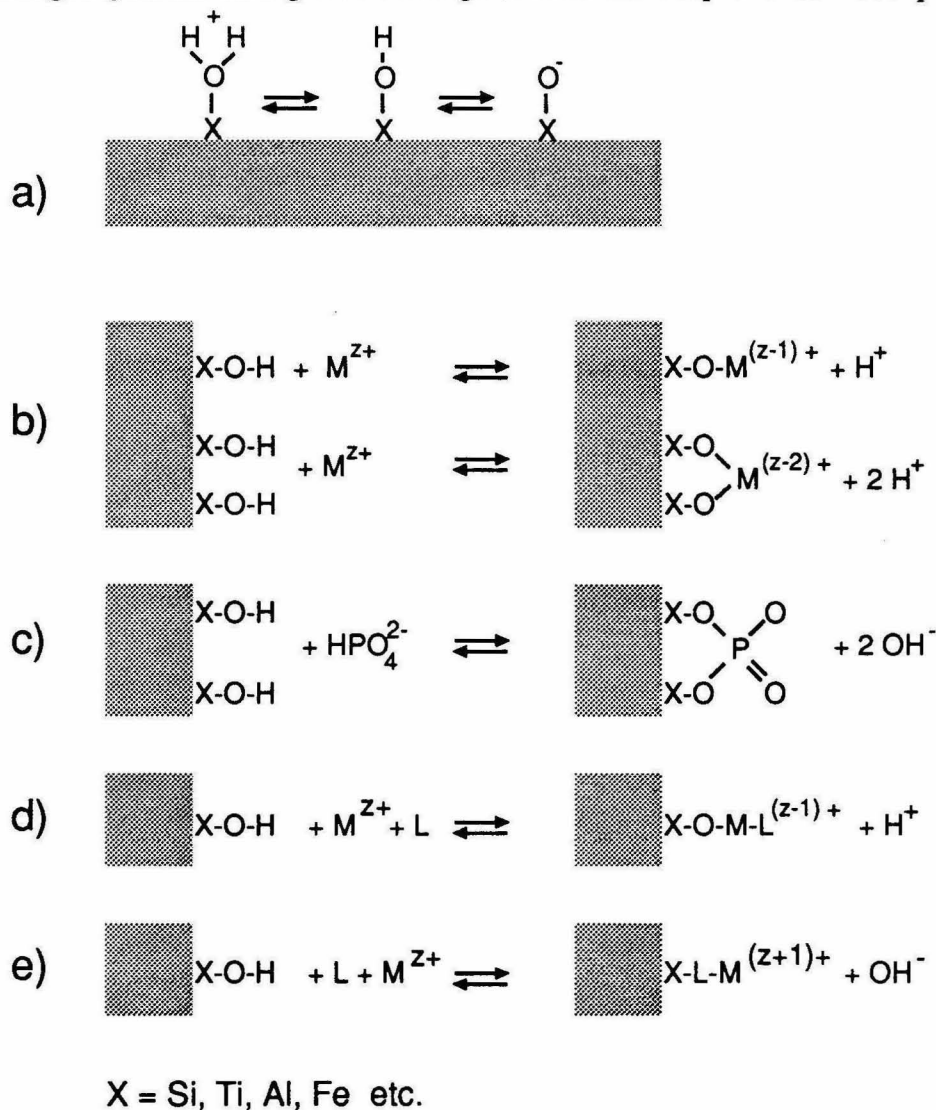


**Figure 1.4:** Coordination phenomena at oxide-water interface (from Schindler, 1981).

- Acid-base reactions of surface hydroxyl groups.
- Deprotonated surface hydroxyls coordinate with dissolved metal ions. Several species may be formed simultaneously.
- Surface hydroxyls are replaced by dissolved ligands.
- A dissolved metal ion coordinates with both deprotonated surface hydroxyls and dissolved ligands.
- A dissolved multidentate ligand coordinate with both X and the dissolved metal ion M.

the best description for the potential-charge relations since the surface double layer can be viewed as a planar capacitor. According to Hayes and Leckie (1985) the triple layer

model closely fits both equilibrium and kinetic adsorption data; however, they do not report the effectiveness of other models in fitting their data.

**The adsorption of lead, cadmium, zinc and copper:** Among these metal centers, lead has the strongest tendency to be adsorbed on am-Fe(OH)<sub>3</sub> and α-SiO<sub>2</sub> surfaces, and copper is the cation whose adsorption edge on δ-Al<sub>2</sub>O<sub>3</sub> is at the lowest pH range (Fig. 1.5). A careful literature review by Dzombak (1986) and Dzombak and Morel (1990) confirmed the adsorption pattern observed on am-Fe(OH)<sub>3</sub>. The mass of iron needed in order to obtain complete adsorption of all metals is ten times lower than δ-Al<sub>2</sub>O<sub>3</sub> and 300 times lower than α-SiO<sub>2</sub> (probably since am-Fe(OH)<sub>3</sub> has the largest specific surface area). Moreover, all metals are fully adsorbed on am-Fe(OH)<sub>3</sub> at lower pH values than on other oxides, making am-Fe(OH)<sub>3</sub> one of the most favorable inorganic adsorbents in natural waters along with gibbsite and silica in clay minerals. MnO<sub>2</sub> and TiO<sub>2</sub>, other studied adsorbing oxides, are much less abundant than Fe(OH)<sub>3</sub>, SiO<sub>2</sub> and Al<sub>2</sub>O<sub>3</sub> in most natural systems. It is well known that both iron and manganese form coating on mineral surfaces in soils and in river sediments, which increases their specific surface area (Buckley, 1989).

**Adsorbate concentration and competition effects:** The adsorption edge of a certain metal on a given amount of adsorbent is also a function of the total adsorbate concentration (Davis and Leckie, 1978; Benjamin and Leckie, 1980). Among the transition and post-transition metals, lead adsorption is the most sensitive to total concentration, while cadmium is the least sensitive (Davis and Leckie, 1978; Benjamin and Leckie, 1980, 1982). Therefore, in order to understand the natural behavior of lead, it is important to study lead adsorption at a very low total lead concentration. In addition, it has been pointed out that competition between trace metals on surface sites shifts the adsorption edge of a trace metal with the lowest surface affinity towards higher pH

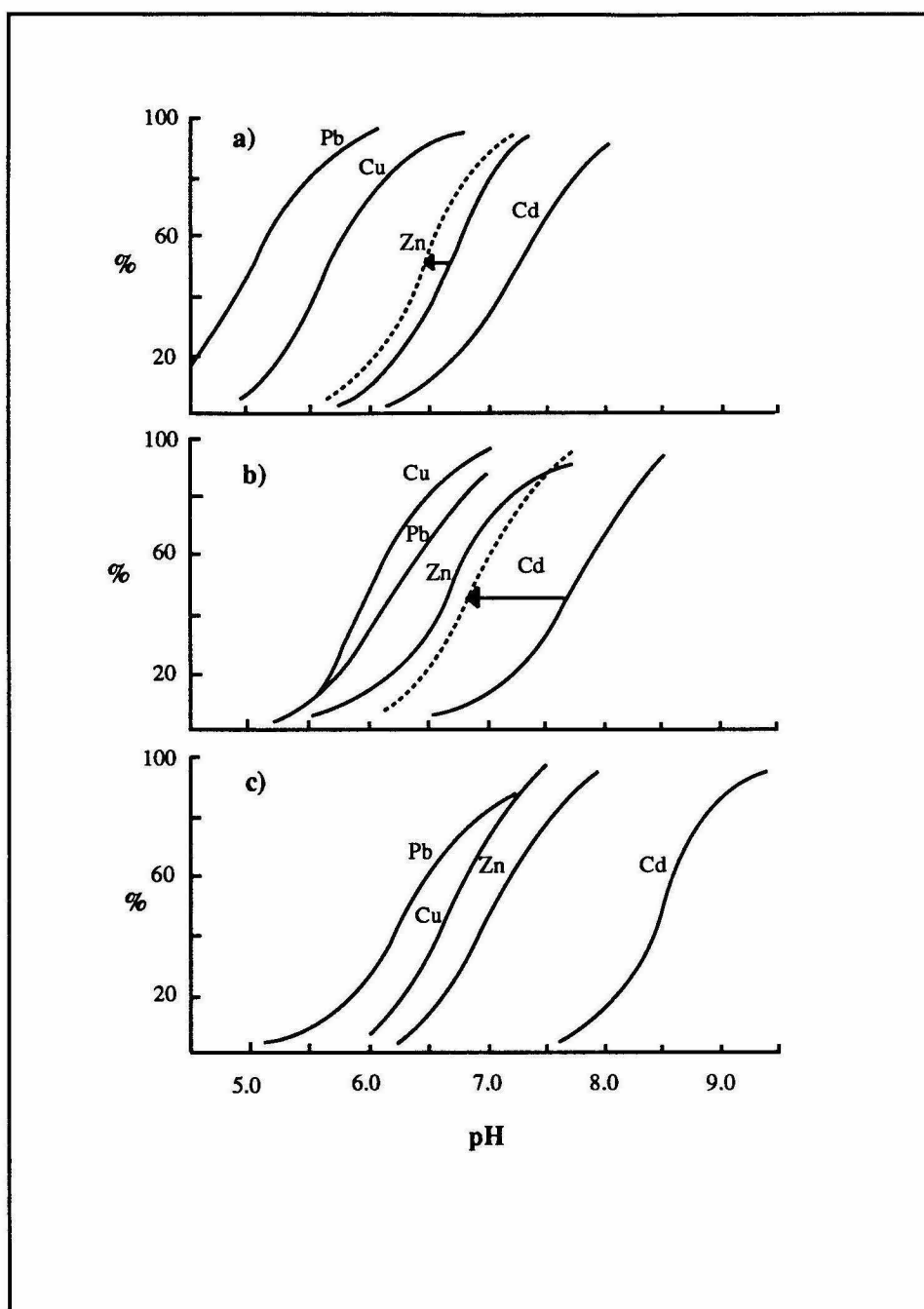


**Figure 1.5:** Fractional adsorption of metals on various substrates. a) 0.1 g/l am-Fe(OH)<sub>3</sub>; b) 1 g/l  $\delta$ -Al<sub>2</sub>O<sub>3</sub>; c) 30 g/l  $\alpha$ -SiO<sub>2</sub>. Solid lines: T.M. conc. = 10  $\mu$ M, dashed lines: T.M. conc. = 0.1  $\mu$ M. (From Salomons and Förstner, 1984; and Leckie et al., 1980.)

values (Benjamin and Leckie, 1980). A minimal effect of a major cation ( $\text{Ca}^{2+}$ ) on the adsorption of zinc on am-Fe(OH)<sub>3</sub> and MnO<sub>2</sub> is reported by Dempsey and Singer (1980). On the other hand, Laxen (1985) reports a substantial decrease of cadmium adsorption on hydrous ferric oxide due to an increase in alkalinity (both  $\text{Ca}^{2+}$  and  $\text{Mg}^{2+}$

concentrations increase). Work done by Huang and Stumm (1973) suggests that among the major cations in water, magnesium is the one with the largest adsorption constant, and therefore the one with the strongest competition effect.

**The effect of complexing ligands:** The effect of inorganic and organic ligands on the adsorption of cations is controlled by the type of complexes they form. If ternary surface complexes are formed, such as between cadmium and  $S_2O_3$  (Benjamin and Leckie, 1982) or between cadmium and humic acid (Laxen, 1985) the adsorption is enhanced. On the other hand, if stable soluble complexes are formed ( $Cd^{2+}$  and  $Cl^-$  or  $SO_4^{2-}$ ; Benjamin and Leckie, 1982;  $Cu^{2+}$  and humic acid; Laxen, 1985) the adsorption decreases. Vuceta (1976) reports a strong competition effect of citrate and EDTA (ethylenediamine tetraacetic acid) on the adsorption of both copper and lead on  $\alpha$ - $SiO_2$ , and Elliot and Huang (1979) describe a strong competition of NTA (nitrilotriacetic acid) with copper on  $\delta$ - $Al_2O_3$  sites.

**Binary oxide particles:** Adsorption experiments of metal ions on binary oxide particles suggest that these particles have different available adsorption sites than single oxide particles, and that the sites of one oxide are either covered with or in competition with the sites of the other oxide (Anderson, 1990; Anderson and Benjamin, 1990a,b). In addition, particle size distributions and surface charges are affected by the interaction between two or more oxides.

**Characteristics of oxy-hydroxide surfaces:** The adsorption constant values decrease with increasing surface coverage mainly for three reasons: (1) surface potential produced by the adsorbed charged species, (2) lateral interaction between adsorbed species, and (3) surface heterogeneities (Schindler and Stumm, 1987). The third factor is probably the most unpredictable. Particles in natural waters have a very wide range of properties such as size distribution, charge densities, shape, degree of organic coating and distribution of surface sites. Even synthetic particles, produced

**Table 1.7:** Surface properties of common particles. Surface area, exchange capacity, pH of zero charge, and site density of synthetic oxy-hydroxide particles (from Scott, 1990). (1) Stumm and Morgan (1981); (2) Davies (1985); (3) Hingston et al. (1971); (4) Hingston (1970); (5) Liang (1988); (6) Battelle (1986); (7) Avotins (1975); (8) Davis (1977); (9) Hohl and Stumm (1976); (10) Huang and Stumm (1973); (11) Young (1982); (12) Yates (1975); (13) Wehrli (1987); (14) Oscarson et al. (1983); (15) McKenzie (1971); (16) Scott (1990).

mineral form	surface area (m <sup>2</sup> /g)	exchange cap. (mmole/g)	site density (OH groups/nm <sup>2</sup> )	Ref.
<b>Iron oxides: pH ZPC = 7 - 8 (1)</b>				
$\alpha$ -FeOOH	34	0.734	13.0	(2)
$\alpha$ -FeOOH	60	0.588	5.9	(3)
$\alpha$ -FeOOH	28	0.31	6.7	(4)
$\alpha$ -Fe <sub>2</sub> O <sub>3</sub>	40	0.316	4.7	(5)
$\alpha$ -Fe <sub>2</sub> O <sub>3</sub>	13	0.216	10.0	(6)
am-Fe(OH) <sub>3</sub>	159	-	-	(7)
am-Fe(OH) <sub>3</sub>	182	2.72	9	(8)
am-Fe(OH) <sub>3</sub>	700	-	-	(8)
am-Fe(OH) <sub>3</sub>	300	-	-	(8)
<b>Aluminum oxides: pH ZPC = 8 - 8.5 (1)</b>				
Al(OH) <sub>3</sub>	31	0.302	5.9	(3)
Al(OH) <sub>3</sub>	58	1.46	15.2	(4)
$\delta$ -Al <sub>2</sub> O <sub>3</sub>	117	0.25	1.3	(9)
$\delta$ -Al <sub>2</sub> O <sub>3</sub>	125	1.66	8.0	(10)
<b>Silica: pH ZPC = 1 - 2 (1)</b>				
SiO <sub>2</sub>	182	1.50	5.0	(11)
SiO <sub>2</sub>	182	0.725	2.4	(11)
<b>Titanium oxide: pH ZPC = 6 (1)</b>				
TiO <sub>2</sub>	20	0.40	12.0	(12)
TiO <sub>2</sub>	50	0.46	5.5	(13)
<b>Manganese oxides: pH ZPC = 4 - 5 (1)</b>				
$\alpha$ -MnO <sub>2</sub>	346	-	-	(14)
$\alpha$ -MnO <sub>2</sub>	58	-	-	(15)
$\alpha$ -MnO <sub>2</sub>	222	-	-	(15)
$\delta$ -MnO <sub>2</sub>	72	2.39	20	(16)

under controlled conditions in the laboratory have a very wide range of properties mainly because of the large range of size distributions (Table 1.7). The surface properties of clay minerals can be viewed as a combination of alumina and silica surface

properties. For example, the ZPC of montmorillonite is 2.2, very close to the ZPC of synthetic silica particles (Table 1.7).

**Organic and biological particles:** Many of the oxide particles present in natural waters are coated by organic film (Hunter, 1980; Stumm and Morgan, 1981; Salomons and Förstner, 1984). Hunter and Liss (1982) demonstrated that most inorganic particles entering the marine environment are rapidly coated with a thin organic film, which alters their surface charge. The adsorption of trace metals on organic surfaces is pH-dependent, probably due to the acid-base properties of the surface carboxylic and phenolic functional groups. However, the adsorption of metal on organic surfaces is less sensitive to pH changes than the adsorption on oxide surfaces (Davis, 1984).

It has been pointed out that microorganisms are capable of concentrating specific metals in the marine environment. While essential elements like zinc and copper are actively accumulated by microorganisms, cadmium is probably being uptake by analogy with zinc (Bruland and Franks, 1983; Boyle, 1988; Morel and Hudson, 1987; Whitfield and Turner, 1987). Coombs (1979) presents a large set of cadmium concentrations in fresh water and in aquatic organisms. According to his data, most microorganisms enrich Cd  $10^3$ - $10^4$ -fold compared with the surrounding water. Those levels of cadmium in organisms are approximately ten times less than its average toxicity level (Wong, 1987). Bradford (personal communication) reports an enrichment factor of about  $10^3$  for cadmium in algae from evaporation ponds at the San Joaquin Valley in California. In addition to ingestion as food, live and dead microorganisms provide surfaces available for metal adsorption (Baudo, 1982). The interaction between microorganisms and metals sometimes have a moderate pH dependence (like other organic particles), which might be related to the fact that cadmium and other trace metals are strongly bound to extra-cellular sulfur groups (Fig. 1.6).

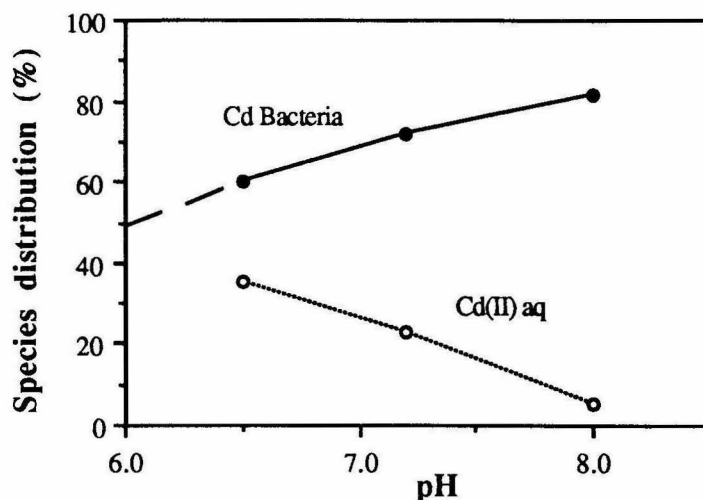


**Figure 1.6:** Cadmium uptake by bacteria surfaces as a function of pH (from Nelson et al., 1981).

#### 1.4.5. Modeling of lead, cadmium, zinc and copper speciation in water, including $\text{Fe}(\text{OH})_3(\text{s})$ surfaces

Table 1.8 gives the speciation of lead, cadmium and zinc in fresh water at pH 6.0 and pH 9.0 and in sea water at pH 8.2 in the presence of am- $\text{Fe}(\text{OH})_3$  particles. The speciation of the metal ions are calculated using the SURFEQL program (Westall, 1980, 1987) with stability constants reported by Smith and Martell (1976) for dissolved complexes and by Dzombak (1986) for surface complexes. The concentration of major components in the water are the ones used by Turner et al.(1981) for their calculations (see Table 1.5). The concentration of total iron is assumed to be  $7.1 \times 10^{-7} \text{M}$  (Taylor and McLennan, 1985), and the concentration of the surface sites is  $1.4 \times 10^{-8}$  (2% of the total iron concentration; Dzombak, 1986). The concentrations of lead, cadmium and zinc are  $1.1 \times 10^{-10} \text{M}$ ,  $8.9 \times 10^{-13} \text{M}$  and  $1.22 \times 10^{-10} \text{M}$ , respectively, calculated from their ratio with iron in the upper continental crust (see Table 1.2). Zinc speciation and lead speciation, even more so, are highly affected by the presence of iron particles in fresh

water both at pH 6.0 and at pH 9.0. In sea water most of the lead is desorbed from the surfaces due to complexation by chloride and carbonate, while most of the zinc remains on the surface. The actual desorption of lead and zinc in the presence of sea water is probably smaller than the model prediction because of other processes such as coagulation and flocculation (see section 4.3.2). Cadmium speciation both in sea water and in fresh water at pH 6.0 is not affected by the presence of iron particles; however, it is moderately affected by the presence of these particles in fresh water at a higher pH.

**Table 1.8:** Model speciation of metal cations with major anions and iron hydroxide surfaces; a) fresh water, pH 6.0; b) fresh water, pH 9.0; c) sea water, pH 8.2. All metal values in percent of total. Calculated with the SURFEQL program (Westall, 1980, 1987). Total concentrations of major anions are given in Table 1.5.

cation	free	OH <sup>-</sup>	F <sup>-</sup>	Cl <sup>-</sup>	SO <sub>4</sub> <sup>2-</sup>	CO <sub>3</sub> <sup>2-</sup>	<FeOH <sup>o</sup>
<b>a) model fresh water, pH=6.0</b>							
Cd <sup>2+</sup>	96	<1	<1	2	2	<1	<1
Pb <sup>2+</sup>	9	<1	<1	<1	<1	2	89
Zn <sup>2+</sup>	61	<1	<1	<1	1	<1	38
<b>b) model fresh water, pH=9.0</b>							
Cd <sup>2+</sup>	32	2	<1	1	1	30	34
Pb <sup>2+</sup>	<1	<1	<1	<1	<1	2	98
Zn <sup>2+</sup>	<1	<1	<1	<1	<1	<1	99
<b>c) model sea water, pH=8.2</b>							
Cd <sup>2+</sup>	3	<1	<1	96	1	<1	<1
Pb <sup>2+</sup>	<1	<1	<1	57	<1	33	9
Zn <sup>2+</sup>	10	<1	<1	<1	4	<1	85

#### 1.4.6. Kinetic consideration

It has been shown by Eigen and Wilkins (1965) that the rate determining step for the reaction between transition metals (e.g. Zn, Cu) or post-transition metals (e.g. Cd, Pb) with protonated and free ligands is the loss of water from the inner coordination sphere. However, the rate of interaction in a more complex environment is also

determined by competition with major cations such as  $\text{Ca}^{2+}$  and  $\text{Mg}^{2+}$ . In sea water (or any high ionic strength solutions), copper tends to bind first to weak ligands, since the stronger ligands are consumed by more abundant  $\text{Ca}^{2+}$  (Hering and Morel, 1988). This mechanism may increase dramatically the time required to reach an equilibrium distribution between strong ligands and metal centers.

From an analogy with solution reactions, the adsorption of trace metals on oxide surfaces probably involves formation of inner sphere surface complexes. It has been noticed that the rate of desorption is generally slower than adsorption (Lion et al., 1982). Schultz et al. (1987) report that lead, zinc and copper adsorption is an irreversible process on the time scale of hours, while for cadmium complete desorption takes place in a shorter amount of time. Hayes and Leckie (1985) suggest that the rate determining step for the desorption of lead from goethite is the breaking down of the surface-inner sphere bond.

### **1.5. Human use of lead and cadmium**

Both lead and cadmium from anthropogenic sources have been extensively emitted into the atmosphere and hydrosphere on a global scale (Salomons and Förstner, 1984; Nriagu, 1989). The ratio between anthropogenic emission and natural emission to the atmosphere is presently 100 for lead, 19 for cadmium, 23 for zinc, and 13 for copper, whereas a relatively unpolluted metal like manganese has a ratio of 0.53 (Table 1.9). Therefore, the contemporary levels of lead, cadmium and other polluted trace metals should far exceed their natural levels in the atmosphere and in the hydrosphere. The degree of lead contamination in the environment has been repeatedly documented (Patterson, 1965; Murozumi et al., 1969; Boyle et al., 1986; Grant, 1986; Patterson and Settle, 1987; Shen and Boyle, 1987; Sturges and Barrie, 1987; Maring et al., 1989). However, the degree of cadmium contamination is less known since there is no isotopic distinction between natural and anthropogenic cadmium, and since cadmium

concentrations in marine waters are largely determined by biological activities (Yeats and Bowers, 1982, 1987; Bruland and Franks, 1983; Boyle, 1988; Morel and Hudson, 1987).

**Table 1.9:** Emission to the atmosphere of lead, cadmium, zinc, copper, and manganese; natural versus anthropogenic sources. Emission in  $10^9$  g/yr. (From Salomons and Förstner, 1984.)

element	natural	anthropogenic	ratio
Cd	0.3	5.5	19
Cu	19	260	13
Mn	610	320	0.53
Pb	4	400	100
Zn	36	840	23

Emission of lead and other metals to the environment by human activities have been going on for the last several thousand years. Usually, an increase of lead production and emission is related to a technological and economical growth, while a decrease in lead emission is related to a period of major economical and political recession (Fig. 1.7). Anthropogenic lead has been accumulating in lake and marine sediments, as well as in polar ice (Murozumi et al., 1969; Shirahata et al., 1980; Ng and Patterson, 1982), reflecting the continued anthropogenic emission (Fig. 1.8). In recent studies, it has been pointed out that levels of lead in the Mississippi sediments, in corals, and in many U.S. rivers have declined during the last fifteen years in response to the decrease in the use of leaded gasoline in automobiles (Trefry et al., 1985; Boyle et al., 1986; Alexander and Smith, 1988). Most of the excess industrial lead has been accumulating in soils and sediments and has been continually released to surface and ground water reservoirs at low rates, as a result of the high affinity of lead for solid surfaces.

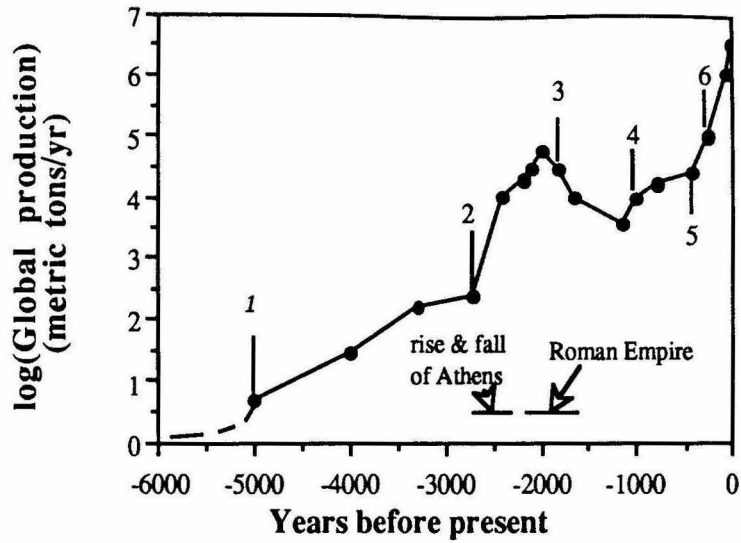


**Figure 1.7:** Production of lead during the last 5000 years, and its relation to major historical events (from Settle and Patterson, 1980). (1) Discovery of Cupellation, (2) use of coinage, (3) exhaustion of Roman lead mines, (4) silver production in Germany, (5) Spanish production of silver in the New World, (6) Industrial Revolution.

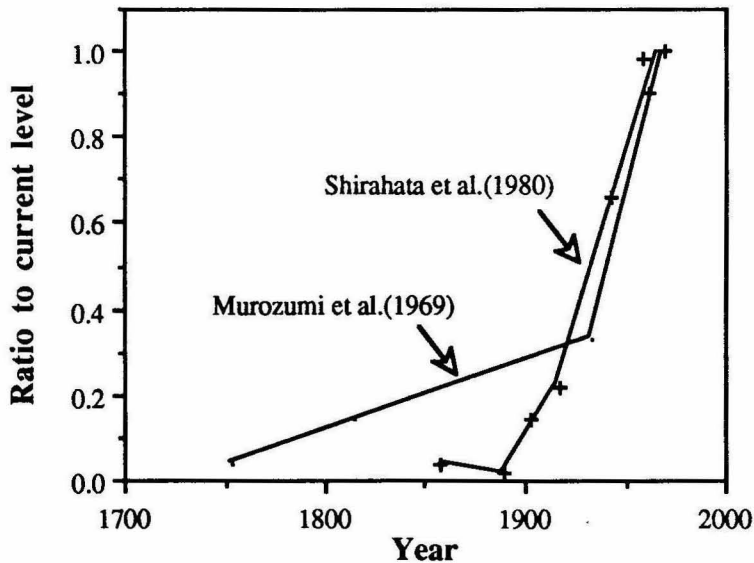


**Figure 1.8:** Amounts of lead in snow strata (Murozumi et al., 1969) and pond sediments (Shirahata et al., 1980) relative to current levels.

In the last few years, concerns have been raised that the release of man-made organic chelators (e.g. nitrilotriacetic acid, NTA; ethylenediamine tetraacetic acid, EDTA; AIS, 1987; Frimmel et al., 1989) may increase the desorption of trace metals from solid surfaces (Salomons and van Pagee, 1981; Dietz, 1982).

### 1.6. Isotopic composition of lead: Systematics of changes during weathering of rocks and minerals

Lead has four stable isotopes:

- 1)  $^{206}\text{Pb}$  (25%) which is the radiogenic daughter of  $^{238}\text{U}$  with a half-life of  $4.7 \times 10^9$  yr,
- 2)  $^{207}\text{Pb}$  (21%) which is the radiogenic daughter of  $^{235}\text{U}$  with a half-life of  $7 \times 10^8$  yr,
- 3)  $^{208}\text{Pb}$  (52%) which is the radiogenic daughter of  $^{232}\text{Th}$  with a half-life of  $1.4 \times 10^{10}$  yr,
- 4)  $^{204}\text{Pb}$  (2%) which is a primordial isotope.

The ratios  $^{206}\text{Pb}/^{204}\text{Pb}$ ,  $^{207}\text{Pb}/^{204}\text{Pb}$ , and  $^{208}\text{Pb}/^{204}\text{Pb}$  are measures of the amount of radiogenic lead in a sample, which in turn is related to the concentrations of uranium and thorium and to the age of the sample. Since  $^{235}\text{U}$  has a short half-life compared with the age of the solar system, only a small fraction is still left in crustal rocks, approximately 1/138 of the  $^{238}\text{U}$  concentration. In rocks younger than a billion years,  $^{207}\text{Pb}$  is not changing much with time since most of the  $^{235}\text{U}$  has already decayed away. Therefore, it is possible to use  $^{207}\text{Pb}$  as a non-radiogenic isotope, just like  $^{204}\text{Pb}$ .

**Magmatic rocks:** Two types of lead are found in magmatic rocks: common lead and radiogenic lead. Common lead is found in minerals whose Pb/U and Pb/Th ratios are very large (mainly sulfides such as galena and pyrite, and in some rock-forming minerals like K-feldspar). The  $^{206}\text{Pb}/^{204}\text{Pb}$ ,  $^{207}\text{Pb}/^{204}\text{Pb}$ , and  $^{208}\text{Pb}/^{204}\text{Pb}$  ratios of common lead measured in K-feldspar are around 18, 15 and 38, respectively (Table 1.10a). Radiogenic lead is found in minerals whose uranium and/or thorium contents are relatively high and the rocks are old enough so that considerable amounts of uranium and thorium have already decayed to produce lead. Many of the radiogenic

minerals have been used for rock dating (zircon,  $\text{ZrSiO}_4$ ; sphene,  $\text{CaTiSiO}_5$ ; apatite,  $\text{Ca}_5\text{FP}_3\text{O}_{12}$ ; pyrochlore,  $\text{NaCa}(\text{Cb},\text{Ta})_2\text{O}_6\text{F}$ ; epidote group,  $\text{Ca}_2\text{Al}_2\text{OHSi}_3\text{AlO}_{12}$ ; monazite,  $\text{CePO}_4$ ; uranium minerals (uraninite,  $\text{UO}_2$ ); allanite, and others). The details of rock dating using U-Th-Pb system is out of the scope of this work; however, the basic concern about rock dating is determining if the minerals have remained as closed systems over time. Values of  $^{206}\text{Pb}/^{204}\text{Pb}$ ,  $^{207}\text{Pb}/^{204}\text{Pb}$ , and  $^{208}\text{Pb}/^{204}\text{Pb}$ , as well as uranium and thorium in some radiogenic minerals, are given in Table 1.10b. Since most of the radiogenic minerals are usually accessory rock minerals, the ratios of  $^{206}\text{Pb}/^{204}\text{Pb}$ ,  $^{207}\text{Pb}/^{204}\text{Pb}$ , and  $^{208}\text{Pb}/^{204}\text{Pb}$  in most whole rock samples are closer to the K-feldspar values than to the radiogenic minerals (Table 1.10c).

**Sedimentary rocks:** Lead isotopic ratios of most Mesozoic and Cenozoic sedimentary rocks are mainly determined by the source rock rather than by the sedimentary rock type. Closed basin sediments which drain Precambrian terrains have highly radiogenic lead and large variability. On the other hand, sediments which drain large areas have uniform, less radiogenic lead values (Doe, 1970).

**Rock and mineral leaching:** It has been observed by many researchers that lead released from both magmatic and sedimentary rocks by leaching with a weak acid or with water is more radiogenic than lead in the whole rock (Chow, 1965; Hart and Tilton, 1966; Shirahata et al., 1980; Silver et al., 1982; Silver et al., 1984; Table 1.10d). Several mechanisms have been proposed to account for the preferential release of radiogenic lead from rocks and minerals:

- 1) Recoil effect: recoil of uranium and thorium atoms because of the release of  $\alpha$  particles during the radioactive decay, which causes damage to the lattice, and makes the decay product more vulnerable to weathering.
- 2) Preferential weathering of radiogenic minerals: It is important to note that some of the most radiogenic minerals in the rock, like zircon and sphene, are among the most

resistant to weathering, while other minerals, like apatite and uraninite, are less resistant to weathering than K-feldspar.

- 3) Release from impurities or minor phases concentrated on crystal surfaces, which contain high concentrations of incompatible elements like uranium and thorium and therefore high concentrations of radiogenic lead.
- 4) Remobilization of uranium during hydrothermal activity, and as a consequence, a high concentration of uranium and its daughters (if the hydrothermal activity took place more than a few millions years ago) along mineral surfaces.
- 5) A combination of some or all of the above processes.

According to Silver et al. (1982), the main mechanism which has released radiogenic lead in the rocks they studied was a preferential weathering of accessory minerals. Other studies (Sturchio et al., 1986; Zielinski et al., 1981) point out that excessive remobilization of uranium took place during hydrothermal events which affected also the distribution of uranium decay products.

Plotting  $^{206}\text{Pb}/^{207}\text{Pb}$  vs.  $^{206}\text{Pb}/^{204}\text{Pb}$  is a measure of the amount of radiogenic lead in a sample. The plot in the  $^{206}\text{Pb}/^{207}\text{Pb}$  vs.  $^{206}\text{Pb}/^{204}\text{Pb}$  plain is usually less scattered than the  $^{206}\text{Pb}/^{204}\text{Pb}$  vs.  $^{208}\text{Pb}/^{204}\text{Pb}$  plot which involves both Th/U ratios and age differences between the various sources. For multisource samples, the  $^{206}\text{Pb}/^{207}\text{Pb}$  vs.  $^{206}\text{Pb}/^{204}\text{Pb}$  plot is also a better presentation than the  $^{206}\text{Pb}/^{204}\text{Pb}$  vs.  $^{207}\text{Pb}/^{204}\text{Pb}$  plot since different sources may be of different ages, thus affecting the shape of the line. Figure 1.9 is an example of the large excess of radiogenic lead released from leaching of plutonic rocks, both Precambrian, uranium-rich rocks and Mesozoic rocks with an average content of uranium.

**Lead isotopes in ore bodies:** There are several genetic types of ore leads: magmatic ores (Butte, Montana; Nelson Batholith, British Columbia), metamorphic ores (The Thackaringa deposits, Australia), and sedimentary ores (Mississippi-Missouri ores). Each type of ore deposit can be divided into subgroups according to

the geological setting, the chemistry and the mineralogy of the ore body. In many cases, lead composition in ore bodies is different than lead composition in the bedrock, and in many (but not all) cases, the ore lead is less radiogenic (Doe, 1970). A summary of  $^{206}\text{Pb}/^{207}\text{Pb}$  ratios of major ore bodies related to lead use in gasoline manufacturing is given in Table 1.11. The low  $^{206}\text{Pb}/^{207}\text{Pb}$  ratios in most ore bodies used for leaded gasoline compared with rock-derived lead, provides a powerful tool to trace mixing of natural (rock-derived) lead with anthropogenic (ore-derived) lead of various sources. Most of the research done so far, using lead isotopes in the environment, focused on atmospheric and marine lead (Tatsumoto and Patterson, 1963; Settle and Patterson, 1982; Flegal and Patterson, 1983; Maring et al., 1987; Patterson and Settle, 1987; Flegal et al., 1989). A few studies of lead isotopes have been done on continental and near-shore sediments (Chow et al., 1973; Shirahata et al., 1980; Ng and Patterson, 1982, Elbaz-Poulichet et al., 1984), and very few studies have been done using lead isotopes in fresh water environments (Elbaz-Poulichet et al., 1986; Elbaz-Poulichet, 1988).

**Table 1.10:**  $^{206}\text{Pb}/^{204}\text{Pb}$ ,  $^{207}\text{Pb}/^{204}\text{Pb}$ , and  $^{208}\text{Pb}/^{204}\text{Pb}$  ratios in rock-forming minerals and common rock types, from Doe (1970): a) K-feldspars; b) radiogenic minerals; c) whole rock (wr) samples (U, Th and Pb in ppm); d) rock leaching. (1) Silver et al. (1984); (2) this work.

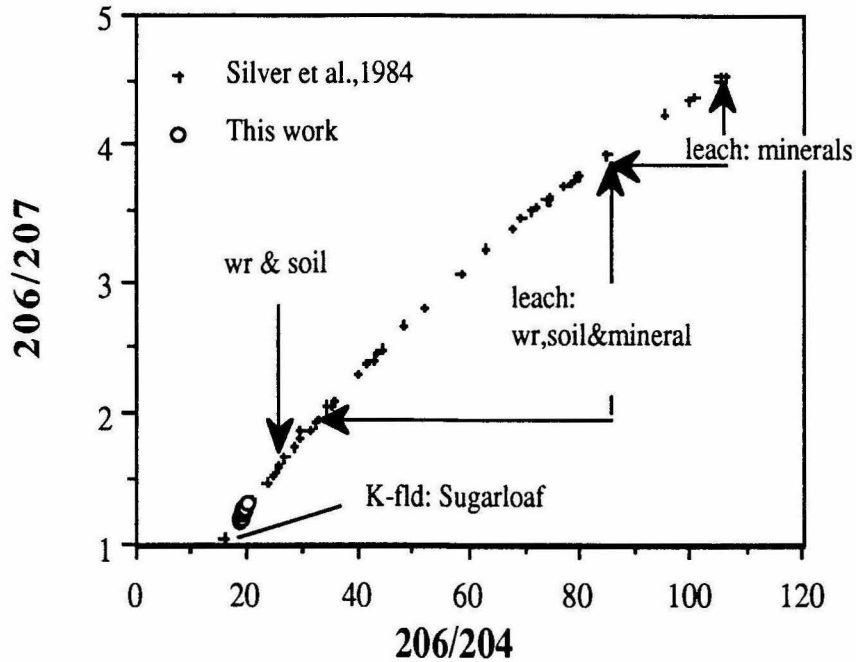
description	$^{206}\text{Pb}/^{204}\text{Pb}$	$^{207}\text{Pb}/^{204}\text{Pb}$	$^{208}\text{Pb}/^{204}\text{Pb}$	U	Th	Pb
<b>a) K-feldspars</b>						
Eldora stock Front Range	17.86	15.49	38.53			
Butte Quartz Monzonite	17.95	15.58	38.19			
Ringing Rocks Pluton	17.96	15.62	38.38			
Unionville Granodiorite	18.02	15.61	38.28			

Table 1.10 cont.

description	$^{206}\text{Pb}/^{204}\text{Pb}$	$^{207}\text{Pb}/^{204}\text{Pb}$	$^{208}\text{Pb}/^{204}\text{Pb}$	U	Th	Pb
<b>b) radiogenic minerals</b>						
3500 m.y. zircon Morton granite	1961	465	147.5	962	-	548
1400 m.y. zircon Leeuwfontein Syenite	516	59.9	163.8	408	415	74.7
1400 m.y. sphene Leeuwfontein Syenite	121.4	24.47	149.5	63.8	230	121.4
1000 m.y. sphene granite along French R. Canada	161.8	26.44	97.2	145.1	-	20.5
allanite Kola Peninsula	30.43	16.41	666.7	0.008	0.66	0.06
1400 m.y. apatite Leeuwfontein suit	38.16	17.6	83.58	20.7	-	28
apatite Tory Hill	31.9	16.3	76.3	90.5	-	136
monazite pegmatoidal granite, Kola Peninsula	364.1	52.3	1011.1	0.65	19.6	3.35
monazite granite gneiss, Little Belt Mnts.	312.5	50.2	3540	0.213	8.84	0.802
<b>c) whole rock</b>						
	<b>1) Precambrian and Paleozoic granites</b>					
3000 m.y. Aldon Shield	14.1	14.87	36.78			
1100 m.y. Essonville	20.25	15.65	48.73			
Paleozoic Rhode Island	18.42	15.63	38.98			
1400 m.y. Lawler Peak (1)	29.84	16.59	39.87	20.9	26.7	35.8

Table 1.10 cont.

description	$^{206}\text{Pb}/^{204}\text{Pb}$	$^{207}\text{Pb}/^{204}\text{Pb}$	$^{208}\text{Pb}/^{204}\text{Pb}$	U	Th	Pb
	<b>2) Cretaceous granodiorite</b>					
88 m.y. Sugarloaf, CA (2)	19.27	15.75	39.6			
88 m.y. Paradise, CA (2)	18.89	15.55	39.08			
<b>d) rock and mineral leaching</b>						
1400 m.y. Lawler Peak whole rock (1)	29.84	16.59	39.87	20.9	26.7	35.8
rock leach, 1M HNO <sub>3</sub> (1)	79.10	21.11	50.89	6.8	10.2	8.5
Qz,feldspar leach, 1M HNO <sub>3</sub> (1)	67.87	20.07	48.76	0.46	1.1	0.2
opaque leach, 1M HNO <sub>3</sub> (1)	105.4	23.43	57.72	22.5	25.3	29.8
88 m.y. Sugarloaf,CA(2)	19.27	15.75	39.6	6.8	28.8	14.7
Sugarloaf leach, 0.1M HNO <sub>3</sub> (2)	20.34	15.34	39.48			0.003



**Figure 1.9:** Systematic of changes in the isotopic composition of lead during rock leaching and weathering. Figure 3.2.3a. gives a more detailed plot of the results from the present study. wr = whole rock.

**Table 1.11:**  $^{206}\text{Pb}/^{207}\text{Pb}$  ratios in selected major lead-bearing ores (from Sturges and Barrie, 1987).

source	$^{206}\text{Pb}/^{207}\text{Pb}$
North Star, B.C.	1.06
Federal Metals, Quebec	1.16
Buchans, Newfoundland	1.15
Flin Flon, Manitoba	1.01
Pine Point, N.W.T.	1.16
Monarch, B.C.	1.19
Brunswick, N.B.	1.16
Keymet, N.B.	1.16
Manitouwadge, Ontario	0.92
Mississippi Valley, Missouri	1.39
Durango, Mexico	1.20
Taxco, Mexico	1.19
Cerro de Pasco, Peru	1.20
San Cristobal, Peru	1.20
Mt. Isa, Australia	1.04
Broken Hill, Australia	1.04

## Chapter 2: Experimental methods

Much of the sampling, preparation and analytical methods described here have been developed in Dr. Patterson's laboratory during the last thirty years. Nevertheless, some new clean sampling techniques have been developed, according to the ideas of Dr. Morgan, which take into consideration speciation and rate of reactions in aquatic media.

### 2.1. Sampling

The low concentrations of lead and cadmium in all samples and of other elements in some water samples required a good control on blank, precision and accuracy of sample collection, preparation, and analysis.

#### 2.1.1. Preparation and precleaning procedures

All of the ware and the reagents used both in the laboratory and in the field were carefully cleaned and checked for blank.

Conventional polyethylene (CPE) bottles were used to collect sample water for lead, cadmium, iron, manganese, aluminum and strontium analyses. They were thoroughly cleaned in a manner described in Appendix 2.1. Millipore filters, filter holders, dialysis bags, digging tools, dust collectors, and rain funnels were thoroughly cleaned in the laboratory before going to the field (Appendix 2.1). Water samples were collected for major cations ( $\text{Na}^+$ ,  $\text{K}^+$ ,  $\text{Ca}^{2+}$ ,  $\text{Mg}^{2+}$ ),  $\text{NH}_4^+$ , dissolved silica, anions ( $\text{Cl}^-$ ,  $\text{NO}_3^-$ ,  $\text{SO}_4^{2-}$ , formate, acetate and oxalate), acid neutralization capacity (ANC) and pH, in linear polyethylene (LPE) containers cleaned according to the procedure described in Appendix 2.1. Samples for total organic carbon (TOC) analysis in water were collected in dark glass bottles which were carefully precleaned to remove any organic contaminant (Appendix 2.1).

**Table 2.1:** Blanks of reagents, ware and procedures. The blanks of the ware are a little different from one set to another, and the blanks of the reagents tend to change from one batch to another. All the values given here represent the current situation in the laboratory.

	Pb blank ng/ml	Cd blank ng/ml	
<b>Reagent</b>			
QDW	0.0002	0.0002	
HNO <sub>3</sub> (NBS)	0.001	0.001	
HNO <sub>3</sub> (Reagent)	1.12	-	
NH <sub>4</sub> OH	0.001	-	
Dithizone	0.011	-	
CHCl <sub>3</sub>	0.0004	-	
Citrate	0.052	-	
CN	0.023	-	
HCl (NBS)	0.001	0.007	
HClO <sub>4</sub> (NBS)	0.018	-	
HF (NBS)	0.012	-	
	Pb blank ng	Cd blank ng	
<b>Ware</b>			
Bottle 1l	0.024	-	
Bottle 2l	0.038	-	
Bottle 30ml	0.005	-	
Extraction bottle w/o Cit	0.005	-	
Extraction bottle w/Cit	0.066	-	
Sep. funnel	0.007	-	
<b>Process</b>			
Evap., 20 ml Qz beaker	0.01	-	
Evap., 250 ml Qz beaker	0.026	-	
Evap., 30 ml FEP beaker	0.005	-	
Filter digestion	0.1	0.1	
Filtration (in Lab)	0.043	-	
Dialysis equilibration	0.184	0.154	
Column separation	0.032	-	
Filament loading	0.003	-	
Tot. extr. w/o Cit & CN	0.04	0.04	
Tot. extr. w/ Cit & CN	0.097	0.083	
lead IC of blank	<sup>206</sup> Pb/ <sup>207</sup> Pb	<sup>206</sup> Pb/ <sup>208</sup> Pb	<sup>206</sup> Pb/ <sup>204</sup> Pb
	1.181±.1%	0.49125±.1%	18.03±.2%

### 2.1.2. Collection sites

From each site, rock, soil, and water samples were collected at the same time, and were delivered to the laboratory with extreme care to avoid contamination. Most of the work was done in an area with granodiorite bedrock, whereas three other sites that have granite, basalt and carbonate bedrocks were used for comparison.

#### 2.1.2.1. Granodiorite site

Samples of stream water, ground water, stream-bed, soil, and rock were collected from Moraine Creek, a small tributary of the Kings River in the central part of the Sierra Nevada, during the fall of 1987, and the spring and fall of 1988 (Fig. 2.1). Moraine Creek drains a region with granodiorite bedrock, composed of the Paradise and the Sugarloaf plutons. The upper part of the stream cuts through the Paradise Granodiorite (83-86 Ma U-Pb age; Chen and Moore, 1982), and the lower part of the stream cuts through the Granodiorite of Sugarloaf (<88 Ma U-Pb age; Chen and Moore, 1982; Moore and Sisson, 1987). The plutons exposed along Moraine Creek have similar mineralogical and chemical compositions but a different lead isotopic composition. Norm calculations of the compositions of the two rocks exposed in the area yield 50% andesine, 20% K-feldspar and 20% quartz (Table 3.2.1). Modal analyses agree with these proportions and, in addition, there is almost 10% biotite and more than 1% hornblende. A common and distinctive feature of the rocks is the occurrence of granoblastic, subhedral plagioclase phenocrysts.

#### 2.1.2.2. Granitic site

Thompson Canyon is located in a remote part on the crest of the Sierra Nevada near the northern border of Yosemite National Park (38°09'N, 119°30'W). Samples of stream water, ground water, soil moisture, soil, and bedrock were collected during the spring of 1986. This site has been intensively studied since the early 1970s as a

pristine ecosystem (Patterson et al., 1973; Hirao and Patterson, 1974; Hinkley, 1975; Elias et al., 1976; Shirahata et al., 1980; Elias et al., 1982).

The canyon is cut into a single granitic pluton (Cathedral Peak) with a relatively uniform mineralogy and chemistry (Table 3.1.1). More than half the canyon surface consists of bare rock, talus and grus which is derived from the granite. Several andesite dikes are exposed in the upper canyon, but their relative contribution to the material in the canyon is negligible (Patterson et al., 1973).

#### **2.1.2.3. Basalt site**

Rock and ground water samples were collected from the Miocene Lower Basalt Formation, Northern Israel (32°44'N, 35°28'E). The bedrock is an alkali olivine basalt with 30-60% plagioclase (mainly labradorite), 14-27% pyroxene, 5-23% olivine, 5-18% ore deposit, and 3-18% vesicular matter (calcite, chlorite, zeolite; Oppenheim, 1959). The Lower Basalt Formation supports local aquifers which are used extensively for irrigation. The spring sampled at this site (Ein Mizrav) is one of the few unspoiled springs in the area, and has been sampled for major ion analyses several times during the last decade. The major ion concentrations obtained in this study were very similar to previous measurements (Sandler, 1981).

#### **2.1.2.4. Carbonate site**

Rock and ground water samples were collected from the Soreq Formation, Central Israel (31°45'N, 35°13'E). The formation is composed of approximately 130 m of stratal, well-bedded dolomites interbedded with shales and marls (Sass and Katz, 1982). The rock has a heterogeneous chemical composition indicated by large variations of Sr/Ca and Na/Ca values. Nevertheless, the Mg/Ca ratios are very constant, ranging from 0.85 (some calcite is present) to 1.01 (Sass and Katz, 1982). The samples collected from the spring vicinity for this study have approximately 1% insoluble

residue, which is in the very low range of concentrations reported by Sass and Katz (1982). The spring sampled in this study (Ein Bikura) is located 15 m above the base of the Soreq Formation, and has been sampled previously by other researchers for major element concentration analyses. The concentrations obtained in this study were similar to previous measurements (Starinsky, personal communication).

#### **2.1.2.5. Minerals**

Mineral separates were provided by L. T. Silver, Caltech. Biotite concentrate (98%±1 pure), containing accessory inclusions (e.g. apatite, sphene, allanite, zircon) was separated from the Jossi Spring Tonalite, located along the northeast flank of Thomas Mountain, Riverside County, California (33°39'N, 116°44'W). The biotite minerals were coarser than 50 mesh. The feldspar sample (77% K-feldspar, 19% plagioclase (albite), 3% quartz, and 1% impurities) was separated from pegmatite bodies intruding into the tonalite in Blair Valley, San Diego County, California (33°01'N, 116°24'W). The feldspar grains were 50-100 mesh.

#### **2.1.3. Collection methods**

Samples for lead, cadmium and other trace metal analyses were collected with care to minimize contamination. The collection methods of stream water, ground water, atmospheric deposition and soil for total lead and cadmium analyses were developed by Patterson and coworkers in Thompson Canyon during the 1970s. The following requirements on water sampling were made:

- 1) Stream and ground water samples to be analyzed for lead and cadmium concentrations and isotopic compositions of lead should be collected before collection of other samples;
- 2) a minimum of two people sample the water;

- 3) both people wear plastic hand gloves, in addition, the main sampler wears shoulder gloves;
- 4) before touching the bottle itself, both the sampler and his helper put on an additional pair of new gloves;
- 5) the keeping solution is to be drained just before the sampling;
- 6) the sample is to be taken from the top third of the water column, away from the sediment, and upstream from the sampler.

The same care was applied to soil, soil moisture and atmospheric deposition collection. In addition to total water samples, filtered and dialysed water samples were collected in the field. This work is the first attempt to combine clean collection techniques at such low concentrations of trace metals with rigorous speciation study; therefore, both the filtration and the dialysis techniques were checked for contamination (Table 2.1).

#### **2.1.3.1. Lake water**

The lake at the top of Moraine Creek was sampled only during the spring, immediately after the major portion of 1988 spring-melt had flowed out of the watershed, but when meltwater from remnants of the 1987-88 winter snowpack was still draining to the lake (Fig. 2.1). Two samples of lake water were collected, one unfiltered (for total measurement) and the other filtered through a 0.45  $\mu\text{m}$  pore diameter Millipore filter.

#### **2.1.3.2. Stream water**

Stream water samples were collected only in Moraine Creek and Thompson Canyon. Stream water samples from Moraine Creek were collected for lead and cadmium analyses and for major cation and anion analyses at stations 1-7 during the fall of 1987, at station 5 during the spring of 1988, and at stations 1-5 during the fall of

1988 (Fig. 2.1). In addition, particles for SEM analysis were collected by filtering stream water through 0.1, 0.2, 0.4 and 2  $\mu\text{m}$  pore diameter Nuclepore filters. Stream water samples were also collected for particle size distribution and for microelectrophoresis measurements. The discharge of the stream was determined at stations 1-5 during the base flow in the fall, and at station 5 during the spring flow (Fig. 2.1). The discharge was computed from the measured velocity (with an Ott current meter) and the cross section area. Stream water samples from Thompson Canyon were collected during the spring of 1986 (Appendix 2.5).

#### **2.1.3.3. Ground water**

Five pits were dug to depths of 50 to 100 cm at stations 1 through 5 in Moraine Creek during the fall of 1988, and in Thompson Canyon during the spring of 1986 (Fig. 2.1). The initial digging was done with acid washed shovels, and the final digging (from 5 cm above the ground water table) was done with acid cleaned stainless steel scoops. Ground water seeped in at depths of between 30 and 70 cm, and the pits were bailed several times before sample collection. In addition, spring waters were collected from the basalt and carbonate sites (winter 1988) and from the upper meadow in Moraine Creek during the fall of 1987.

Stream waters at stations 1, 3, and 5 and ground water at station 4 in Moraine Creek were filtered through a 0.45  $\mu\text{m}$  pore size Millipore filter using a vacuum hand pump (Fig. 2.1). In addition, at the same stations, 1000 molecular weight cutoff (about 1nm) Spectra/Por dialysis bags filled with the purest laboratory water were left in the stream for a few hours. Rate of diffusion, contamination and uptake of metals by the dialysis membrane were checked in the laboratory prior to the use in the field (Appendix 2.2).

#### **2.1.3.4. Soil, rock and stream-bed samples**

Basalt and dolomite samples were collected from the vicinity of each spring (see section 2.1.2). Granodiorite rock samples were collected from two sites in Moraine Creek; Paradise Granodiorite was sampled from an outcrop near station 1 and the granodiorite of Sugarloaf was sampled on the ridge west of Roaring River near station 6 (Fig. 2.1). Soil samples were collected at various depths from the wall of each pit above the ground water table. The samples were collected with care to avoid any cross contamination between shallow and deep layers. Stream-bed samples were collected at stations 1-5 in Moraine Creek, a few meters downstream from the water collection sites (Fig. 2.1).

#### **2.1.3.5. Atmospheric deposition**

Dry deposition samples were collected in Moraine Creek during May 1988 and September 1988 using both dry and wet passive dust deposition collectors. The collectors had a 100 cm<sup>2</sup> collection area and were placed on a stand two meters high. The collection site was near station 1 in an open area, on the crest of Moraine Ridge (Fig. 2.1). A rain sample was collected near station 3, in a relatively open area, during a rain storm in the fall of 1988 (Fig. 2.1).

### **2.2. Sample preparation and experimental procedures**

Much thought and effort was put into reducing the magnitude of changes taking place in water and soil samples between the time of collection and analysis (e.g. separation between particulate matter and solution was done in the field). At the same time, contamination of trace metal samples was controlled and monitored.

### 2.2.1. Stream water and ground water

Samples for trace metal analysis and for measurement of lead isotopic composition were not acidified in the field. They were acidified a few hours before analysis in order to minimize leaching of lead from the walls of the bottles (Maring et al., 1989). Samples for total cation analysis, dissolved silica,  $\text{NH}_4^+$  and for  $\text{Fe}^{2+}$  determination were acidified in the field, those for  $\text{Fe}^{2+}$  analysis were also kept in the dark. Samples for anion analysis were spiked in the field with chloroform in order to avoid any bacterial activity between sampling and analysis. Samples for TOC measurements were spiked with a 50  $\mu\text{l}$  saturated solution of  $\text{HgCl}_2$  for the same reason. All samples were kept in the dark at  $4^\circ\text{C}$  prior to analysis.

Three different preparation schemes were applied for both stream and ground water samples: 1) acidification ( $\text{pH}=1.0$ ), 2) filtration followed by acidification, and 3) digestion with aqua regia (mainly for lead and cadmium analyses in order to compare the  $\text{pH}=1$  "total" value with the conventional total value after digestion). Only the particulate matter collected on the filters was analyzed for lead and cadmium, since the filtrate, under field conditions, was too contaminated. The filters were digested with a mixture of  $\text{HNO}_3$  and  $\text{HClO}_4$  acids, and the amounts of lead and cadmium on the particles were determined directly (Appendix 2.3). Other elements were measured both in the filtered water and in the particulate matter. During the adsorption laboratory experiments an improved filtration apparatus was used, which enabled me to analyze lead and cadmium in solution after filtration (Table 2.1). Lead and cadmium from lake water, atmospheric deposition, stream water, and ground water samples for concentration and isotopic composition measurements were extracted using the dithizone (diphenylthiocarbazone) method (Appendix 2.3). The yield of the extraction process was checked by double spiking. The yield of both lead and cadmium extraction was always larger than 90%. The amount of contamination involved with each step of sample acquisition and with reagent and ware was determined for both lead and

cadmium. The total amount of contaminated lead and cadmium introduced to a water sample during its processing (not including filtration) was 40-100 pg (Table 2.1).

Some researchers claim that our laboratory has reported such low concentrations of lead because we have been failing to analyze a large fraction of the lead present in the sample (Jaworowski et al., 1983). An experiment was designed in order to verify a complete recovery of lead from water samples. A known amount of lead salt was added to a water sample, then the sample was spiked, and the lead was extracted and analyzed. The measured lead concentration was less than a percent different from the actual value.

### **2.2.2. Soil, stream-bed and rock samples**

One portion of rock sample was ground to 200 mesh size and homogenized, and another portion was sawed for thin sections preparation. Ground rock and soil samples were dissolved for total chemical analyses using the  $\text{LiBO}_2$  technique described by Feigenson and Carr (1985). Soil and stream-bed samples were dried at  $60^\circ\text{C}$  upon arriving at the laboratory and sieved through acid cleaned polyethylene 2 mm sieves. Then, the samples were homogenized and a portion was ground to 200 mesh size. In addition, soil samples for exchangeable cation analysis (Thomas, 1982), free hydroxide-oxide analysis (using dithionite; Mehra and Jackson, 1960), particle size distribution (Gee and Bauder, 1986), organic carbon content (Nelson and Sommers, 1982), and pH determination (Richards, 1954) were prepared for analysis at the Department of Soil and Environmental Sciences, University of California, Riverside. A few soil and rock samples were leached with a solution at  $\text{pH} = 1$ . The amount of iron released by leaching with  $\text{pH} 1$  solution for six days was roughly equivalent to the amount released by the dithionite method (Thomas, 1982) from soil samples and was three times the amount released by the dithionite method from rock samples (Table 3.2.4).

Rock and soil samples were dissolved for lead and cadmium analysis according to the method described in Appendix 2.3. Dissolved rock and soil samples (in 1.0M

HCl solution) for lead and cadmium analyses were passed through a Bio-Rad, AG-1 (mesh 200) resin in a quartz column prior to the dithizone extraction. The total contamination of lead and cadmium analyses was 250-500 pg.

### **2.2.3. Leaching experiments**

Rock and soil samples collected from the sites described above were used for leaching experiments. Rock samples were leached with 0.1M HNO<sub>3</sub> acid, followed by measurements of lead, iron and other components in the leached phase. The leaching experiments were combined with analysis of natural water samples collected in the same sites in order to examine the relations between lead and iron upon their release from rock and soil minerals.

Granodiorite and basalt rock samples were ground to 200 mesh size before leaching, while the biotite and feldspar separates were coarser. Large pieces of dolomite samples were washed with double distilled water before the acid dissolution, in order to reduce possible contamination of the carbonate fraction, where the lead content is relatively low. Known amount of the dolomite samples were dissolved with a 10% HCl. The residue was collected on a filter, dried and weighted. Soil samples were dried and passed through a 2 mm sieve immediately upon getting to the laboratory. Some soil samples were split into three fractions: 1) soil samples which were passed through a magnetic separator (Franz) and were examined under a binocular microscope to remove iron-rich minerals from the feldspar-quartz fraction (therefore, most of the iron released came from mineral coating in the sample), 2) soil samples which were ground to 200 mesh before leaching, and 3) a fraction that was leached without any treatment except for initial drying and sieving through a 2 mm screen.

#### 2.2.4. Adsorption experiment

Two aliquots of biotite (1g each; > 50 mesh) from Jossi Spring Tonalite were leached with 1.5 liters of 0.1 M HNO<sub>3</sub> solution (pH 1) to provide the initial composition of the solution for the experiment (Table 1). Biotite has high concentrations of Fe, Al, Si and Mg which has the highest tendency among the major alkali earth cations to be adsorbed on oxide surfaces (Huang and Stumm, 1973). A low pH solution was used in order to avoid any precipitation of iron hydroxides during the leaching process. The samples were kept at 25°C, in contact with the atmosphere, and were agitated for two hours every day. After thirty days, when iron levels in the solution were high enough to prevent a substantial dissolution of Fe(OH)<sub>3</sub>(s) above pH 4, the solids were separated from solution by filtration through a 0.45 µm pore size Millipore filter, using a mechanical vacuum pump. An aliquot of 30 ml was taken for determination of solution composition, including lead concentration and isotopic composition (Table 1). The pH of the solution was then raised with purified NH<sub>4</sub>OH to pH 8.5. NH<sub>4</sub>OH rather than NaOH solution was used because of its low lead blank, although there was a risk of formation of lead-ammonium complexes in solution. The base was added in small increments and the whole process of base addition took approximately 30 minutes. Upon raising the pH, light-scattering particles started to form, and at pH 8.5 the particles had a brown color, typical of some iron hydroxides. The solution was left at 25°C in contact with the atmosphere for ten days to stabilize the particles and to make sure that the adsorption of lead on the particles reached equilibrium (Benjamin and Leckie, 1981; Schneider and Schwyn, 1987; Combes et al., 1989). An aliquot of about 100 ml for X-ray diffraction analysis was taken, and then a <sup>208</sup>Pb spike (99.7427% <sup>208</sup>Pb, 0.2006% <sup>206</sup>Pb and 0.0567% <sup>207</sup>Pb) was added and left to equilibrate with lead in the solution for two days. The pH was lowered to 6.0, 5.2, 4.5 and 3.5 using HNO<sub>3</sub> acid. The time required for the desorption process to reach an equilibrium was monitored at each step. At least seven days passed before the

desorption process reached equilibrium (Hayes and Leckie, 1985; Schultz et al., 1987). At each step, 30 ml of the sample were filtered through a 0.025  $\mu\text{m}$  pore size Millipore filter (Table 1). The particles collected on the filters were examined with a scanning electron microscope and on an X-ray diffraction analyzer. The solution was then analyzed for lead, iron, aluminum, manganese, dissolved silica, calcium, magnesium, sodium, and potassium concentrations (Table 2). Two kinds of lead were present in the solution, the first one derived from the biotite and the second added as a spiked lead.

### **2.2.5. Desorption experiment**

A portion of the solution obtained from the biotite leaching was used for desorption experiments. The pH of the solution was raised to 8.5 as described in the previous section. After the particles stabilized, spiked lead was added and the system was left to equilibrate. One milliliter of the spiked solution was diluted 1000 times with a  $1.15 \times 10^{-7} \text{M}$  EDTA solution (solution blank,  $3.6 \times 10^{-11} \text{M Pb}$ ), and another milliliter was diluted 1000 times with deep ocean water (sea water blank,  $1.9 \times 10^{-11} \text{M Pb}$ ). After thirty days, 30 ml of each solution was filtered through a 0.025  $\mu\text{m}$  pore filter and analyzed (Table 1).

## **2.3. Analysis**

All instruments used for analysis were calibrated before any quantitative measurement, and were cross checked by running interlaboratory and NBS standards.

### **2.3.1. Water, rock and soil samples**

Concentrations of lead and cadmium were determined by the isotope dilution mass spectrometry (IDMS) technique, using  $^{116}\text{Cd}$  and  $^{208}\text{Pb}$  spikes. The spikes were regularly checked against known NBS standards. A multicollector VG-Sector solid-source mass spectrometer was used for concentration and isotopic composition

determination (Appendix 2.4). The mass spectrometer had a limit of detection of approximately  $5 \times 10^{-15}$  M lead and cadmium and a standard deviation (STD) of approximately 0.1% for isotopic ratio measured with Faraday Cups ( $5 \times 10^{-13}$  < beam <  $10^{-10}$  amp), and STD of 0.5-1.0% for isotopic ratios measured with a Daly multiplier (beam <  $5 \times 10^{-13}$  amp).

Na, K, Ca, Mg, Al, dissolved silica, Fe, Mn and Sr were analyzed with an ARL SpectroSpan VB direct current plasma (DCP) spectrometer. The lower linearity ranges of the instrument used were: 2.6, 4.1, 1.3, 0.4, 1.9, 3.6, 0.9, 0.9, and 0.1  $\mu\text{M}$ , respectively (Appendix 2.4). The DCP had STD of at the most 10% for stream water and ground water samples and 2-5% for soil and rock samples. Samples with low concentrations of Fe, Mn, Al and Sr were analyzed with a 3030 Perkin Elmer Graphite Furnace atomic absorption spectrometer (detection limits: 0.02, 0.002, 0.2, and 0.01  $\mu\text{M}$ , respectively), with a STD of 20%.

### 2.3.2. Water samples

Only stream water and ground water samples were analyzed for anion and  $\text{NH}_4^+$  concentrations.  $\text{Cl}^-$ ,  $\text{NO}_3^-$ ,  $\text{SO}_4^{2-}$ , oxalate, formate, and acetate were analyzed with a Dionex 2020i Ion Chromatograph (limit of detection =  $1 \mu\text{eq/l}$ , CV = 10%).  $\text{NH}_4^+$  was measured by the phenol-hypochlorite method (Solorzano, 1967) using an Alpkem flow injection analyzer.  $\text{Fe}^{2+}$  in stream and ground water was measured within a week of sampling.  $\text{Fe}^{2+}$  was determined with the ferrozine method described by Stookey (1970) and Carter (1971), using an HP 8452 Diode Array Spectrophotometer (a limit of detection of  $5 \times 10^{-8}$  M). In order to detect possible changes in the amount of  $\text{Fe}^{2+}$  during its storage, five random samples were measured twice: once a week after the field sampling and then one week later. There was up to 20% difference between the two measurements, indicating that the reported  $\text{Fe}^{2+}$  values have at least a  $\pm 20\%$  uncertainty. TOC in stream water was measured with a Rertex Dohmann Carbon

Analyzer with a Horiba PIR 2000 CO<sub>2</sub> IR detector (detection limit 1mg/l). The pH of stream water and ground water samples was measured in the field with a VWR digitized mini pH meter. The pH of the solution in the adsorption-desorption experiments and of stream water and ground water samples (in the laboratory) was measured with a Radiometer PHM 80 standard pH meter with a GK2320c semi-micro combination electrode. ANC of stream water and ground water samples was determined (in the laboratory) by titration with a 0.01M HCl using the Gran Method (Stumm and Morgan, 1981; Butler, 1982).

Particle size distribution analyses of stream water samples were carried out by a Photon Correlation Spectroscopy (PCS) method with a sub-micron particle analyzer, Malvern 4700M/SM. One sample was also analyzed with a Coulter counter (model TAU) to determine size distribution of particles larger than three microns. Electrophoresis measurements of particles in one sample of stream water were done with a Particle Micro-Electrophoresis instrument (Mark II, Rank Brothers). Gold-plated filters with particles collected from stream water and from the adsorption experiment solution were examined using a CamScan scanning electron microscope at 15 kV. A Tracor Northern 5500 energy dispersive spectrometer system was used for qualitative chemical analysis of the particles. X-ray diffraction analyses of the particles formed in the adsorption experiment were done on a Scintag PADv automated  $\theta/2\theta$  goniometer stage X-ray diffractometer.

### **2.3.3. Soil, stream-bed and rock samples**

Organic carbon in soil was measured with a modified Coleman Nitrogen Analyzer. The pH of water-saturated soil samples was measured in the laboratory using an Orion 811 pH meter with Ross combination glass electrode. The available P in soil samples was determined by the sodium bicarbonate extraction method (Nelson and

Sommers, 1982), while phosphate in rock samples was determined with the DCP (CV of 10%).

Thin sections of fresh and weathered rock samples were examined for qualitative mineral identification and to detect mineral alteration. Dry, sieved soil minerals immersed in a 1.542 refractory index oil were examined under a petrographic microscope to determine the degree of iron coating. The same sample was examined after mineral separation with a magnetic separator (Franz) and after leaching with a pH 1 solution for six days.

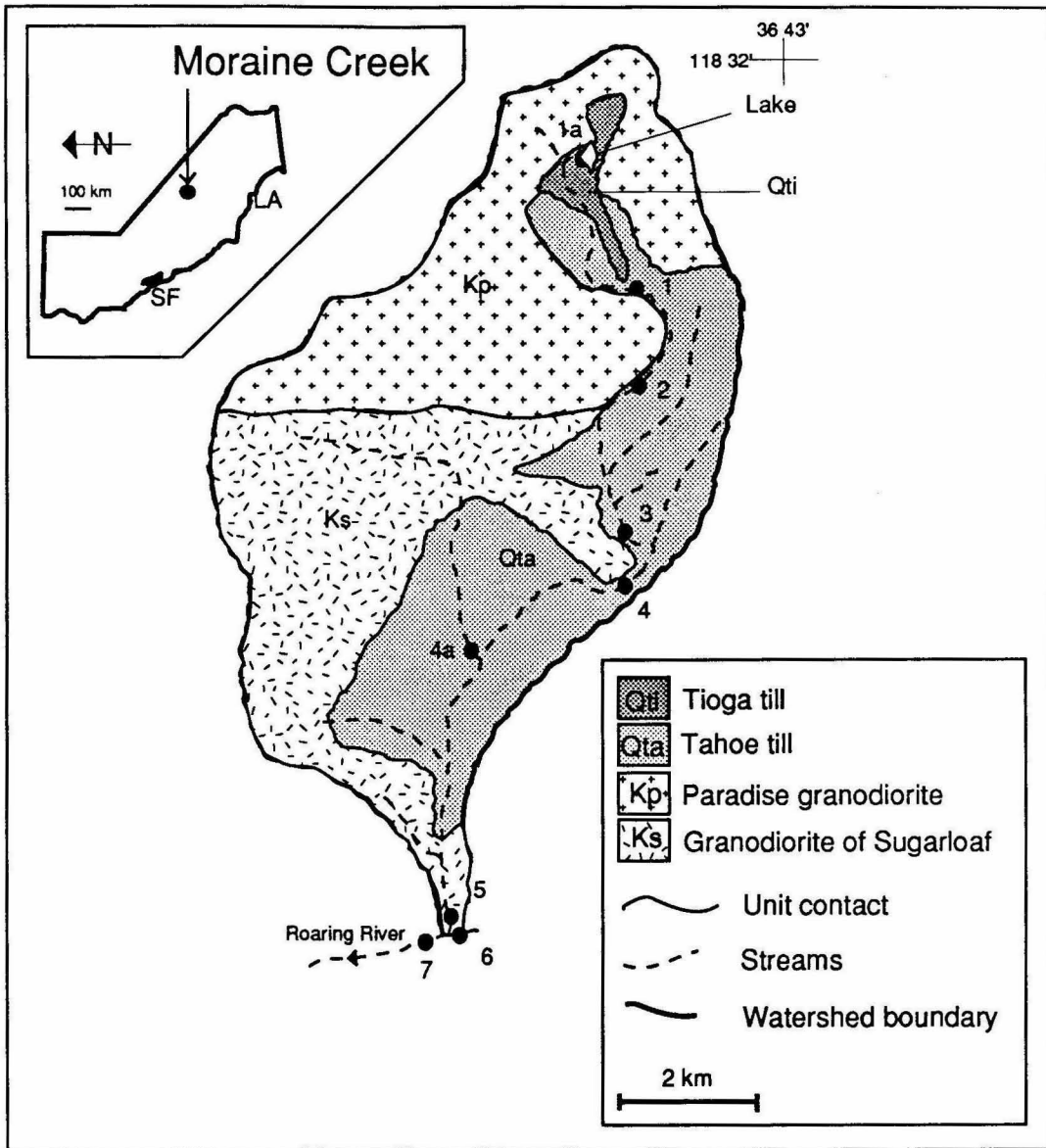


**Figure 2.1:** A map of the Moraine Creek drainage area and the location of the sampling stations.

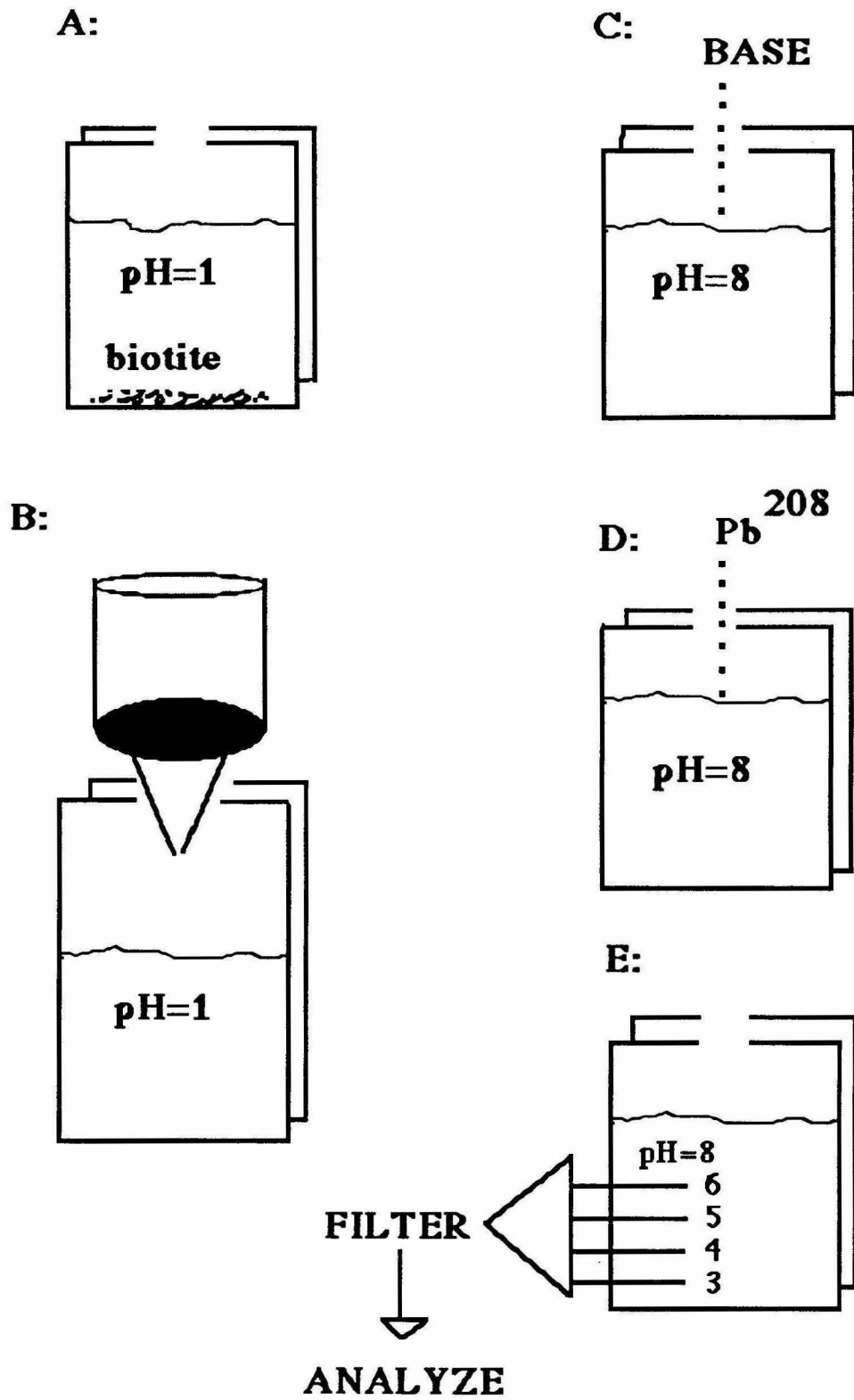


Figure 2.2: Schematic description of the adsorption experiment.

## Appendix 2.1: Precleaning of field and laboratory ware

### 1. Water bottles

Narrow mouth, conventional polyethylene (CPE) bottles have been found to be the least contaminating type of water container. 30 ml, 1000 ml and 2000 ml bottles were used to sample water for lead, cadmium, iron, manganese, aluminum and strontium analyses. These bottles were precleaned in the following manner:

- 1) rinsing with triple distilled water (TDW)
- 2) rinsing with a reagent grade chloroform
- 3) rinsing the chloroform with TDW until no chloroform was detected
- 4) soaking in 25% reagent grade  $\text{HNO}_3$  at  $55^\circ\text{C}$  for three days (1<sup>st</sup> bath)
- 5) rinsing 4 times with quadruple distilled water (QDW)
- 6) soaking in 0.1% NBS  $\text{HNO}_3$  at  $55^\circ\text{C}$  for three days (2<sup>nd</sup> bath)
- 7) rinsing 4 times with QDW
- 8) soaking in 0.1% NBS  $\text{HNO}_3$  at  $55^\circ\text{C}$  for three days (3<sup>rd</sup> bath)
- 9) soaking in 1<sup>st</sup> bath for an hour
- 10) rinsing 4 times with QDW
- 11) soaking in 2<sup>nd</sup> bath for three days
- 12) rinsing 4 times with QDW
- 13) soaking in 3<sup>rd</sup> bath for three days
- 14a) rinsing plastic bags, three per bottle. The inner-most bag is acid washed on both sides (reagent grade) and then washed with QDW; the 2<sup>nd</sup> bag is acid washed on the inside only and with QDW on both sides; and the outer bag is washed with TDW water only
- 14b) drying the bags
- 14c) soaking rubber bands in sodium-free liquid soap
- 14d) rinsing the bands with TDW
- 14e) soaking the bands in dilute reagent grade acid for a day

- 14f) rinsing the bands with TDW and with QDW and drying under cover
- 15) rinsing the bottles 4 times with QDW
- 16) filling the bottles with QDW and 0.1% NBS HNO<sub>3</sub>
- 17) wrapping each bottle with the three plastic bags

The whole process of bottle cleaning took more than two weeks, and approximately 18 bottles were cleaned simultaneously.

60 ml linear polyethylene bottles for major cation (Ca<sup>2+</sup>, Mg<sup>2+</sup>, Na<sup>+</sup>, K<sup>+</sup>), dissolved silica, NH<sub>4</sub><sup>+</sup> and Fe<sup>2+</sup> analysis were passed through stages 1 to 7. All bottles were then filled with QDW and transported to the field in water-washed plastic bags.

60 ml linear polyethylene bottles (LPE) for major anion analysis (Cl<sup>-</sup>, NO<sub>3</sub><sup>-</sup>, SO<sub>4</sub><sup>2-</sup>, formate, acetate, and oxalate), acid neutralization capacity (ANC) and pH measurements were rinsed several times in TDW, filled with TDW, and then were transported to the field in water-washed plastic bags.

30 ml brown glass bottles were used for TOC analysis. The bottles were soaked in concentrated HNO<sub>3</sub> at 55°C overnight, rinsed in TDW, and were put in the oven at 400°C for four hours. The caps were cleaned in dilute HNO<sub>3</sub> and thoroughly washed with TDW, and then were dried in a 55°C oven. The bottles were transported dry to the field.

## **2. Millipore filters, filter holders and dialysis membranes**

Two types of Millipore filters were used: (1) 0.45 μm mixed cellulose acetate and nitrate, 47 mm diameter filters, and (2) 0.025 μm mixed cellulose acetate and nitrate, 47 mm diameter. The 0.45 μm filters were used in the field since the field hand pump did not produce the vacuum needed for the 0.025 μm filters, and since I wanted to compare my results with "dissolved" (<0.45μm) values reported in the literature. Both filter types were cleaned in the following manner:

- 1) 10 -12 filters of the same kind and from the same box are put in a 150 ml teflon FEP beaker
- 2) laying a teflon disk on the filters
- 3) adding 30 ml of 10% NBS HF solution slowly, so the teflon disk remains floating and the filters are not pressed together
- 4) overnight on a 55°C hot plate, covered
- 5) pouring the HF solution and washing the filters 5 times, 30 ml QDW each time
- 6) checking the pH with a pH paper (around 5 after the 5<sup>th</sup> wash)
- 7) adding 30 ml 10% NBS HCl solution slowly
- 8) overnight on a 55°C hot plate, covered
- 9) pouring the HCl solution and washing the filters 5 times, 30 ml QDW each time
- 10) checking the pH with a pH paper (around 5 after the 5<sup>th</sup> wash)
- 11) repeating stages (7-10) 2 more times, each time in clean solution
- 12) drying the filters undercover and weighing

Note: The handling of the filter was done with acid wash tweezers. One filter from each batch was analyzed for blank. Both types of filters were used in teflon PFA filter holders with 300 ml PFA funnel. The filter holders and the CPE tubes were cleaned in the following way:

- 1) disassembling the filter holders
- 2) the tubes were treated the same way as the CPE bottles
- 3) the filter holders were cleaned using the same process as for the CPE bottles except that the first bath has concentrated HNO<sub>3</sub>
- 4) assembling the filter holders, and wrapping in plastic bags (cleaned like the ones used for CPE bottles).

The dialysis bags used for this study were Spectra/Por 7 (1000 molecular weight cutoff) wet tubing. The bags were cleaned in the following way:

- 1) rinsing 3 times with QDW, approximately 100 ml each time

- 2) soaking in a 1% NBS HCl overnight at 55°C
- 3) rinsing 3 times with QDW, approximately 100 ml each time
- 4) checking the pH with a pH paper, (around 5 after the 3<sup>rd</sup> wash)
- 5) soaking in a 0.1% NBS HCl overnight at 55°C
- 6) rinsing 3 times with QDW, approximately 100 ml each time
- 7) checking the pH with a pH paper (around 5 after the 3<sup>rd</sup> wash)
- 8) repeating steps 5-7 four more times, each time soaking in a new, clean solution
- 9) wrapping in clean plastic bags. The innermost bag is cleaned like a CPE bottle

Note: QDW was added to the wrapped dialysis bags, to prevent drying. Bag closures were first soaked in 25% HNO<sub>3</sub> to remove any color and then were cleaned like CPE bottles.

### **3. Atmospheric deposition collectors**

Dust collectors, both the dry and the wet collector, were made of CPE and were cleaned and transferred to the field as the CPE bottles were.

Rain collector was made of a bottle and a funnel, both were cleaned and were transferred to the field like the other CPE bottles.

### **4. Digging tools and plastic bags for soil and rock samples**

Digging tools (stainless steel scoops and spatulas) were cleaned in the following way:

- 1) rinsing with TDW
- 2) soaking in 25% reagent grade HNO<sub>3</sub> for a few minutes
- 3) rinsing with QDW
- 4) drying and wrapping with plastic bags and rubber bands (cleaned as the CPE bottles bags were).

Shovels used for the first part of the digging were acid washed and then rinsed with TDW.

## 5. Laboratory ware

The ware used for trace metal analysis was made only of teflon, ultra pure quartz and CPE, and was cleaned as follow:

- 1) rinsing 4 times with TDW
- 2) soaking in a concentrated reagent grade  $\text{HNO}_3$  at  $55^\circ\text{C}$  for a few hours (1<sup>st</sup> bath)
- 3) rinsing 4 times with QDW
- 4) soaking in 0.1% NBS  $\text{HNO}_3$  at  $55^\circ\text{C}$  overnight (2<sup>nd</sup> bath)
- 5) rinsing 4 times with QDW
- 6) soaking in 0.1% NBS  $\text{HNO}_3$  at  $55^\circ\text{C}$  overnight (3<sup>rd</sup> bath), and leaving in the 3<sup>rd</sup> bath.

Note: 1) CPE ware was put in 25% reagent grade  $\text{HNO}_3$  instead of the concentrated  $\text{HNO}_3$ . 2) Upon switching from one set of samples to another set, all the CPE ware was replaced and extra cleaning steps were applied to the quartz and teflon ware.

quartz ware was cleaned as follows:

- a) soaking overnight in an extra bath of concentrated  $\text{HNO}_3$  before the 1<sup>st</sup> bath
- b) soaking in QDW bath overnight
- c) rinsing 4 times with TDW
- d) soaking in 1<sup>st</sup> bath, and proceeding from stage 3

teflon ware was cleaned as follows:

- a) soaking overnight in a 5% HF (reagent grade) bath
- b) soaking in QDW bath overnight
- c) rinsing 4 times with TDW
- d) soaking in an extra bath of concentrated  $\text{HNO}_3$  overnight
- e) soaking in QDW bath overnight

f) rinsing 4 times with TDW

g) soaking in 1<sup>st</sup> bath, and proceeding from stage 3

## 6. Reagents

The **acids** used in this study for clean work were NBS acids. A blank was determined from each bottle of a new acid, and the acid was titrated to determine its molarity.

Reagent grade **chloroform** ( $\text{CHCl}_3$ ) was cleaned before use by washing with 10% HCl (reagent grade). The acid washed chloroform was washed with QDW and then distilled three times in a quartz distillation unit.

**NH<sub>4</sub>Cit** and **KCN** salts were dissolved in QDW and then were cleaned by 4 consecutive extractions with chloroform and dithizone. After each of the first 3 extractions, the pH was lowered with NBS HCl, and the mixture was left for a few hours.

The column **resin** (Bio-Rad, AG-1) was cleaned by soaking and washing with 6 M HCl. A reagent grade HCl was used for the first 3 washings, and NBS HCl was used for the final 2 soakings and washings.

**NH<sub>4</sub>OH** was prepared by bubbling ultra pure ammonia gas through QDW. **Dithizone** was dissolved in clean chloroform, then it was washed several times, first with an alkaline solution (QDW and  $\text{NH}_4\text{OH}$ ) and then with an acidic solution (QDW and  $\text{HNO}_3$ ). The final solution was evaporated to dryness.

## Appendix 2.2: Dialysis membrane calibration

The dialysis bags, Spectra/Por 1000 molecular weight cutoff (1000 MWCO) membrane (about 1nm pore size), were checked in the laboratory for the following:

1) the time required to reach a steady state across the membrane wall, 2) contamination of lead and cadmium involved with the dialysis process, and 3) possible uptake of metals by the membrane (Benes and Steinnes, 1974). The process of dialysis is not solely diffusion controlled, since there is an upper limit to the amount of a certain element which can cross the membrane. According to Truit and Weber (1981), the upper limit of cadmium transfer through a 1000 MWCO membrane is  $7.8 \times 10^{-8}$  M per hour. They also report that the rate of Cd transfer is four times higher than Cu. The higher Cd transfer rate cannot be explained by diffusion per se, since  $\text{Cu}^{2+}$  has a smaller ionic radius than  $\text{Cd}^{2+}$  and, therefore, based on the Stokes-Einstein equation, has a higher diffusivity. Since the transfer through the membrane is also dependent on interaction of certain aqueous species with the dialysis membrane, Truit and Weber (1981) suggested that certain copper species preferentially interact with the membrane. Therefore, it is very difficult to predict the rate of material transfer through a dialysis membrane (especially in natural waters), and the rate of lead and cadmium transfer was determined experimentally, using Moraine Creek stream water samples. It was found that both lead and cadmium reached constant concentrations in the bag within two hours (Fig. 2.3). Approximately  $3 \times 10^{-11}$  M Cd passed through the membrane in two hours, much less than the upper limit reported by Truit and Weber (1981), and the amount of Pb was even lower ( $2 \times 10^{-11}$  M). The amount of contamination involved with the dialysis process was  $9 \times 10^{-13}$  M for lead and  $10^{-12}$  M for cadmium. By controlling the concentrations of both metals and the amount of water evaporated during the experiment it was estimated that 10-20% of the dissolved metals were adsorbed onto the membrane walls.

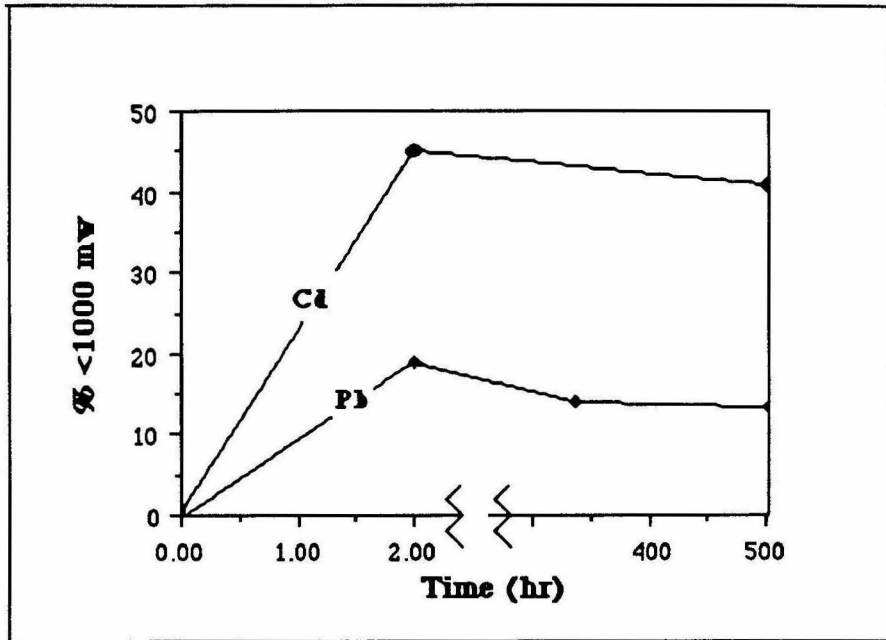


**Figure 2.3:** Rate of lead and cadmium transfer through a 1000 MWCO dialysis membrane.

### **Appendix 2.3: Digestion, extraction and separation techniques**

The techniques used in this study were developed and presented by Patterson and Settle (1976), and Settle and Patterson (1982).

#### **1. Digestion of filters and organic matter**

- 1) weigh a dry sample in a quartz dish (add spike to IDMS sample)
- 2) add 2 ml NBS HNO<sub>3</sub>, 0.3 ml NBS HClO<sub>4</sub> and cover
- 3) let equilibrate and start evaporating
- 4) when bubbling ceases remove the cover
- 5) evaporate to dryness and, if necessary, add more HNO<sub>3</sub> until the residue is fully oxidized
- 6) add 0.1-0.3 ml Cit, 0.1-0.3 ml CN, and 4 ml of QDW and extract.

#### **2. Digestion of rock, soil and sediment**

- 1) weigh 0.2 g of homogenized, dry sample in a teflon beaker
- 2) add 5 ml NBS HF, 3 ml NBS HNO<sub>3</sub>; cover and let stand overnight
- 3) evaporate slowly (6-8 hrs) to dryness
- 4) repeat stages 2, 3 once more
- 5) add 0.5 ml NBS HClO<sub>4</sub> and evaporate slowly to dryness
- 6) add 5 ml NBS HCl and evaporate slowly to dryness
- 7) add 20 ml 1 M NBS HCl and split: 30% for IDMS (add spike to IDMS sample) and 70% for IC.

Note: If the sample is not completely dissolved after stage 6, either centrifuge and proceed with the supernate, or start again, repeating stages 2, 3 for more than two times, or start again and use a teflon bomb.

**3. Column separation of rock and soil samples**

- 1) prepare 1-5 ml of resin in 6M NBS HCl solution
- 2) precondition with 1 M NBS HCl
- 3) pass the sample (dissolved in 1 M HCl)
- 4) wash the column with 1 M NBS HCl
- 5) elute lead with 6 M NBS HCl
- 6) evaporate to dryness and extract

**4. Extraction of water sample for lead and cadmium analyses**

- 1) acidify the sample (add spike to IDMS sample)
- 2) raise pH to 7-9 with  $\text{NH}_4\text{OH}$
- 3) add 0.1-0.3 Cit, 0.1-0.3 CN and extract with dithizone dissolved in  $\text{CHCl}_3$
- 4) wash the organic fraction (where the lead and cadmium are) with water
- 5) back extract with 0.5 M NBS  $\text{HNO}_3$
- 6) evaporate to dryness and load

Note: Some of the water samples with low iron concentration were extracted without Cit and CN in order to reduce the lead and cadmium blank. Extraction of digested samples starts at stage 3. Samples were loaded on outgassed Re filament in the presence of silica gel and 0.75 M  $\text{H}_3\text{PO}_4$  acid.

#### Appendix 2.4: Calibration of a multicollector VG-Sector solid-source mass spectrometer

A new solid source sector mass spectrometer was calibrated and used for the first time to analyze lead and cadmium concentrations at  $10^{-12}$  to  $10^{-10}$  M levels and the lead isotopic composition at  $5 \times 10^{-11}$  to  $5 \times 10^{-10}$  M levels.

In order to account for the machine fractionation of small size samples, 100 ng Pb ( $5 \times 10^{-10}$  M), 70 ng Pb ( $3.5 \times 10^{-10}$  M), and 10 ng Pb ( $5 \times 10^{-11}$  M) 981, 982 NBS standards were run at various temperatures (Fig. 2.4a,b,c). The  $^{206}\text{Pb}$ ,  $^{207}\text{Pb}$ , and  $^{208}\text{Pb}$  were detected on three Faraday cups and the  $^{204}\text{Pb}$  was detected either on a Daly multiplier or on a Faraday cup. The following observations were made:

- 1) in the temperature range  $1200^{\circ}$ - $1500^{\circ}\text{C}$ , the fractionation per unit mass is 0.1 - 0.15%
- 2) a 10 ng sample is more sensitive to temperature (and time) changes during the analysis than a larger sample
- 3)  $^{204}\text{Pb}$  in small samples can be measured only with a Daly multiplier
- 4) the precision of the Faraday cups measurements was approximately 0.1% ( $1\sigma$ ).
- 5) by calibrating the Daly multiplier before and after each set of measurements, the precision was found to be 0.5 - 1.0% ( $1\sigma$ )
- 6) calibrating the Daly both with  $^{206}\text{Pb}$  and with  $^{208}\text{Pb}$ , it was found that the Daly has a mass discrimination factor of  $0.6 \pm 0.1\%$ .

Most natural samples are more contaminated by hydrocarbons than pure standards. Usually the  $^{206}\text{Pb}/^{204}\text{Pb}$  and  $^{206}\text{Pb}/^{207}\text{Pb}$  ratios in natural samples increase at lower temperatures (burning of hydrocarbons), then they stabilize, and finally the  $^{206}\text{Pb}/^{204}\text{Pb}$  ratio starts to decrease (probably faster diffusion rate of  $^{204}\text{Pb}$ ). Therefore, each sample was measured at various temperatures above  $1200^{\circ}\text{C}$ . The best results were obtained when data were collected near a maximum  $^{206}\text{Pb}/^{204}\text{Pb}$  ratio, and when the ratios measured at various temperatures were less than one standard error apart (confidence interval of 95%).

Most ID measurements (both Pb and Cd) were done using the Daly multiplier to detect the unspiked isotopes ( $^{206}\text{Pb}$ ,  $^{207}\text{Pb}$ ,  $^{114}\text{Cd}$ ), therefore, the results have STD of 0.5-1.0%.

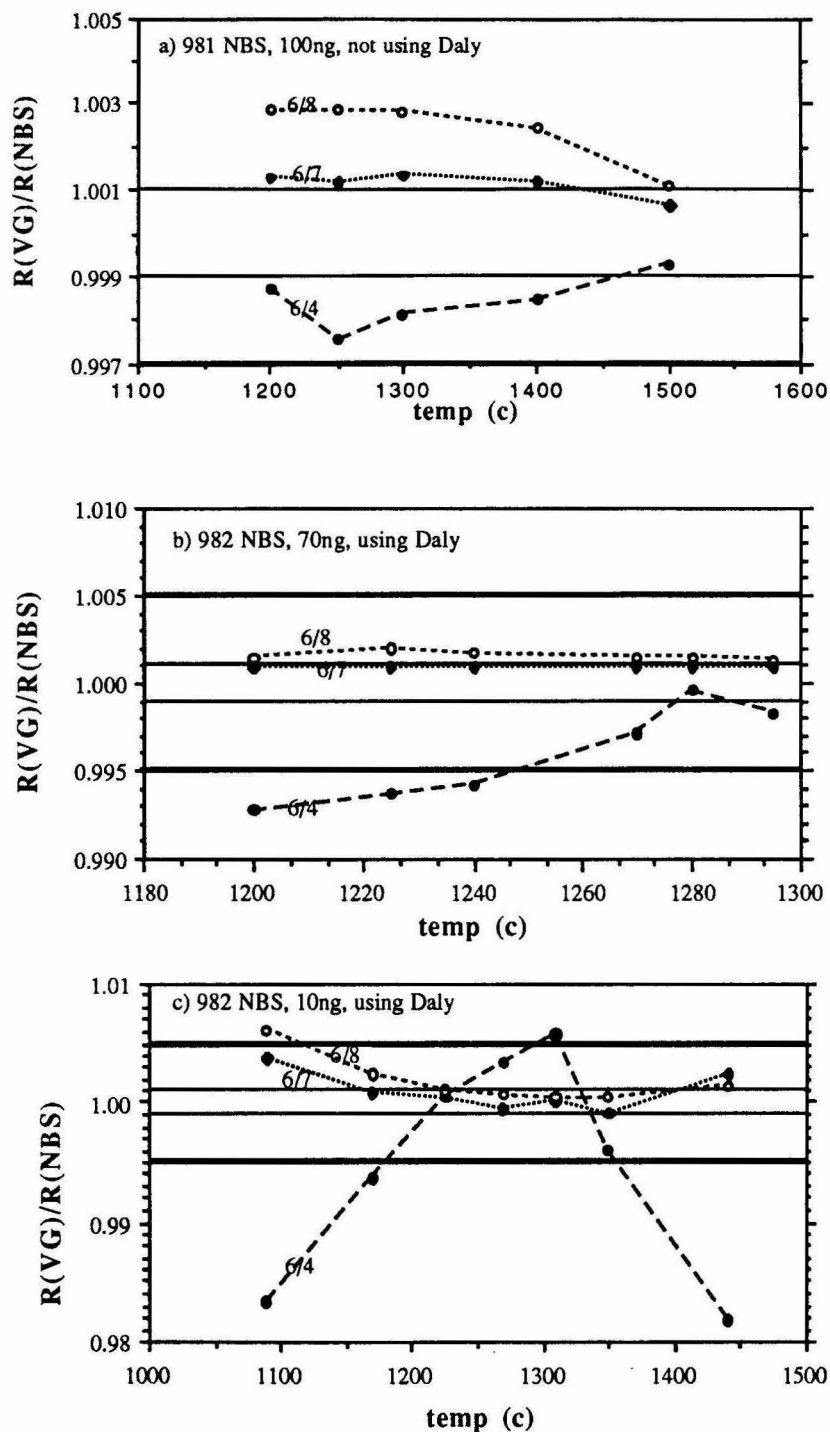


**Figure 2.4:** Fractionation of the mass spectrometer as a function of temperature (and time). The lines present the ratio between the measured values and the values reported by NBS (Table 2.2). The bold horizontal lines represent  $\pm 0.5\%$  errors and the plain horizontal lines represent  $\pm 0.1\%$  error.

**Table 2.2:** Isotopic composition of lead in NBS standards measured by the VG MS and other mass spectrometers at Caltech.

SAMPLE	$^{206}\text{Pb}/^{207}\text{Pb}$	$^{208}\text{Pb}/^{206}\text{Pb}$	$^{206}\text{Pb}/^{204}\text{Pb}$
<b>NBS 981:</b>			
NBS:	$1.09333 \pm 39$	$2.16812 \pm 80$	$16.9371 \pm 110$
Lunatic II CIT, 100 ng	$1.0932 \pm 3$	$2.1652 \pm 4$	$16.948 \pm 16$
Lunatic IV CIT, 100 ng	$1.0940 \pm 16$	$2.1664 \pm 10$	$16.950 \pm 20$
VG-MS CIT, 100ng	$1.0934 \pm 15$	$2.1675 \pm 9$	$16.941 \pm 48$
VG-MS CIT, 250ng	$1.0935 \pm 10$	$2.1674 \pm 5$	$16.9326 \pm 49$
VG-MS CIT, 250ng	$1.0932 \pm 3$	$2.16715 \pm 12$	$16.9373 \pm 13$
<b>NBS 982:</b>			
NBS:	$2.14101 \pm 6$	$1.00016 \pm 36$	$36.7390 \pm 27$
Lunatic I CIT, 100ng	$2.14362 \pm 9$	$0.99795 \pm 26$	$36.7013 \pm 80$
Lunatic I CIT, 100ng	$2.14335 \pm 9$	$0.99839 \pm 26$	$36.7013 \pm 80$
Pat MS CIT, 50ng	$2.148 \pm 3$	$0.9921 \pm 16$	$36.400 \pm 197$
VG-MS CIT, 100ng	$2.1421 \pm 3$	$0.99998 \pm 40$	$36.516 \pm 75$
VG-MS CIT, 10ng	$2.1466 \pm 3$	$1.0040 \pm 6$	$36.613 \pm 15$

## Appendix 2.5: Experimental methods used in Thompson Canyon

Since the samples collected in Thompson Canyon (see section 2.1.2) were collected before the other samples, somewhat different analytical techniques were applied there.

### Sampling

Samples of stream water, ground water, soil moisture, and soil were collected from Thompson Canyon immediately after the major portion of 1986 spring-melt had flowed out of the canyon. Meltwater from ice-firn remnants of the 1985-86 winter snowpack were draining from the canyon side-walls both into the meadows and directly into the main canyon drainage stream at the time of collection. I did not determine either the concentration or the isotopic composition of lead in the snowpack at that time. Instead, I used literature values to estimate lead concentrations and  $Pb^{206}/Pb^{207}$  ratios in that snowpack by comparing values obtained from similar reservoirs in the Sierra during the 1970s and 1980s (Elias et al., 1982; Shirahata et al., 1980; Laird et al., 1986).

A pit was dug to a depth of approximately 50 cm in the meadow. The tools used for digging and bailing were acid cleaned and transported to the field in acid cleaned plastic bags. Ground water seeped in at a depth below 30 cm. The pit was bailed several times before samples collection. Soil and soil moisture were sampled from the wall of the pit above the ground water table. Soil moisture was extracted in the laboratory from moist soil as described by Elias et al. (1982).

Samples analyzed for lead concentrations and isotopic compositions were collected before collection of other samples, using great care to minimize contamination. Collection procedures, types of containers used, as well as preconditioning techniques and amount of contamination involved during sample acquisition were described previously. Samples collected and analyzed for major

cations and anions, ANC and pH, were collected in containers suitably cleaned in ways that did not interfere with those measurements (Clesceri et al., 1989).

### Sample preparation

Ground water samples were centrifuged (7000 rpm) for 20 minutes prior to acidification. All water samples for cation analysis were acidified to pH ~ 1.5 and allowed to stand in the original sample bottle for 1-2 hours immediately before aliquots were separated.

The soil was dissolved for cation analysis using two different techniques:

1) The HF, HNO<sub>3</sub>, HClO<sub>4</sub> technique (McQuaker et al., 1979) was used for Na, K, Fe, Al analyses.

2) The LiBO<sub>2</sub> technique (Boar and Ingram, 1970) was used for Si, Ca, Mg analyses.

Lead from stream water and ground water samples, for concentration and isotopic composition measurements, was extracted using the dithizone method.

### Chemical analysis

Lead concentration was determined by the isotope dilution technique (Patterson et al., 1973). The mass spectrometer used for concentration and isotopic composition determination (Patterson et al., 1973) had a limit of detection of  $5 \times 10^{-5}$  picomole/g Pb and a coefficient of variance (CV) of 0.1% for concentration and a Pb<sup>206</sup>/Pb<sup>207</sup> ratio measurement of samples whose lead content was about 1000 times above the detection limit.

Na, K, Ca, Mg, and silica (only in soil samples) were analyzed with a CRA-90 Varian Techtron atomic absorption flame spectrophotometer (detection limit = 0.001 micromole/g). Al (only in soil samples) and Fe (both in soil and water samples) were analyzed with a 360 Perkin Elmer Graphite Furnace atomic absorption

spectrophotometer (detection limit = 40 and 20 picomole/g, respectively). The coefficient of variance of cation analysis was approximately 10% in stream water and ground water samples and 2% in soil samples. Only stream water and ground water samples were analyzed for anion concentration. Chloride, nitrate, sulfate, and formate were analyzed with a Dionex 20-20i Ion Chromatograph (limit of detection = 0.0005 micromole/g, CV = 10%). Phosphate was determined using absorption spectrometry analysis (Eisenreich et al, 1975); however, its concentrations in all the water samples fell below the limit of detection.

pH was measured in the field both with Merck Colorphast pH papers and with a Radiometer PHM 80 portable pH meter. ANC (measured in the laboratory) of stream water and ground water was determined by titration with 0.01N HCl using the Gran Method (Stumm and Morgan, 1981; Butler, 1982). Moisture content of soil was determined by vacuum drying the sample.

The term "labile reservoir" refers to the soil fraction that was leached after a soil sample was treated with 1N HNO<sub>3</sub> at room temperature. (Ng and Patterson, 1979, 1982; Shirahata et al., 1980). This type of treatment causes a dramatic increase of proton activity which enhances nonspecific release of cations from all mineral surfaces. In addition, it dissolves iron hydroxides and manganese oxides releasing bound metals and organic matter. Therefore, all the relatively mobile cations in the soil were released. This leaching method is very crude, however, it avoids both the ambiguity involved with soil leaching by water (Hinkley, 1975) and the contamination associated with more complicated leaching schemes (Tessier et al., 1979). The leached phase is composed of organic matter, iron hydroxides and manganese oxides. The fraction remaining after acid treatment is called the "non labile reservoir," composed of bedrock minerals and allophane.

## Chapter 3: Field study

The primary goal of the field study was to measure natural lead and cadmium in streams, and to distinguish between natural and anthropogenic lead. The lowest values of lead in streams reported in the literature were measured by Patterson et al. (1973) in Thompson Canyon, California (see section 2.1.2.2). The initial part of the field work was carried out at this site because it was hoped that the signal of anthropogenic lead was low. In Thompson Canyon, concentrations and  $^{206}\text{Pb}/^{207}\text{Pb}$  ratios of lead were used to follow both the path of industrial lead in snowmelt as it exchanged with chelator reservoirs in soil and the path of natural rock-lead at ground water depths. These two different kinds of lead were traced as they enter the stream water and ground water in order to determine the fraction of the original industrial lead contained in snowmelt which was retained soil, and the fraction which drained off in streams. The data from this study were combined with findings obtained at the same site in earlier years to provide a coherent explanation of my observations. In this part of the field study I found out that natural (rock-derived) lead can be detected in remote mountain streams as long as the water in the stream comes from subsurface reservoirs. Therefore, I concluded that it is most appropriate to study the transport of natural (rock-derived) lead in mountain streams during the fall, when the streams are fed by ground water.

In order to trace both the horizontal and the vertical movements of lead in stream water-ground water system, I undertook a second field study at a site in which the isotopic composition of lead in the bedrock changes spatially. In accordance with this criterion, I chose to study Moraine Creek, in Kings Canyon National Park, California (see section 2.1.2.1). In order to assess the variability of trace metal behavior in natural systems, I studied another trace metal whose aquatic chemistry is similar to lead. Cadmium was chosen because of its similarity to lead, because it is highly polluted in most aquatic environments, and since not much is known about the natural levels and behavior of cadmium in streams (see section 1.4).

### **3.1. Transport of industrial lead in snow through soil to stream water and ground water**

#### **3.1.1. Introduction**

##### **3.1.1.1. Industrial lead and the hydrological cycle**

Industrial lead concentrations have increased approximately 100-fold in the atmosphere of the Northern Hemisphere since the Industrial Revolution (Patterson, 1965; Murozumi et al., 1969; Patterson, 1972; Settle and Patterson, 1980). At present, virtually all atmospheric lead originates from industrial sources. The atmospheric lead is rapidly removed from the atmospheric reservoir by precipitation in snow, rain and dust (Ng and Patterson, 1981; Settle and Patterson, 1982; Patterson and Settle, 1987). Lead is known to have low mobility in surface waters and in soils, hence, atmospheric lead is expected to be trapped at the upper soil horizons (Benninger et al., 1975; Lewis, 1976; Lewis, 1977; Turekian, 1977; Nriagu, 1978).

The  $^{206}\text{Pb}/^{207}\text{Pb}$  ratio can be used to distinguish industrial from natural lead (see section 1.6). Industrial lead is produced from ore bodies whose isotopic composition differs from that of lead in rocks. During the formation of ore bodies, lead is separated from uranium so that  $^{206}\text{Pb}$ , derived from  $^{238}\text{U}$  decay, is no longer accumulated after the ore is formed. Consequently the  $^{206}\text{Pb}/^{207}\text{Pb}$  ratios in most lead ores are lower than in most bedrock, where accumulation of  $^{206}\text{Pb}$  has continued. Radioactive accumulation of  $^{207}\text{Pb}$  is minor during the last billion years since its parent,  $^{235}\text{U}$ , possesses a 0.7 Ba half-life and has essentially decayed away. Therefore, the  $^{207}\text{Pb}$  isotope is used as an accurately measured normalizing isotope for the  $^{206}\text{Pb}$  isotope. The  $^{206}\text{Pb}/^{207}\text{Pb}$  ratio of airborne lead in the study area was relatively constant at about 1.150 before 1967 according to Shirahata et al. (1980), because during that period most of it came from nonradiogenic ores. However, after 1967 that ratio increased in atmospheric lead to about 1.22 in 1979, due to a shift to the dominant use of Missouri ore lead in

manufacturing lead-tetraethyl and lead-tetramethyl (Shirahata et al., 1980). Missouri ore lead possesses an anomalously high  $^{206}\text{Pb}/^{207}\text{Pb}$  ratio and was an important source of gasoline lead used in North America until 1984 (Doe, 1970; Sturges and Barrie, 1987).

Recent addition of Missouri lead, with large  $^{206}\text{Pb}/^{207}\text{Pb}$  ratios to soils containing previously incorporated ore leads, with small  $^{206}\text{Pb}/^{207}\text{Pb}$  ratios, would result in overall  $^{206}\text{Pb}/^{207}\text{Pb}$  ratios which might be indistinguishable from  $^{206}\text{Pb}/^{207}\text{Pb}$  ratios in the bedrock. However, by combining measurements of the isotopic composition of lead in stream water, ground water, soil and bedrock with other geochemical and geological parameters (i.e., concentrations of other elements, mineralogy, field observations), I was able to use isotope tracers to determine what fraction of industrial lead in snow is incorporated into the soil and what fraction escapes into stream water and ground water.

#### 3.1.1.2. Study area

Thompson Canyon is located in a remote site on the crest of the Sierra Nevada Mountains Range near the northern border of Yosemite National Park (see section 2.1.2.2). The soil is derived entirely from post-Wisconsin weathering of the granite rock, is subalpine, relatively immature, acidic and sterile (Patterson et al., 1973; Hinkley, 1975). The main minerals in the soil are clay (allophane), white mica and bedrock minerals (plagioclase, quartz, microcline, biotite and magnetite). The organic content of the soil is approximately 5% dry weight.

The 14 km<sup>2</sup> snow collection and drainage area of Thompson Canyon feeding the stream we sampled receives an average of  $2 \times 10^7$  m<sup>3</sup> of precipitation annually. Most of the precipitation is added in the form of snow during the winter months, and leaves the canyon as flood water during the spring thaw (Patterson et al., 1973). During the spring flood times, ground water levels are about 30 cm below the surface, while during most of the year depths of water-saturated soil are at about 50 cm.

### **3.1.2. Character of data**

#### **3.1.2.1. Rock lead: $^{206}\text{Pb}/^{207}\text{Pb}$ ratio and storage in the nonlabile reservoir**

The original source of natural lead in Thompson Canyon soil is bedrock, with a  $^{206}\text{Pb}/^{207}\text{Pb}$  ratio of 1.212 in whole rock samples (Table 3.1.1). The average chemical composition of the soil is similar to the bedrock composition except for the relative abundances of some elements in the soil caused both by incongruent weathering and by fluvial sorting of igneous minerals (Table 3.1.1). Lead concentrations in nonlabile reservoir strata (bedrock minerals and clays), as shown in Table 3.1.2, do not change much with depth, and the  $^{206}\text{Pb}/^{207}\text{Pb}$  ratio of lead in this reservoir remains rather constant at 1.210-1.215.

#### **3.1.2.2. Rock lead: $^{206}\text{Pb}/^{207}\text{Pb}$ ratio and storage in the labile reservoir**

Total amounts of soil moisture film (in unsaturated soil), organic matter, iron hydroxides and manganese oxides make up the bulk of the labile reservoir of lead in soil and decrease rapidly with depth (Table 3.1.3). At depths unaffected by additions from the atmosphere of industrial lead (below 2cm), the concentrations of lead incorporated into organic matter in the labile reservoir increases as the amount of organic matter in soil decreases ("Natural trend," Fig. 3.1.1). I believe that this is the result of retaining and accumulation of lead in organic matter as its mass is reduced by oxidation. The isotopic composition of lead in this reservoir is determined by several mechanisms (see sections 1.6 and 3.2). The net result of these processes is that the mixture of leads from weathered minerals, which is added to the labile reservoir, contains a disproportionately greater amount of radiogenic lead with high  $^{206}\text{Pb}/^{207}\text{Pb}$  ratios (1.280-1.300) than is contained in total bedrock (1.212).

### 3.1.2.3. Industrial lead: $^{206}\text{Pb}/^{207}\text{Pb}$ ratio and storage in the labile reservoir

Elias et al. (1982) estimated that the industrial lead added to Thompson Canyon by snow, rain and dust amounted to about  $15 \mu\text{g}/\text{cm}^2$  in 1976. Approximately two-thirds of this atmospheric lead came from dry deposition, while the remaining one-third was introduced by snow and rain. Hirao and Patterson (1974) report an average of 3.0 nanomole/kg lead in the 1973 snowpack in Thompson Canyon, which they sampled in April 1973. The concentration of lead in snow collected during March 1983, from nine stations along the Sierra Nevada near Thompson Canyon was reported by Laird et al. (1986) to average about 0.5 nanomole/kg (Table 3.1.4). The six-fold decline during this period conforms with a three-fold nationwide decline in the burning of lead alkyls during the last 15 years (Trefry et al., 1985) which may have been accentuated in the central and southern California region. Concentrations of lead in organic matter of both litter and the labile reservoir decrease with depth and are linearly related to the decrease in the amount of organic matter in the total soil within the shallow surface strata ("Anthropogenic trend," Fig. 3.1.1). Lead isotope tracers of this soil profile also indicate that industrial lead introduced into Thompson Canyon is trapped within the labile reservoir of the upper two cm of soil (Table 3.1.2). This lead constitutes most of the total lead in that reservoir, with the remainder originating from weathered rock minerals (Elias et al., 1982; Patterson and Settle, 1987).

As shown by Shirahata et al. (1980), the  $^{206}\text{Pb}/^{207}\text{Pb}$  ratio of atmospheric lead in Thompson Canyon was about 1.15 until 1967 when it began to increase as a result of increased burning of gasoline lead derived from Mississippi ores. The levels approached 1.22 in the late 1970s. Based on scattered measurements of  $^{206}\text{Pb}/^{207}\text{Pb}$  ratios of industrial lead in urban atmospheres of the Western U.S., I estimate that the value of the  $^{206}\text{Pb}/^{207}\text{Pb}$  ratio in present day atmospheric lead incorporated in Thompson Canyon is still about 1.22 (Patterson and Settle, 1987; Sturges and Barrie, 1987). By integrating

the data from Shirahata et al. (1980; Figs. 5, 6, and 7) with data from Trefry et al. (1985), Boyle et al. (1986), Patterson and Settle (1987) and Sturges and Barrie (1987), I estimate the average  $^{206}\text{Pb}/^{207}\text{Pb}$  ratio of industrial lead entering Thompson Canyon via the atmosphere since 1860 until now to be approximately  $1.17 \pm 0.01$ . (Note: Later on in the study I measured present day anthropogenic lead and found a  $^{206}\text{Pb}/^{207}\text{Pb}$  ratio of 1.18, however, the average  $^{206}\text{Pb}/^{207}\text{Pb}$  ratio remains 1.17.)

The  $^{206}\text{Pb}/^{207}\text{Pb}$  ratio of lead stored in the labile phase of the upper two cm of soil in Thompson Canyon is about 1.20 (Table 3.1.2). Combining the estimated average industrial  $^{206}\text{Pb}/^{207}\text{Pb}$  ratio (1.17) with the  $^{206}\text{Pb}/^{207}\text{Pb}$  ratio of 1.300 for rock-derived lead, I calculate that about 75% of the lead in the labile phase in the upper two cm of the soil in Thompson canyon comes from industrial sources.

### **3.1.3. Results**

#### **3.1.3.1. Meltwater-soil relationships**

The concentration of lead in stream water is an order of magnitude less than that in snow (Table 3.1.4), indicating that 90% of the lead in snow is incorporated into the surface strata of soil upon melting during percolation of melt water through surface soil in its downhill flow. In addition, during the period between 1973-1983, lead concentrations in spring flood stream water decreased by only 40% in comparison to a six-fold decrease of lead concentrations in snow (Table 3.1.4). The observed relatively uniform concentration of lead in stream water appears to be independent of changes of lead concentrations in snow. This suggests that lead is leached into surface runoff from the labile reservoir of lead in the upper two cm of soil and that the concentration of lead in this reservoir is changing very slowly with time.

The concentration of lead in surface runoff during spring determines, for the most part, the concentrations of lead in stream drainage (at this time). The similarity of the  $^{206}\text{Pb}/^{207}\text{Pb}$  ratio of lead in stream water (1.215) to the value of that ratio of lead in the

labile reservoir in the upper two cm of soil (1.20) permits this interpretation (Fig. 3.1.2). However, this comparison is not definitive, since the estimated  $^{206}\text{Pb}/^{207}\text{Pb}$  ratio of lead in the 1986 snow pack (1.22) is also similar to that in stream water.

### 3.1.3.2. Soil-stream water-ground water relationships

Although the chemical compositions of stream water and ground water are similar (Fig. 3.1.3), the lead in them appears to originate from two different sources. The  $^{206}\text{Pb}/^{207}\text{Pb}$  ratio of lead in stream water during spring runoff (1.215), is similar to that in the upper two cm of soil labile reservoir, and differs from the lead in both soil moisture films at a depth of 15 cm and ground water at depth below 30 cm (1.274-1.275; Fig. 3.1.2). Lead in stream water comes mainly from a shallow labile reservoir in soil during spring floods, and from a different deep labile reservoir strata during the remainder of the year (see section 3.2.4). This indicates that during spring floods, when streams are fed mainly by surface runoff, lead in stream water originates from labile reservoirs at the soil surface which are heavily contaminated with industrial lead.

The  $^{206}\text{Pb}/^{207}\text{Pb}$  ratios of lead in nonlabile reservoirs (1.210-1.215) do not vary with depth, a characteristic that is different from the large variations of this ratio with depth exhibited by lead contained in soil moisture films and in ground water (Fig. 3.1.2). This indicates that lead in these waters does not originate from interactions with nonlabile reservoirs of lead in soil. Nevertheless,  $^{206}\text{Pb}/^{207}\text{Pb}$  ratios of lead, both in soil moisture films below 10 cm and in ground water, are slightly less than  $^{206}\text{Pb}/^{207}\text{Pb}$  ratios in labile reservoirs of lead at those depths (Fig. 3.1.2), which suggests that some industrial lead (up to 15%, based on mass balance calculations), perhaps bound to colloids, accompanies snowmelt and rain waters as they percolate through the soil to ground water depths.

The mobility of lead in a precipitation-soil-ground water-stream water system is markedly less than that of calcium. Concentrations of lead in stream water and in

ground water are similar and are one order of magnitude lower than its concentration in snow. Concentration of calcium in stream water and in ground water are similar; however, calcium concentration in snow is about one order of magnitude less. The relative mobilities of the two elements are shown by changes in Ca/Pb molar ratios during their transit from snow and weathered rock, through soil to stream water (Table 3.1.5). The primary source of calcium in stream water is weathered bedrock, where the Ca/Pb ratio is about 5,300, in contrast to a Ca/Pb ratio of about 270 in snow, which is the major source of lead. This ratio increases sharply to 3,530 in films of moisture contacting soil particles in unsaturated soil due to stronger adsorption of lead relative to calcium in the labile reservoir. In ground water, a more dilute medium whose greater mass is outside the steep concentration gradients within thin films next to soil particles, the ratio increases to 120,830. The ratio increases to 229,170 in flowing stream water.

#### 3.1.4. Conclusions

The isotopic composition of lead and concentrations of lead and other cations in soil, ground waters, and stream waters measured in a mountain creek were combined with lead concentration and isotopic data measured previously by others in snow, ground waters, stream waters, and soil profiles in the same study area to yield the following conclusions.

Approximately 90% of lead in snow (>95% industrial) is removed from snowmelt and trapped in the labile component of soil (which is made up of humus plus iron hydroxides and manganese oxides) before it is incorporated into the pristine mountain stream water during spring snowmelt runoff. The  $^{206}\text{Pb}/^{207}\text{Pb}$  ratio of Pb in the accumulation reservoir in the upper two cm of soil is different from that of industrial Pb added from snow each year, because it is a mixture of isotopically distinct natural rock-derived lead from weathering, and industrial lead. Additional isotope variation results from the fact that  $^{206}\text{Pb}/^{207}\text{Pb}$  ratio of industrial Pb accumulated from

atmospheric inputs during the past century has changed considerably during that period as isotopically distinct ore bodies successively provided the industrial lead within the United States.

During spring melt, the  $^{206}\text{Pb}/^{207}\text{Pb}$  ratio of lead in stream waters is the same as that in the surface soil accumulation reservoir, demonstrating that some lead from this soil reservoir is released back into surface runoff and then into stream water. This lead, which is approximately 70% industrial, accounts for most of the lead in streams at this time. However, the amount introduced into streams by this process is equivalent to only 10% of the quantity of industrial lead contained in the immediate past winter's snow pack.

Variations of isotopic compositions and concentrations of lead in soil profiles indicate the virtual absence of industrial lead in the labile lead accumulation reservoir below two cm depths. Below 10 cm depths this increment contains an undetectable amounts of industrial lead. However, measured  $^{206}\text{Pb}/^{207}\text{Pb}$  ratios of lead in ground waters at depths of 30 cm indicate that the lead is a mixture of approximately 15% industrial and 85% natural lead. This conclusion is based on the comparison with  $^{206}\text{Pb}/^{207}\text{Pb}$  ratios measured in lead in deep accumulation reservoirs and with an estimate for the average  $^{206}\text{Pb}/^{207}\text{Pb}$  ratio of industrial lead in the canyon (1.17). The industrial component is believed to originate from colloids in snowmelt which do not release their lead to the accumulation reservoir during downward percolation. Due to the extremely low concentration of lead in water, the isotopic composition of lead in the ground water is extremely sensitive to isotopic changes of its sources.

Although concentrations of lead in stream water remain the same, both throughout different seasons when rates of water discharge change 20-fold and over a decade when lead inputs from snow decreased six-fold, the  $^{206}\text{Pb}/^{207}\text{Pb}$  ratios of lead in those stream waters in spring and fall vary. This relationship demonstrates that during spring snowmelt most of the lead is of industrial origin, while during other times, when

streams are fed by underground aquifers, most of the lead is of natural rock-lead origin. This study exhibits that measurements of isotopic compositions of lead in precipitation, soil, ground water and stream water can provide a powerful tool for characterization of the pathways by which lead contained in precipitation is transported over and through soils to enter streams in ways which permit it to be distinguished from lead which is weathered from the bedrock and also added to stream water.

**Table 3.1.1:** A comparison between bedrock and soil at the south drainage, Thompson Canyon. Rock values from Patterson et al. (1973).

COMPONENT	GRANITE	SOIL
	WT %	DWT %
SiO <sub>2</sub>	68.5	45.6
Al <sub>2</sub> O <sub>3</sub>	15.83	4.6
Fe <sub>2</sub> O <sub>3</sub>	1.4	1.1
MgO	0.9	0.4
CaO	1.5	2.1
Na <sub>2</sub> O	4.2	5.9
K <sub>2</sub> O	2.9	1.6
ORG.	-	5.0
H <sub>2</sub> O	0.5	22
Pb	22 ppm	15 ppm
<sup>206</sup> Pb/ <sup>207</sup> Pb	1.212	1.190-1.300

**Table 3.1.2:** Lead concentration (micromoles/kg) and  $^{206}\text{Pb}/^{207}\text{Pb}$  ratios in the labile and nonlabile reservoirs at various depths in meadow soil (from G. Kolbasuk, R. Elias and C.C. Patterson, unpublished data).

DEPTH (cm)	LABILE RESERVOIR		NONLABILE RESERVOIR	
	Pb conc	$^{206}\text{Pb}/^{207}\text{Pb}$	Pb conc	$^{206}\text{Pb}/^{207}\text{Pb}$
0	157	1.190	-	-
0-0.5	81	1.192	44	1.210
0.5-1.0	37	1.217	-	-
2.0-2.5	15	1.300	-	-
4.5-5.2	14	1.280	72	1.211
14.5-15.0	13	1.295	82	1.215
35-45	8	-	-	-

**Table 3.1.3:** Concentrations of water, organic matter and labile reservoir in meadow soil at various depths (from G. Kolbasuk, R. Elias and C.C. Patterson, unpublished data). WTR = amount of water in the soil. LR = the amount of matter in the dried soil leachable by dilute acid plus organic matter. ORG = the amount of organic matter in the soil.

Depth (cm)	%in soil		
	WTR	LR	ORG
0	40	90.0	80.0
0-0.5	68	54.3	50.7
0.5-1.0	60	31.0	31.0
2.0-2.5	37	11.3	6.0
4.5-5.2	14	18.7	11.0
14.5-15.0	24	6.8	2.3
35-45	14	8.3	2.6

**Table 3.1.4:** Concentrations of lead (nanomole/kg) and  $^{206}\text{Pb}/^{207}\text{Pb}$  ratios in snow, stream water (SW), ground water (GW) and soil moisture (SM). Data from the present study as well as from Hirao and Patterson (1974) and Laird et al. (1986).

depth (cm)	water type	year	conc.	$^{206}\text{Pb}/^{207}\text{Pb}$
0-330	snow	1973	2.95	1.20
0-10	snow	1983	0.483	1.22
0-10	SW	1972	0.068-0.082	-
0-10	SW	1986	0.048	1.215
14-16	SM	1972	33.82	1.274
30-40	GW	1986	0.072	1.275

**Table 3.1.5:** Ca/Pb ratio in the hydrological cycle.

cycle stage component	Pb conc mole/kg	Ca conc mole/kg	Ca/Pb
snow	4.8E-7	1.3E-7	270
bedrock	1.1E-4	0.58	5270
soil moisture	3.4E-8	1.2E-4	3530
ground water	7.2E-11	8.7E-6	120,830
stream water	4.8E-11	1.1E-5	229,170

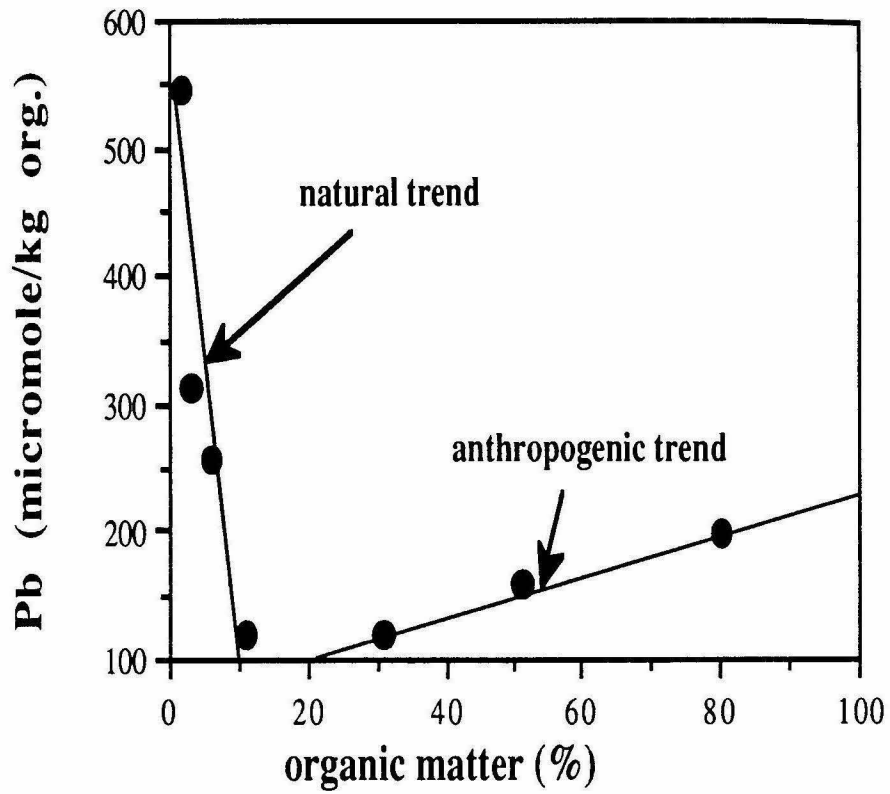


**Figure 3.1.1:** The relations between the concentration of lead, incorporated by organic matter, and the concentration of organic matter in soil. Data from Tables 3.1.2 and 3.1.3.

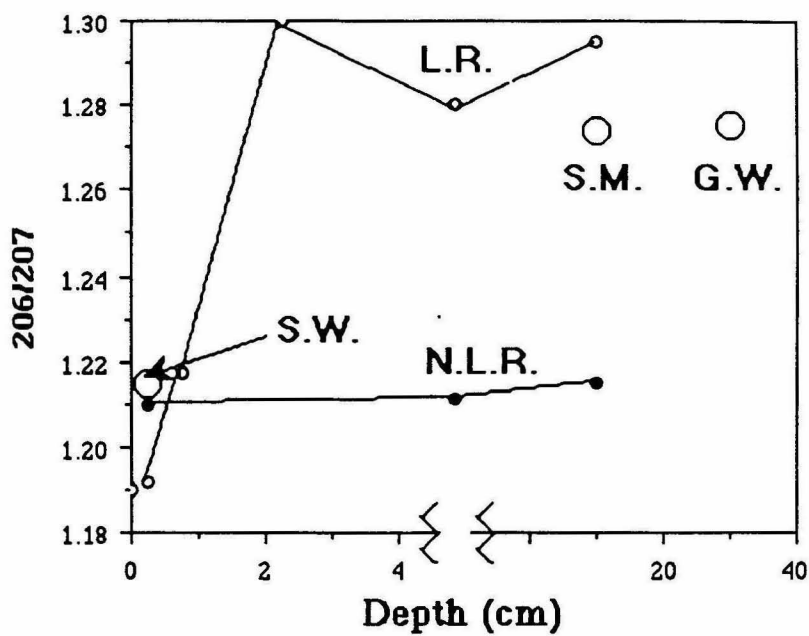


**Figure 3.1.2:**  $^{206}\text{Pb}/^{207}\text{Pb}$  ratios in the labile reservoir (L.R.), in nonlabile reservoir (N.L.R.), in stream water (S.W.), soil moisture (S.M.) and in ground water (G.W.) as a function of depth. Data from Tables 3.1.2 and 3.1.4.

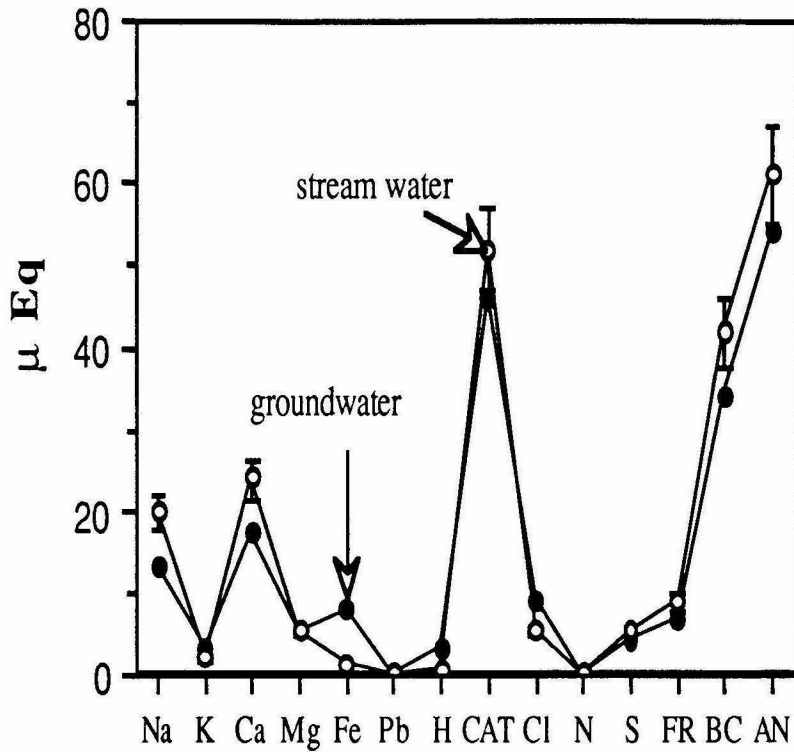


**Figure 3.1.3:** The general composition of stream water and ground water in Thompson Canyon, spring 1986 (N =  $\text{NO}_3^-$ , S =  $\text{SO}_4^{2-}$ , FR = formate, BC =  $\text{HCO}_3^-$ , CAT = total cations, AN = total anions).

### 3.2. Natural levels of lead and cadmium in remote mountain streams

#### 3.2.1. Introduction

As discussed in the previous section, it was found that during the spring snowmelt, most of the lead in a remote Sierra Nevada stream comes from industrial sources, while the lead in a shallow ground water at the same site is dominated by lead released from the bedrock. This suggests that most of the atmospheric lead (99% industrial) is trapped in the upper part of the soil, and that during the fall, when the stream runoff is dominated by ground water flow, lead and other trace metals in the stream are derived from rock weathering. The present work is an attempt to measure trace metals at their natural levels in streams, to understand the mechanisms of transport of natural lead and cadmium in a mountain stream environment, and to draw some general conclusions from a specific site study concerning the transport of trace metals in larger, more contaminated rivers.

#### 3.2.2. Study area

Moraine Creek is a typical western U.S. mountain stream having high ratios of  $(\text{HCO}_3^- + \text{CO}_3^{2-})/(\text{Cl}^- + \text{SO}_4^{2-})$  and comparable  $\text{Ca}^{2+}$  and  $\text{Na}^+$  concentrations (Landers et al., 1987). Moraine Creek is located in a relatively remote part of the Kings Canyon National Park (Fig. 2.1). The creek lies approximately 20 km northeast of Emerald Lake which was used as a study area for the California Air Research Board acid precipitation project during the last few years (Amar, 1988). Some of the work done at Emerald Lake has provided useful background and comparative information about the composition of dry and wet atmospheric precipitation, soil and water chemistry, and the geology of Moraine Creek watershed (Lund et al., 1987; Moore and Sisson, 1987; Melack et al., 1987; Bytnerowicz and Olszyk, 1988).

As mentioned before, the upper part of the stream cuts through the Paradise Granodiorite, and the lower part of the stream cuts through the Granodiorite of

Sugarloaf. The plutons have different lead isotopic compositions and both values are different from values of industrial lead used in California. Therefore, changes of isotopic composition of lead in the stream water are monitored in order to study lead transport and to distinguish between natural and anthropogenic lead inputs. Most of the creek surface is covered by moraine deposits, as the terrain has been modified by glacier activity during the Wisconsin Ice Age, approximately 10,000 years ago. The work done in Thompson Canyon indicates that freshly glaciated rock surfaces preferentially release radiogenic lead, which is different from both the whole rock lead and industrial lead (see section 3.1).

Moraine Creek starts its path in a small glacier lake at approximately 3200 m elevation, and in the course of 15 km drops to 2200 m where it flows into the Roaring River (Fig. 2.1). The stream flows most of the way through a pine (Westernwhite pine, Lodgepole pine) and redwood forest. The stream drains approximately 50 km<sup>2</sup>, with an estimated snow volume (as water) of  $8 \times 10^6$  m<sup>3</sup> (during the relatively dry 1987-88 winters; Meixner, 1988). The stream goes through a several regimes of flow (Fig. 2.1). It originates in a series of cascades down from the lake and then enters a small meadow (upper meadow) a few hundreds meters upstream from station 1. About half a kilometer down from station 1 it goes through another set of cascades (upper cascades). Stations 2 and 3 are located along this section. A few hundred meters down from station 3 the stream slows when it enters a large meadow extending for more than 2 km (lower meadow, stations 4, 4a). Then it flows again through a set of cascades (lower cascades, station 5) until it merges with the Roaring River (stations 6 and 7).

### 3.2.3. Results

As mentioned before, the Sugarloaf and Paradise plutons exposed in the study area have similar bulk compositions (Table 3.2.1). The soils developed on both plutons are sand containing 1-5% clay and 2-7% silt (Table 3.2.2). The clay and silt content of

the soils in the lower and upper meadows is twice those in the cascade part of the stream. The pH of the soil along the stream varies between 6.13 (upper meadow, B horizon) and 6.86 (upper cascades, B horizon) (Table 3.2.2). The water saturation percent of all soil samples analyzed is approximately 30%. The amount of organic carbon in the soil is relatively low (2-4%), and the organic carbon content varies with depth more than with location (Table 3.2.2). The exchangeable cations of the soil are dominated by  $\text{Ca}^{2+}$  (>80%), although the concentrations of  $\text{Na}^+$  in stream water and ground water are either equal or higher than  $\text{Ca}^{2+}$  concentrations. The total exchangeable cations of the soil at the pH of the soil varies as a function of depth and location, and is approximately 1.5 meq/100g (Table 3.2.3).

The amount of iron, aluminum and manganese oxides and hydroxides in all the soil samples analyzed is less than 1% (Table 3.2.4a). The soils developed on the Granodiorite of Sugarloaf contain mostly iron oxides and hydroxides while those developed on the Paradise Granodiorite contain mainly aluminum oxides and hydroxides. The leaching of soil samples (developed on the Granodiorite of Sugarloaf) with a pH 1 solution dissolved a substantial fraction of the coating of quartz and feldspar in the soil, as indicated by comparing the appearance of soil minerals under a petrographic microscope before and after the leaching. The amount of iron released from the 200 mesh sample by leaching with pH 1 solution for six days was roughly equivalent to the amount released by the dithionite method (Thomas, 1982) in soil samples, and was three times the amount released by the dithionite method in rock samples (Table 3.2.4b). The Fe/Pb ratios in the leached soil and rock samples were close to the ratios found in the bedrock (Table 3.2.1).

The major cations in Moraine Creek stream water and ground water are  $\text{Na}^+ \geq \text{Ca}^{2+} > \text{Mg}^{2+} > \text{K}^+$  (all  $\text{NH}_4^+$  values are below 1  $\mu\text{M/l}$ ), and the major anion is bicarbonate, reported as acid neutralization capacity ANC (Table 3.2.5a,b).  $\text{Cl}^-$ ,  $\text{NO}_3^-$ ,  $\text{SO}_4^{2-}$  concentrations are much lower than  $\text{HCO}_3^-$  in all stations both in the fall and in

the spring (1-4  $\mu\text{M}$ ), and formate, acetate and oxalate concentrations are below the detection limit. The pH of the stream water is slightly higher in the fall than in the spring, and the ANC is almost twice as high in the fall (450  $\mu\text{eq/l}$ ; station 5) as in the spring. Usually, the concentrations of all elements in the stream water do not fluctuate more than 30% at a given station and season (Table 3.2.5a). During the spring, all cations, except Al, have lower concentrations in stream water than during the fall. During the spring, the concentrations of lead, cadmium, sulfate, and chloride are higher in the snowmelt lake water than in the stream at station 5. The TOC levels in all the stream water samples analyzed are very close to the limit of detection, ranging between 1 to 2 mg/l.

The amount of lead, cadmium, manganese and iron in atmospheric dry deposition and rain is presented in Table 3.2.5c. One of the reasons for the higher concentrations measured in the fall atmospheric deposition was due to the usage of a different dust collector with a higher collection efficiency.

### **3.2.4. Discussion**

#### **3.2.4.1. Anthropogenic input of lead and cadmium to Moraine Creek**

Because of the remote location of Moraine Creek, atmospheric deposition is the only way anthropogenic lead and cadmium can be introduced to the stream. The  $^{206}\text{Pb}/^{207}\text{Pb}$  ratio of lead in the stream water at station 5 in the spring is 1.218, and is very close to its value in the snow-fed lake water (1.183) and in the atmospheric dust (1.19; Fig. 3.2.1; Table 3.2.5d). Both the lake  $^{206}\text{Pb}/^{207}\text{Pb}$  ratio and the dust  $^{206}\text{Pb}/^{207}\text{Pb}$  ratio are very close to the  $^{206}\text{Pb}/^{207}\text{Pb}$  ratios of contemporary leaded gasoline in California (Flegal, unpublished data). The concentrations of lead and cadmium in the snow-fed lake water at the top of the creek are higher than in the stream water (Table 3.2.5a). Therefore, most of the lead and probably cadmium in the stream

during the spring come from anthropogenic sources through snowmelt and atmospheric dust.

A fall storm provided an opportunity to observe massive transport of atmospheric lead and cadmium to the stream (Fig. 3.2.1). The concentrations of both elements were elevated seven to eight times, while the discharge increased two-fold, and the  $^{206}\text{Pb}/^{207}\text{Pb}$  ratio of the stream water dropped from 1.249 to 1.21 (at the implied station). The rain probably washed out some of the dry deposition accumulated on the forest canopy and introduced large amounts of anthropogenic lead and cadmium to the stream (Turner et al., 1985).

In the fall, the isotopic composition of lead in station 5 ( $^{206}\text{Pb}/^{207}\text{Pb} = 1.297$ ) is different from the isotopic composition of atmospheric lead ( $^{206}\text{Pb}/^{207}\text{Pb}$  of dust = 1.19,  $^{206}\text{Pb}/^{207}\text{Pb}$  of lake water = 1.183,  $^{206}\text{Pb}/^{207}\text{Pb}$  of rain = 1.18; Table 3.2.5d), yet is very close to the isotopic composition obtained from the leaching of a rock sample from the Granodiorite of Sugarloaf with a pH 1 solution ( $^{206}\text{Pb}/^{207}\text{Pb} = 1.326$ ), and to the  $^{206}\text{Pb}/^{207}\text{Pb}$  ratio of ground water sampled in the upper meadow ( $^{206}\text{Pb}/^{207}\text{Pb} = 1.279$ ). This suggests that most of the lead in stream water during the fall is released from the bedrock, since the stream is only fed by ground water flow. It has been shown previously that atmospheric lead is retained in the upper part of the soil, and that most of the atmospheric lead does not reach a shallow ground water table (see section 3.1).

The  $^{206}\text{Pb}/^{207}\text{Pb}$  ratios of the stream water in the fall change as a function of distance from the lake at the head of the stream. The  $^{206}\text{Pb}/^{207}\text{Pb}$  ratio is 1.247 in station 2, 5 km from the lake, and 1.297 at station 5, 15 km from the lake. As mentioned before, the  $^{206}\text{Pb}/^{207}\text{Pb}$  ratio of Granodiorite of Sugarloaf leached lead is 1.326 (Fig. 3.2.2a). Thus, the fraction of natural lead in stream water in the fall can be calculated as mixing between anthropogenic lead with a  $^{206}\text{Pb}/^{207}\text{Pb}$  ratio of 1.183 and a natural, rock-derived lead with a  $^{206}\text{Pb}/^{207}\text{Pb}$  value of 1.326. According to this

calculation, the proportion of natural lead in the stream during the fall increases from 46% at 5 km to 80% at 15 km downstream from the lake (Fig. 3.2.2b).

#### **3.2.4.2. Changes of the isotopic composition of rock-derived lead during weathering**

Lead leached from magmatic rocks such as granite, monzonite, leucogranite and granodiorite is more radiogenic than the total lead in the rock (Shirahata et al., 1980; Silver et al., 1984). Both radiogenic rocks examined by Silver et al. (1984) and less radiogenic rocks examined by Shirahata et al. (1980) preferentially release radiogenic lead during leaching and weathering. Silver and coworkers reported that  $^{206}\text{Pb}/^{204}\text{Pb}$ ,  $^{207}\text{Pb}/^{204}\text{Pb}$  and  $^{208}\text{Pb}/^{204}\text{Pb}$  ratios increase by 5 to 100% in solutions ( $10^{-4}\text{M}$  to  $0.1\text{M}$   $\text{HNO}_3$ ) used to leach fresh and weathered rocks (see Fig. 1.6). Relative to the whole-rock leach, leached phase of certain minerals such as magnetite and biotite increased by up to a few hundred percent.

Recoil of U and Th decay product ( $^{206}\text{Pb}$ ,  $^{207}\text{Pb}$  and  $^{208}\text{Pb}$ ) damaging the mineral lattice is the conventional explanation for the relative enrichment of radiogenic lead in weathering products; however, recoil effect by itself cannot account for the higher rate of  $^{206}\text{Pb}$  release compared with  $^{208}\text{Pb}$  in a bedrock whose Th/U ratios are approximately four (Tables 3.2.1 and 3.2.5d; Fig. 3.2.3a,b). Therefore, the results of this study support the mechanism proposed by Shirahata et al. (1980) and Silver et al. (1982) that a preferential weathering of uranium-rich accessory minerals (mainly apatite) as well as pegmatite and vein mineral assemblages, is the primary mechanism for the enrichment of radiogenic lead in leaching solutions and weathering products of freshly exposed rocks.

### 3.2.4.3. The chemical composition of Moraine Creek water

Most elements are diluted during the snowmelt spring flow (Table 3.2.5a). Aluminum is the only element that has higher concentrations during the spring flow, probably as a result of organic complexation (Lund et al., 1987). In spite of high concentrations in the lake water, both lead and cadmium have three-fold lower concentrations down the stream, and both (like most other elements) have lower concentrations in stream water during the spring than during the fall, suggesting an efficient removal of excess (anthropogenic) lead and cadmium from the water column (Table 3.2.5a). Approximately two-thirds of the lead in the lake water is attached to particles larger than 0.45  $\mu\text{m}$ . At the same time, the concentration of lead in the stream at station 5 is one-third of its total concentration in the lake (Table 3.2.5a), implying that most of the lead attached to particles larger than 0.45  $\mu\text{m}$  settles down in the lake before entering the stream.

In order to assess this possibility, the magnitude of the settling time is compared with the residence time ( $\theta$ ) of the water in the lake.

Where:

$$\theta = V/Q$$

$$\theta = (h \cdot A)/Q$$

$$V = \text{lake volume} = \text{area (A)} \cdot \text{depth (h)} = 12500\text{m}^2 \cdot h$$

$$Q = \text{the discharge of the stream at the lake outlet} = 0.05 \text{ m}^3 \cdot \text{s}^{-1}$$

Therefore:

$$h/\theta = Q/A = 0.05/12500$$

$$h/\theta = 4 \times 10^{-6} \text{ m} \cdot \text{s}^{-1} = 4 \times 10^{-4} \text{ cm} \cdot \text{s}^{-1}$$

Since the depth of the lake is unknown, the ratio  $h/\theta$  is compared with the settling velocity ( $u$ ) calculated from Stokes' Law:

$$u = \frac{[(\rho_s - \rho) \cdot g] \cdot d^2}{18\mu}$$

$\rho_s$  = density of the particles = 3 g/ml, for oxides

$\rho$  = density of the water at 11°C = 1 g/ml

$g$  = gravity acceleration = 981 cm·s<sup>-2</sup>

$d$  = particle diameter = 2 μm, estimated with SEM pictures

$\mu$  = viscosity of water at 11°C = 0.0127 g·cm<sup>-1</sup>·s<sup>-1</sup>

If  $h/\theta$  is larger than  $u$ , the particulate lead is likely to enter the stream before it reaches the bottom of the lake. On the other hand, if  $u$  is equal to or larger than  $h/\theta$ , it is likely that a large fraction of the particulate lead reaches the bottom before entering the stream.

The calculated settling velocity,  $u$ , is  $3.5 \times 10^{-4}$  cm·s<sup>-1</sup>, roughly equivalent to the ratio  $h/\theta$ , suggesting that most of the particulate lead in the lake is removed from the water column by settling before entering the stream.

A few stream water samples were subdivided using a 0.45 μm pore Millipore filter and a 1000 molecular weight cutoff dialysis membrane (approximately 1 nm pore size), creating three size fractions of components in the water: 1) smaller than 1 nm, 2) larger than 1 nm and smaller than 0.45 μm, and 3) larger than 0.45 μm. Both lead and cadmium distributions among these three fractions show a spatial variation (Fig. 3.2.4a,b). Usage of the conventional filtration through a 0.45 μm filter together with a 1000 molecular weight cutoff membrane demonstrates that transition between solution and particulate matter is a continuous rather than a sharply defined process, and that large fractions of lead and cadmium are attached to small particles or large organic molecules which pass through the 0.45 μm pores.

The amount of lead in "solution" (<1 nm) decreases with increasing distance from the lake, and from spring (pH = 5.5 in station 5) to fall (pH = 6.2 in station 5), suggesting a continuous uptake of lead by particles at a remarkably constant rate of about 5.5-6% per kilometer. The rate of lead uptake is around  $10^{-15}$  M·s<sup>-1</sup>, based on an

average lead concentration of  $5 \times 10^{-11} \text{M}$  (Table 5a) and an average water velocity of  $0.5 \text{ m}\cdot\text{s}^{-1}$ . The amount of lead attached to particles at station 5 both in the spring and in the fall can be explained by adsorption of lead on am- $\text{Fe}(\text{OH})_3$  surfaces at equilibrium (Fig. 3.2.4a). A SURFEQL program is used to calculate the dissolved and surface species of lead (Westall, 1980, 1987). The adsorption model takes into account the total concentration of  $\text{Fe}^{3+}$  and major ions in the water, as well as the water pH (Table 3.2.5a). The model is based on the rough assumption that concentration of surface sites available for lead adsorption is 2% of the total  $\text{Fe}^{3+}$  concentration, and it uses the empirical surface equilibrium constant reported by Dzombak (1986), and a Gouy-Chapman diffuse layer model.

Similar calculations done in order to examine the possibility of lead adsorption on silica, alumina and  $\text{MnO}_2$  particles, predict that only negligible fractions of the lead in the stream water will be adsorbed on any one of them. Moreover, all adsorption models on oxide surfaces, including am- $\text{Fe}(\text{OH})_3$ , fail to describe the observed behavior of cadmium in station 5 (Fig. 3.2.4b). The model predicts that at both pH 5.5 and pH 6.2 cadmium will exist dominantly in solution, and less than one percent of the cadmium will be adsorbed on am- $\text{Fe}(\text{OH})_3$  surfaces; however, the actual fractions of particulate cadmium in the stream vary from 52% to 88%. Attachment of cadmium to particles does not increase with distance from the lake, and there is a large difference between spring (85% particulate) and fall (52% particulate) behavior in station 5. These relations suggest that a large fraction of the cadmium in stream water is attached to particles other than oxy-hydroxides, and that the attachment is not determined by pH or by time of travel in a simple way.

The nature of the particles in Moraine Creek stream water, as in many other natural fresh water environments, is very diverse. Approximately 97% of the particles are smaller than  $1.0 \mu\text{m}$  and 99% are smaller than  $2.0 \mu\text{m}$ . The discrepancy ratio (the ratio between the median diameter of particles by volume and their median diameter by

frequency) is larger than three, indicating a polydisperse particle distribution; however, the size distribution of the colloidal particles along the stream is rather constant. There is no difference between particle size distribution along the cascades at stations 2 and 5 and the meadow at station 4.

Many of the particles examined under the SEM in this work are biological in their origin (e.g. pollen, diatoms); others are rock minerals and clays (probably kaolinite). Many of the particles, including fragments of microorganisms, contain iron as indicated by an EDS analysis of more than 100 particles collected from Moraine Creek stream water. The amount of iron increases towards the edges and cracks of the particles, suggesting that iron provides a partial surface coating (Nowlan, 1976; Fox, 1988; Buckley, 1989). On the other hand, a microelectrophoresis measurement done at the pH of the water (6.2) shows that the particles have negative surface charge, suggesting that amorphous iron ( $ZPC > 7.5$ ) is not the dominant surface phase. The possibility that most of the surfaces, including the ones coated with iron, are further coated with organic matter (a possible source of the negative surface charge of the particles in the stream) has not been examined closely.

#### **3.2.4.4. Transport of lead and cadmium in Moraine Creek**

In order to determine the transport of lead and cadmium in Moraine Creek, a mass balance approach is taken. The stream is divided along its length into two segments in which the discharge increases by the same factor (approximately 1.6) between the upper and the lower ends of the segments. The first segment begins at station 2 and ends at station 4, while the second segment begins at station 4 and ends at station 5. In the first segment, the stream flows mainly through the middle cascades, while in the second segment the stream flows one-third of its way through the lower meadow and the rest of its way through the lower cascades. Each segment is treated as a continuous flow reactor:

$$V (dc/dt) = C_i^u Q^u + C_i^g Q^g - C_i^d Q^d + R_i - S_i$$

at steady state  $dc/dt = 0$  and:

$$C_i^u Q^u + C_i^g Q^g = C_i^d Q^d + R_i - S_i$$

The input of an element  $i$  to a stream segment from the upper station ( $U_i$ ) is calculated by multiplying its concentration in stream water at the upper station ( $C_i^u$ ) with the discharge at this point ( $Q^u$ ). Similarly, the downstream ( $D_i$ ) output is the product of  $C_i^d$  and  $Q^d$ , and the contribution from ground water ( $G_i$ ) is the product of  $C_i^g$  and  $Q^g$ . It is assumed that  $Q^g$  is equal to the difference between  $Q^d$  and  $Q^u$ . Thus, the total input of a conservative tracer  $i$  to a stream segment is the sum of  $U_i$  and  $G_i$ , and the output equals  $D_i$ . A nonconservative tracer should also have a source term ( $R_i$ ) and a sink term ( $S_i$ ). Therefore, for a conservative element :

$$(U_i + G_i) / D_i = 1$$

and for a nonconservative element :

$$(U_i + G_i) / D_i = 1 + (S_i - R_i) / D_i$$

There is no observed difference in the transport behavior between the two segments (the uncertainty associated with our measurements is  $\pm 20\%$ ). The  $U/D$  ratios of all cations and trace metals measured are around 0.5, with no evident difference between alkali and alkali earth elements and trace metals, with the exception of Al (Fig. 3.2.5a). On the other hand, the  $(U+G)/D$  ratio of trace metals is highly dependent on the way the concentrations in ground water are measured (Fig. 3.2.5b). The

concentrations of all trace metals are extremely high in ground water samples, which are acidified before the analysis as a result of the break-down of free oxides and hydroxides at low pH (an apparent source term). Moreover, the technique used for ground water sampling probably introduced large amounts of particles, including oxides and hydroxides.

Alkali and alkali earth cations and silica have a (U+G)/D ratio of approximately unity in pH 1 samples, and slightly below unity in filtered samples (Fig. 3.2.5b). Fe, Mn and Pb in filtered waters have a (U+G)/D ratio slightly lower than the (U+G)/D ratio of alkali and alkali earth cations (Fig. 3.2.5b). The relatively low (U+G)/D ratios of Pb, Fe and Mn in filtered samples may suggest an additional source, such as contribution from particles in the ground water which are excluded by filtration. These particles might break down in the turbulent environment of the stream, allowing them to pass through the 0.45  $\mu\text{m}$  pores. When the (U+G)/D is normalized so that  $((U+G)/D)_{\text{Pb}}$  equals unity, only  $\text{Fe}^{3+}$  and Mn have (U+G)/D ratios of approximately unity, suggesting a similar transport mechanism of these elements. Both Al and Cd in filtered samples have (U+G)/D ratios higher than unity because of their relatively high concentrations in filtered ground water (Fig. 3.2.5c). A (U+G)/D ratios higher than unity requires a sink within the stream. A large fraction of the stream-bed in Moraine Creek is covered with algae which may act as a sink for trace metals like cadmium (Fig. 3.2.5b).

Combining the mass balance model with isotopic measurements of lead provides another line of evidence that the main process which controls the transport of lead in the stream is a simple mixing between ground water and stream water, and that the stream itself behaves almost like a passive carrier (Table 3.2.6). The results shown in Table 3.2.6 exclude any substantial exchange (larger than the uncertainty associated with our measurements, mainly the discharge measurements,  $\pm 20\%$ ) between lead in the stream and lead in the sediment during a fall flow, since the  $^{206}\text{Pb}/^{207}\text{Pb}$  ratio of the stream-

bed is lower than 1.24 and would substantially lower the  $^{206}\text{Pb}/^{207}\text{Pb}$  ratio in the downstream station. In section 3.1 it was shown that an exchange between lead in the water and lead in the sediment takes place in the spring or in a fall storm. In this case, it is likely that most of the interaction takes place during the slope flow out of the stream channel.

A simple mixing between ground water and stream water is an expected mechanism for the transport of relatively conservative elements like the alkali and alkali earth elements, but it contradicts transport behavior of trace element in streams proposed in numerous studies (Kennedy et al., 1984; Kuwabara et al., 1984). The differences between the nature of the present work (steady state situation, natural concentrations) and the nature of the previous studies (transient stage of transport and elevated concentrations) are possible sources for the disagreement. Furthermore, we have indicated already that excess (anthropogenic) lead and cadmium are removed from the stream water during the spring flow (Table 3.2.5a).

A deviation from conservative tracer behavior is observed when applying the constant flow reactor treatment to the system  $\text{Fe}^{+2} - \text{Fe}^{+3}$ . Assuming that  $(U+G)/D$  of both  $\text{Fe}^{+2}$  and  $\text{Fe}^{+3}$  equals unity and that the  $\text{Fe}^{+2}/\text{Fe}^{+3}$  ratio in ground water entering the stream is constant, and using the upper value of  $\text{Fe}^{+2}/\text{Fe}^{+3}$  measured in ground water (5%, Table 2a), there is a excess  $\text{Fe}^{+2}$  in the stream water which cannot be explained without an additional source (Fig. 3.2.6).

Photoreduction of ferric iron in the stream might account for the excess of ferrous iron (McKnight and Bencala, 1989). Knowing the time of travel between stations and the changes of excess ferrous iron, a reduction rate ( $d[\text{Fe}^{2+}]/dt$ ) of approximately  $2.5 \times 10^{-11} \text{ Ms}^{-1}$  is calculated. This value is close to photoreduction rates measured in the laboratory at similar pH values (Hoffmann, personal communication). The amount of lead released from dissolved ferric iron particles due to reduction should be, therefore, on the order of  $10^{-15} \text{ M} \cdot \text{s}^{-1}$ , as the ratio of lead to ferric iron is

approximately 1:10,000 (Table 3.2.5), similar to the observed rate of lead uptake by particles mentioned before ( $10^{-15}\text{M}\cdot\text{s}^{-1}$ ).

#### 3.2.4.5. Iron, lead and cadmium relationships in Moraine Creek

The concentrations of lead in soil, stream water and ground water in Moraine Creek are linearly related to iron concentrations (Fig. 3.2.7). Two kinds of relationships are observed: 1) a natural relationship in which the concentration of iron is more than 10,000 (mole/mole) times higher than lead, and ratios of these elements approach their ratio in the bedrock, and 2) an anthropogenic relation in which the ratio Fe/Pb is almost 5 times lower than in (1). The natural relationship is observed in unfiltered and filtered ground water samples, stream water samples, soil and rock leached phases, and in rock and soil samples from the study area. The Fe/Pb ratio in the bedrock is lower than in the stream water probably because a large fraction of the lead in the rock is stored in K-feldspar, which is more resistant to weathering than biotite (the main source of iron, see section 4.4.1). A sample collected from the Kings River, more than 40 km downstream from Moraine Creek, at a time when the whole area was closed to visitors, has a Fe/Pb ratio similar to the ratio observed in Moraine Creek.

The anthropogenic ratio observed in Moraine Creek is based on four samples consisting of two lake water samples, a stream water sample during a fall storm, and a sample collected from the Kings River at the foothill area outside of the park boundaries. The Fe/Pb ratio determined by these samples is closer to the ratio in major rivers reported in the literature (150-1500, Martin and Meybeck, 1979; Martin and Whitfield, 1983; Salomons and Förstner, 1984; Taylor and McLennan, 1985). It is interesting to note that Fe/Pb ratios measured twenty years ago in 126 high Sierra Nevada lakes vary from two to eight, suggesting contamination of lead during sampling and analysis (Bradford et al., 1968).

The strong tendency of lead to be attached to particles in the water, the fact that many of the particles found in Moraine Creek waters are coated with iron, the high correlation between lead and iron in the system, the similar transport pattern, and the reasonable fit with the adsorption model all strongly suggest that lead in the system is largely adsorbed on surfaces provided by  $\text{Fe}(\text{OH})_3$ . The transport of lead in rivers on oxide and hydroxide surfaces in general, and on iron hydroxides in particular, has been widely documented (Gibbs, 1973; Benninger et al., 1975; Lewis, 1976, 1977; Turekian, 1977; Mouvet and Bourg, 1983; Trefry et al., 1985).

The behavior of cadmium in Moraine Creek is more complicated than that of lead. There is an overall enrichment of cadmium compared with lead throughout the system (Table 3.2.5a,b). The Pb/Cd ratio drops from almost 100 in the bedrock to 10-50 in unfiltered ground water and to 5-10 in stream water, and is less than 1 in filtered ground water. Although a substantial fraction of the cadmium in Moraine stream water is attached to particles, the percent of particulate cadmium is lower than the percent of particulate lead. In addition, at the pH of the stream (5.5-6.2), adsorption models of cadmium on oxide surfaces predict almost no formation of surface species (Dzombak, 1986; Dzombak and Morel, 1990).

The fluctuating concentrations of cadmium in solution along the stream and the lack of a similar transport pattern to that of any other inorganic component (except for a some similarity with aluminum) suggest a possible adsorption on organic particles and microorganisms. Nelson et al. (1981) report that more than 50% of the cadmium is adsorbed on bacteria surfaces at pH 6.5 and that the adsorption of cadmium on these surfaces is relatively insensitive to pH variations in the range of 6.5-8.0. As mentioned previously, algae covers a large fraction of the stream-bed in Moraine Creek. Concentrations of cadmium in algae found in evaporation ponds in the San Joaquin Valley in California, downstream from the Kings Canyon, are 7000 times higher than in the surrounding water, while lead enrichment factor is much smaller (Bradford, personal

communication). A strong association of cadmium in sea water with microorganisms has been observed by many investigators (Bruland and Franks, 1983; Boyle, 1988).

Although this work does not provide conclusive evidence for the mechanisms of cadmium transport in streams, it is likely that the levels of cadmium observed here ( $10^{-11}\text{M}$ ) are mostly natural. These concentrations of cadmium in the stream water are three-fold lower than the concentration in the snow-fed lake at the top of the stream, suggesting that most of the anthropogenic cadmium is removed from the water column either in the lake or on its way downstream.

### 3.2.5. Conclusions

Natural lead and cadmium are measured in a remote mountain stream. The main source of anthropogenic lead and cadmium to the study area is wet and dry atmospheric deposition. During the spring, when the stream is mainly fed by snowmelt water, most of the lead and probably the cadmium in the stream come from anthropogenic sources. In spite of higher concentrations of lead and cadmium in the snow-fed lake water, the concentrations of both elements in the stream during the spring are lower, indicating an efficient removal mechanism of pollution lead and cadmium from the water column.

In the fall, when the stream is fed only by ground water flow, and when most of the atmospheric input of lead and cadmium is by dry precipitation, the percent of natural lead in the stream water varies between 46 to 80%. Most of the lead in the water, both in the spring and in the fall, is associated with particles, probably due to adsorption on iron-hydroxide surfaces. Although a substantial amount of cadmium is also associated with particles, the nature of the interaction between cadmium and surface sites and the type of particles is less clear.

The close relationship between lead and iron and the natural ratio found in this work provide a powerful tool for generalizing the results from a small mountain stream. Comparing the Fe/Pb ratios obtained in this study (10,000-20,000) with Fe/Pb ratios in

major rivers reported in the literature, a 10 to 100-fold difference is found. The difference between the ratio observed in this work and in major rivers cannot be attributed to bedrock effect since the Fe/Pb ratio of the granodiorite bedrock in Moraine Creek is very close to the upper crust average composition, and the main source minerals for lead and iron are the same in many common rocks.

More work is needed in order to examine the possibility that the source of discrepancy in Fe/Pb ratios between the present work and other reports is pollution of lead. As both lead and iron demonstrate rapid removal rates from the water column, the actual magnitude of the influx of anthropogenic lead to larger rivers should be very high in order to account for the observed excess of lead compared with iron.

**Table 3.2.1a:** Chemical composition of bedrock and soil in Moraine Creek. Rock and soil values are in weight percent. Leached sample values are in ppm. All Pb, U and Th values are in ppm. Leached sample values are of elemental concentration. The soil was leached after a magnetic separation with a Franz. P<sub>2</sub>O<sub>5</sub> in soil = the available P (ppm).

	Sugarloaf	pH 1 leach	soil, B horizon	pH 1 leach	soil, A horizon	stream bed	Paradise	soil, B horizon
SiO <sub>2</sub>	67.2	10.9	61.3	2.0	61.7	63.1	67.2	68.8
TiO <sub>2</sub>	0.7						0.6	
Al <sub>2</sub> O <sub>3</sub>	15.4	8.2	12.0	2.2	13.6	12.6	15.5	14.1
Fe <sub>2</sub> O <sub>3</sub>	4.4	8.7	7.8	3.1	5.1	5.3	3.7	1.9
MnO	0.1	0.23	0.12	0.15	0.09	0.09	0.1	0.07
MgO	2.0	4.9	1.1	0.42	1.2	1.2	1.5	1.0
CaO	4.8	3.1	4.1	1.0	3.4	3.9	4.0	3.0
Na <sub>2</sub> O	3.9	1.0	2.6	0.3	2.8	2.6	3.9	3.0
K <sub>2</sub> O	3.3	5.7	3.9	0.26	4.2	4.1	3.7	4.5
P <sub>2</sub> O <sub>5</sub>	0.2		16		21	16	0.2	11
Pb	14.7	0.003		0.0015			15.7	
U	6.8						5.6	
Th	28.8						16.9	
VLTL	-		3.0		5.3	1.7	-	2.2
TOT	102.0		95.9		97.4	94.6	100.4	98.6

**Table 3.2.1b:** Cross, Iddings, Pirsson, and Washington (CIPW) norm analysis.

	Sugarloaf	Paradise
Qz	20.0	20.4
K-fld	19.5	21.9
Plag (andesine)	47.8	46.9
Biotite		
Hornblende	13.2	10.0
Magnetite		
Ilmenite	1.3	1.1
Apatite	0.2	0.2

**Table 3.2.2:** Particle size distribution, organic carbon, pH and water saturation percent of Moraine Creek soil. U.M. = upper meadow, L.M. = lower meadow, M.C. = middle cascades (see Fig. 2.1).

location	bedrock	depth (cm)	particle size distribution (%)			organic C (%)	pH	water satur. (%)
			sand	silt	clay			
U. M.	Paradise	40-50	90	6	4	1.5	6.13	36
L. M.	Sugarloaf	30-40	90	7	3	1.9		
M. C.	Sugarloaf	40-50	97	2	1		6.86	32
M. C.	Sugarloaf	0-5	94	4	2	4.4	6.65	28
M. C.	Sugarloaf	S.BED	96	3	1	1.2	6.76	31

**Table 3.2.3:** Exchangeable cations at the pH of the soil. All values are in mEq/100g.

bedrock	depth (cm)	XCa	XMg	XNa	XK	SUMXbase
Sugarloaf	40-50	1.290	0.195	0.031	0.027	1.543
Sugarloaf	0-5	1.220	0.154	0.023	0.049	1.446
Sugarloaf	S.BED	1.335	0.208	0.038	0.038	1.619
Paradise	40-50	1.100	0.174	0.057	0.052	1.383

**Table 3.2.4a:** Free (secondary) iron, aluminum and manganese oxides and hydroxides in Moraine Creek soil extracted by the dithionate method. All values are in mg/kg.  $Ox_S-Ox_R$  gives the actual free oxide in soil, since the Ox measured in the rock sample comes from other phases that might be present in the soil too (e.g. magnetite). L.M. = low meadow, U.M. = upper meadow (see Fig. 1).

SAMPLE	GRAIN SIZE	Fe	Mn	Al	Fe <sub>S</sub> -Fe <sub>R</sub>	Mn <sub>S</sub> -Mn <sub>R</sub>	Al <sub>S</sub> -Al <sub>R</sub>
Sugarloaf	<200mesh	2394	36	384	-	-	-
Paradise	<200mesh	2176	40	422	-	-	-
L.M. B horiz.	<200mesh	9360	237	943	6966	201	559
L.M. B horiz.	NATURAL	7761	247	485	5368	212	101
L.M. A horiz.	<200mesh	6944	84	1091	4550	49	707
L.M. S.BED	<200mesh	4446	40	766	2052	4	382
U.M. B horiz.	<200mesh	2168	11	1188	-84	-29	766

**Table 3.2.4b:** The ratio between iron leached with a 0.1M HNO<sub>3</sub> solution (Fe lch) and iron extracted by the dithionate method (Fe extr).

SAMPLE	Fe extr	Fe lch	$\frac{\text{Fe lch}}{\text{Fe extr}}$
Sugarloaf	2394	7992	3.3
Paradise	2176	7446	3.4
L.M. B horiz.	9360	6867	0.7
L.M. B horiz.	7761	7446	1.0
L.M. A horiz.	6944	3343	0.8
L.M. S.BED	4446	3167	1.5
U.M. B horiz.	2168	5184	0.7

**Table 3.2.5a:** Stream water composition in Moraine Creek. All elements are in  $\mu\text{M}$ , ANC in  $\mu\text{eq/l}$ , Pb and Cd in  $10^{-11}\text{M}$ . pH and ANC were measured in a nonacidified sample.  
 >.45 = the concentration in the particulate fraction, collected on a  $0.45 \mu\text{m}$  Millipore filter.  
 pH 1 = the concentration in the water after acidifying with HNO<sub>3</sub> acid to pH of 1.  
 <1000 = the concentrations in the water after dialysis through a 1000 MWCO membrane.  
 dgst = digestion with aqua regia.

	<u>spring 1988</u>				
	lake water		<1000	st.#5	
	>.45	pH1		>.45	pH1
Pb	8.5	11.3	0.36	1.0	3.6
Cd		1.9	0.11		0.71
Fe <sub>tot.</sub>	0.09	0.22	0.02	0.8	1.2
Mn	0.0	0.016	0.002	0.031	0.033
Al					
Mg	0	1.6		0	17
Ca	0	15		0	67
K	0	2.8		0	16
Na	0	8.7		0	78
Sr	0	0.03		0	0.41
Si(OH) <sub>4</sub>	<5	36		<5	207
pH		5.5			5.5
ANC		35			248
temp.		11			12

Table 3.2.5a: cont.

fall 1987, 1988

	st.#1		st.#2	st.#3		
	<1000	pH1	pH1	<1000	>.45	pH1
Pb	1.6	2.3	2.3	1.5	0.9	3.0
Cd	0.27	0.8	0.89	0.11	0.27	0.89
Fe <sub>tot.</sub>	0	0.86	0.8-.9	0.1	0.23	0.7-.9
Fe(II)		0.02	0.09		0.09	0.14
Mn	0	0.03	0.02	0.005	0.01	0.013-.016
Al		0.7	0.9-1.2		0.3	1.1
Mg		10	16		0	19-23
Ca		47	62		0	75-85
K		11	11-13		0	15
Na		65	91		0	100-109
Sr		0.3	0.38-.41		0	0.55-.66
Si(OH) <sub>4</sub>		221	246-247		0	278-292
pH		6.5	5.6-6.6			5.5-6.8
ANC		188	235-237			282-297
temp.		13	9-10			10-14

fall 1987, 1988

	st.#4		st.#4a	st.#5		st.#6	st.#7	
	pH 1	dgst	pH 1	<1000	>.45	pH 1	pH 1	
Pb	3.0	3.9	8.1	0.15	1.7	4.1-5.8	0.7	3.2
Cd			1.5	0.25	1.8	0.3-.58		1.6
Fe <sub>tot.</sub>	0.8-.9		1.45	0.11	0.47	1.1-1.3	0.3	0.75
Fe(II)	0.23		0.02			0.52		
Mn	.009-.02		0.09	0.002	.002	.03-.05	0.007	0.02
Al	0.8-1		1.9					
Mg	23-24		40		0	32-35	10	15
Ca	85-87		160		0	11-12	70	80
K	15-18		28		0	20-24	11	13
Na	109-113		130		0	126-130	100	100
Sr	0.5		0.8		0	0.7	0.2	0.3
Si(OH) <sub>4</sub>	253-281		274		<5	263-288	121	164
pH	5.6-6.6		6.6			6.1-6.3	5.6	
ANC	310-316					415-445	173	
temp.	10-11					8-10	11	

**Table 3.2.5b:** Composition of ground water in Moraine Creek. All elements are in  $\mu\text{M}$ , ANC in  $\mu\text{eq/l}$ , Pb and Cd in  $10^{-11}\text{M}$ . pH and ANC were measured in a nonacidified sample. The spring is located near st. #1.

fltr = the concentration in water after filtration through a  $0.45\ \mu\text{m}$  Millipore filter.

pH 1 = the concentration in the water after acidifying with  $\text{HNO}_3$  acid to pH of 1.

dg = digestion with aqua regia.

	<u>spring</u> pH 1	<u>st.#1</u> pH 1	<u>st.#2</u> pH 1	<u>st.#3</u> pH 1	<u>pH 1</u>	<u>st.#4</u> fltr	<u>dgst</u>	<u>st.#5</u> pH 1
Pb	7.05				514	0.58	1240	156
Cd	5.79 dg				129	3.74	102	6.05
Fe <sub>tot.</sub>	1.25	30	40	236	62	0.16	180	31
Fe(II)		1.4	1.5	4	0.9			1.6
Mn	0.053	0.95	2.95	12	15.3	0.03	8.4	0.36
Al	1.15				48	0.3	93	9.3
Mg	17	97	25	81	27	24		42
Ca	72	147	100	182	100	85		135
K	11	29	16	31	21	21		79
Na	91	109	91	96	109	109		135
Sr	0.4	1.1	0.7	1.3	0.7	0.6		0.9
Si(OH) <sub>4</sub>	256	506	292	402	260			306
pH	5.8	5.5	6.1		6.3			6.1
ANC	250	220	235	288	331			475
temp.	8	9	11		12			12.5

**Table 3.2.5c:** Atmospheric deposition, Moraine Creek. Dry deposition in nanomole/m<sup>2</sup> hr, rain in nM.

	<u>dry deposition</u>		<u>rain</u>
	<u>spring 88</u>	<u>fall 88</u>	<u>fall 88</u>
	<u>dry impactor</u>	<u>wet impactor</u>	
Pb	0.057	0.167	6.92
Cd	0.029	0.054	
Mn	0.72	1.4	229
Fe	8.9	8.9	1270

**Table 3.2.5d:** Isotopic composition of lead in stream water, ground water, rock, and soil from Moraine Creek.

SAMPLE	$^{206}\text{Pb}/^{207}\text{Pb}$	$^{208}\text{Pb}/^{207}\text{Pb}$	$^{206}\text{Pb}/^{204}\text{Pb}$
Lake water, spring	1.183 $\pm 0.5\%$	2.422 $\pm 0.5\%$	-
Ground water, upper meadow fall	1.279 $\pm 0.1\%$	2.442 $\pm 0.1\%$	20.00 $\pm 2.2\%$
Stream water, m. cascades fall	1.247 $\pm 0.1\%$	2.466 $\pm 0.1\%$	19.34 $\pm 0.5\%$
Stream water, m. cascades fall	1.249 $\pm 0.1\%$	2.471 $\pm 0.1\%$	-
Stream water, lower meadow fall	1.270 $\pm 0.1\%$	2.454 $\pm 0.1\%$	19.61 $\pm 0.9\%$
Stream water, lower cascades fall	1.297 $\pm 0.1\%$	2.462 $\pm 0.1\%$	-
Stream water, lower cascades spring	1.218 $\pm 0.1\%$	2.445 $\pm 0.2\%$	19.07 $\pm 0.3\%$
Roaring River fall	1.264 $\pm 0.1\%$	2.457 $\pm 0.1\%$	19.65 $\pm 0.7\%$
Soil (30cm deep) leached, pH 1	1.250 $\pm 0.02\%$	2.523 $\pm 0.02\%$	19.07 $\pm 0.5\%$
Sugarloaf leached at pH 1	1.326 $\pm 0.1\%$	2.574 $\pm 0.1\%$	20.34 $\pm 0.5\%$
G. Sugarloaf, WR Moraine Creek	1.224 $\pm 0.1\%$	2.514 $\pm 0.1\%$	19.27 $\pm 0.5\%$
Paradise G.,WR Moraine Creek	1.215 $\pm 0.1\%$	2.514 $\pm 0.1\%$	18.89 $\pm 0.5\%$

**Table 3.2.6:** A comparison between measured and calculated IC based on mixing between ground water and stream water only.

	discharge(L·s <sup>-1</sup> )	Pb(ng/L)	206/207	206/204
<b>measured:</b>				
U. Stream	20	8.0	1.247	19.34
Ground water	12	(X)	1.326	20.34
D. stream	32	7.0	<b>1.270</b>	<b>19.61</b>

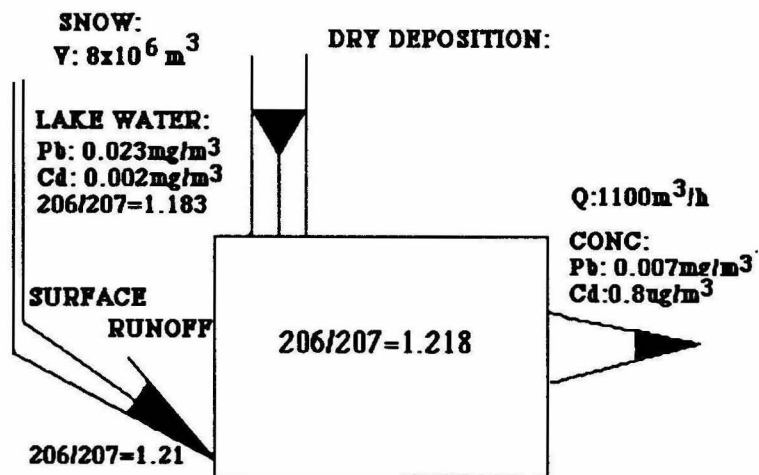
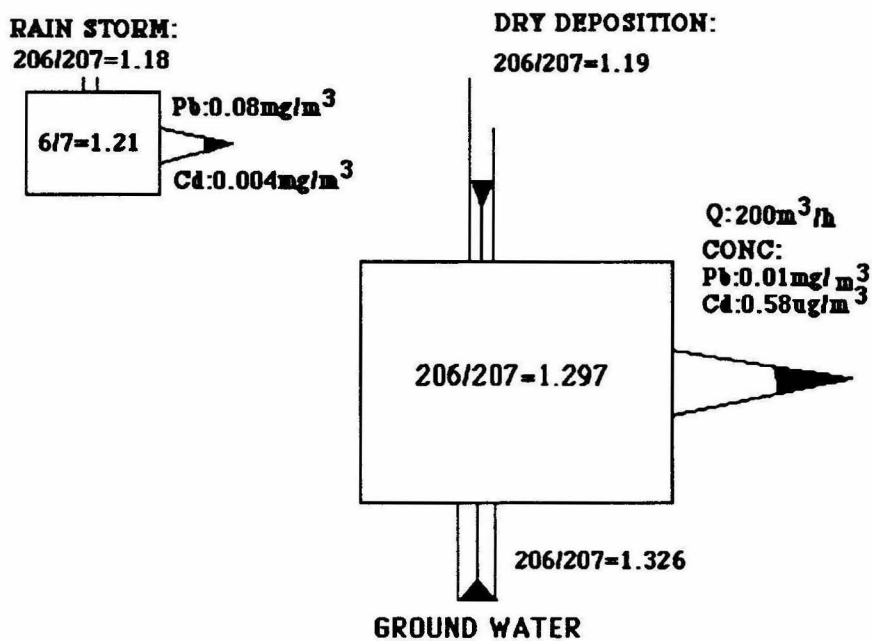
Choose a Pb concentration in ground water (X) so that  $(U+G)/D \rightarrow 1$   
 $X = 5.33$   
 $(U+G)/D = 1.00$

<b>calculated IC of D. Stream station:</b>			206/207	206/204
			<b>1.270</b>	<b>19.63</b>

	Discharge(L·s <sup>-1</sup> )	Pb(ng/L)	206/207
<b>measured:</b>			
U. Stream	32	7.0	1.270
Ground water	18	(X)	1.326
D. stream	50	10.0	<b>1.297</b>

Choose a Pb concentration in ground water (X) so that  $(U+G)/D \rightarrow 1$   
 $X = 15.33$   
 $(U+G)/D = 1.00$

<b>calculated IC of D. stream station:</b>			206/207
			<b>1.301</b>

a) **SPRING:**b) **FALL:**

**Figure 3.2.1:** Isotopic composition of lead in atmospheric precipitations and in stream water in Moraine Creek: (a) spring; (b) fall.

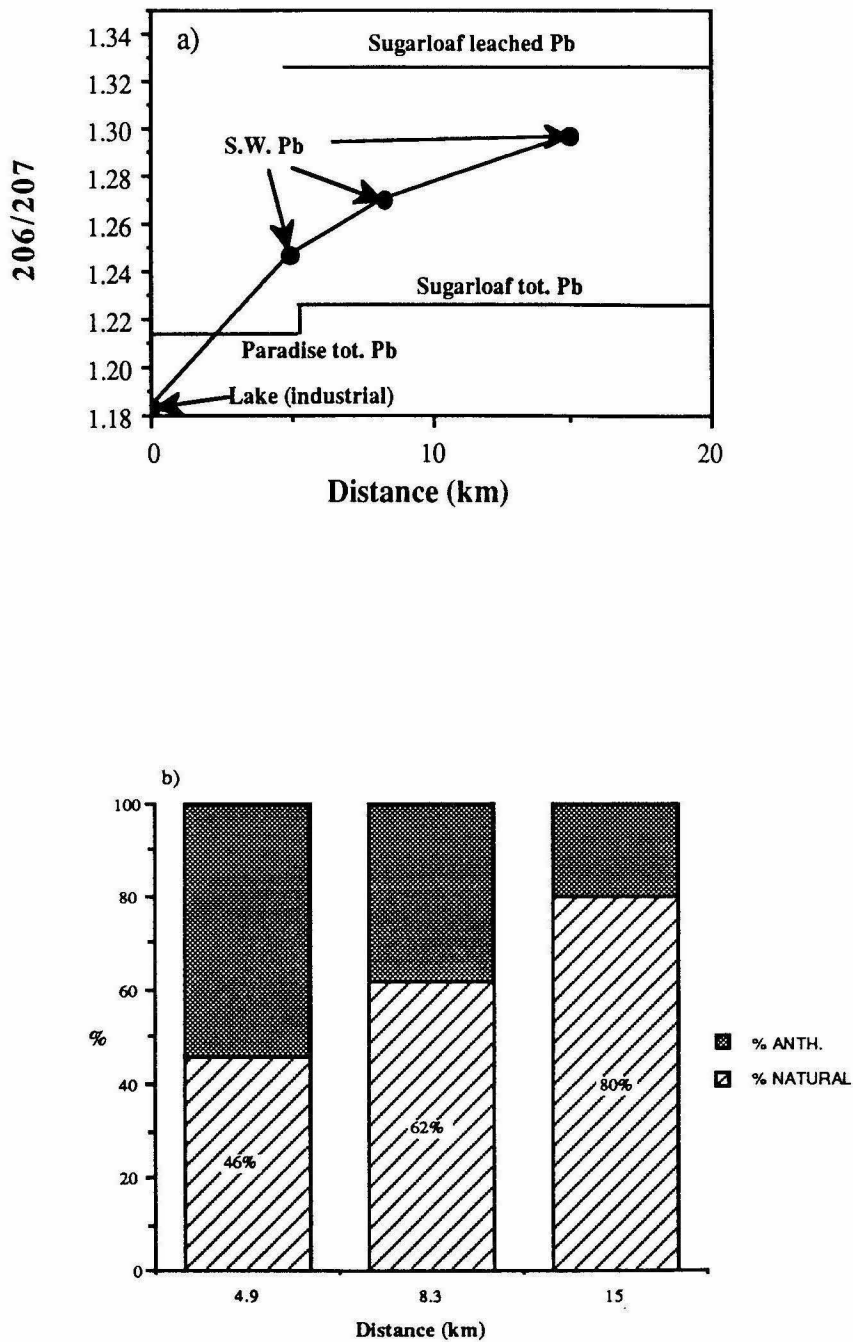


**Figure 3.2.2:** (a) Change of  $^{206}\text{Pb}/^{207}\text{Pb}$  ratios in stream water during the fall as a function of the distance from the lake; (b) the calculated fraction of natural lead in stream water based on mixing between lake lead and rock leached lead.

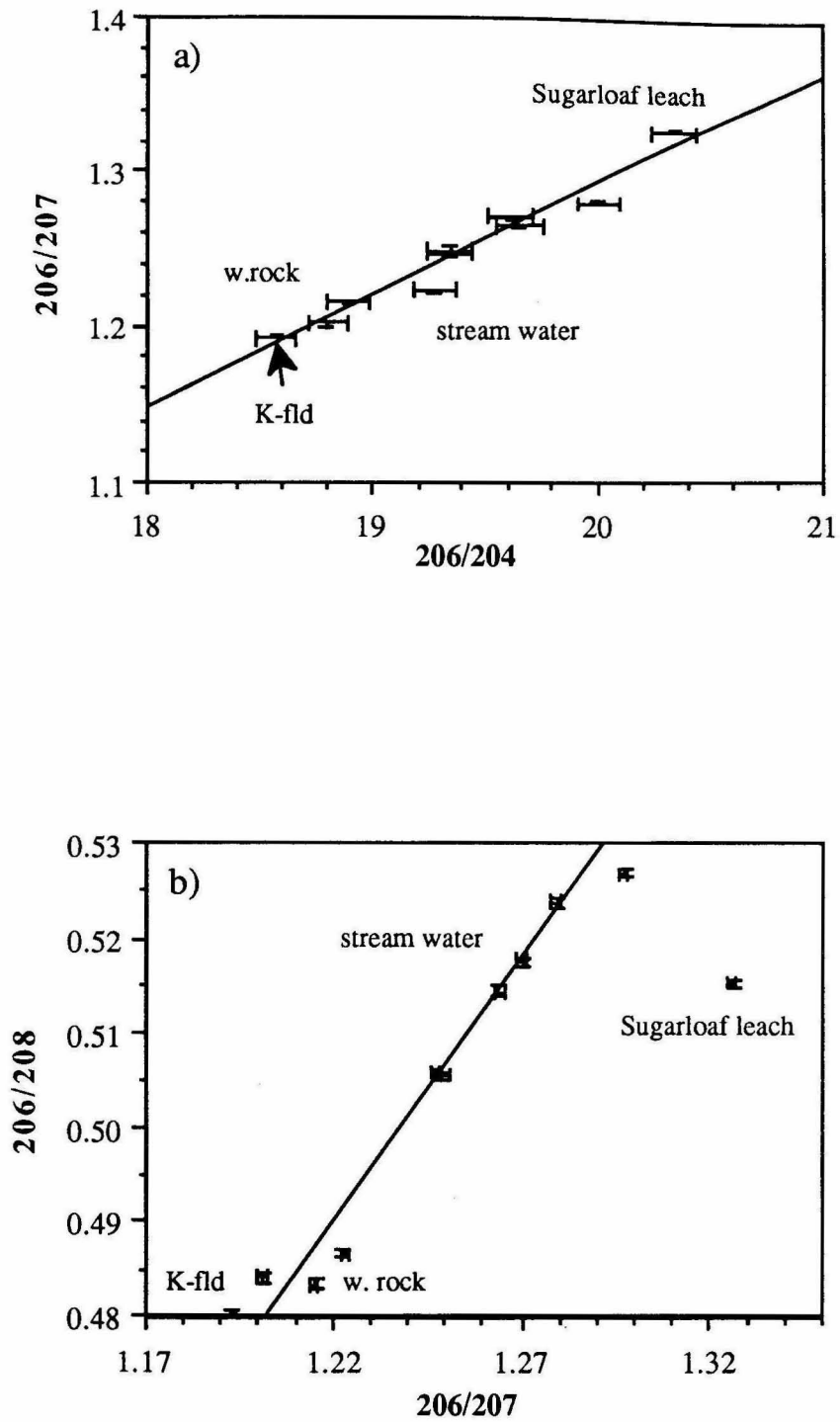


**Figure 3.2.3:** (a)  $^{206}\text{Pb}/^{207}\text{Pb}$  vs.  $^{206}\text{Pb}/^{204}\text{Pb}$  of total lead in rocks (K-feldspars from Chen and Tilton, 1990), rock leached phase and Moraine Creek stream waters; (b)  $^{206}\text{Pb}/^{208}\text{Pb}$  vs.  $^{206}\text{Pb}/^{207}\text{Pb}$  of the same samples.

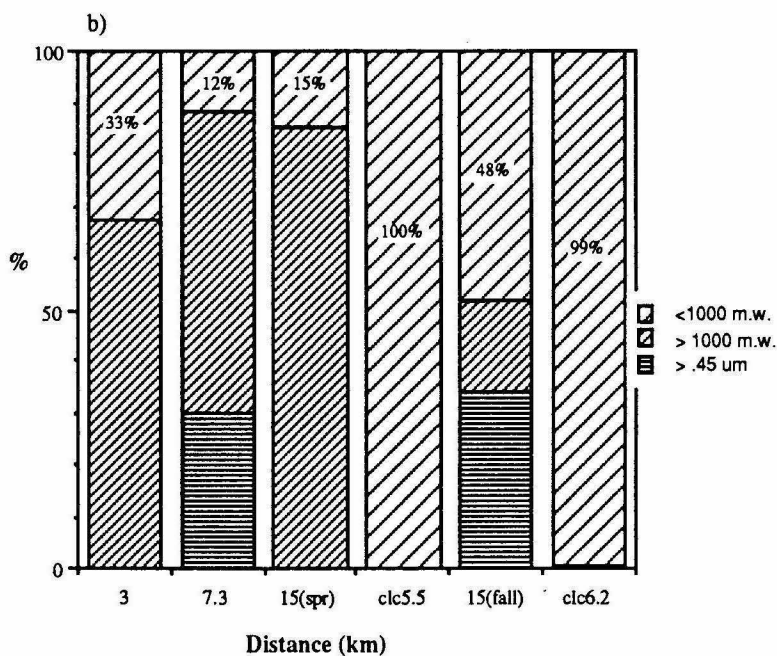
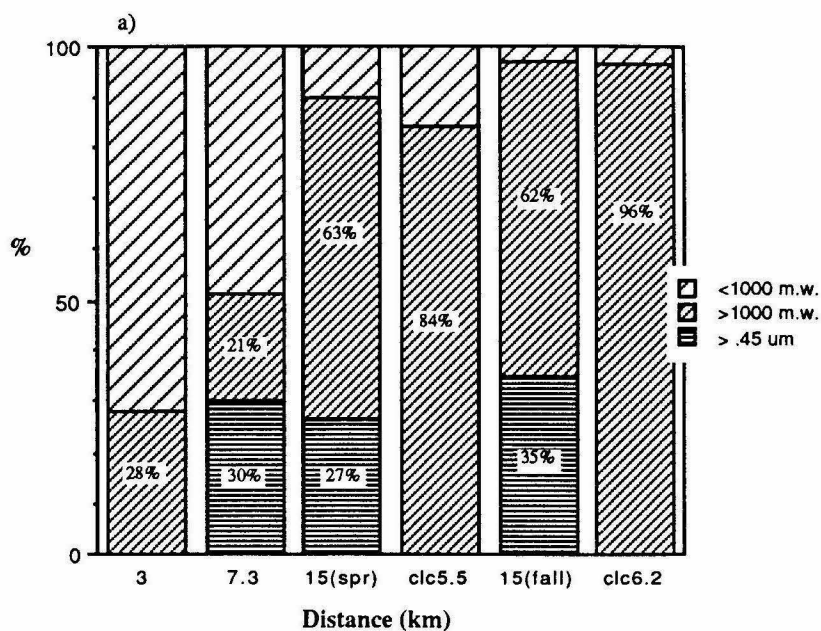


**Figure 3.2.4:** (a) The various forms of lead in stream water compared with the adsorption model of Dzombak (1986); (b) the various forms of cadmium in stream water compared with the adsorption model of Dzombak (1986). 15(spr) = measured at st. 5, 15 km from the lake in the spring. 15(fall) = measured at the same station in the fall. clc 5.5 = the calculated speciation at pH 5.5. clc 6.2 = the calculated speciation at pH 6.2.

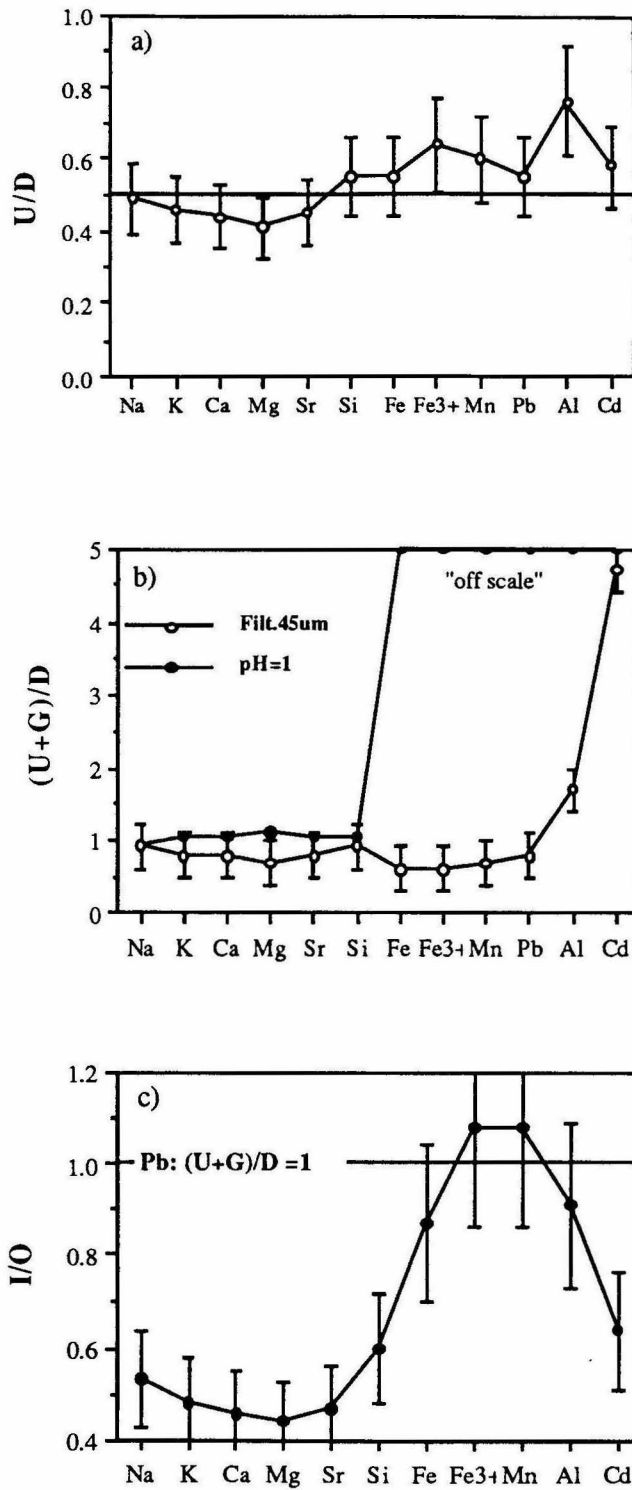


**Figure 3.2.5:** (a) Upstream/downstream (U/D) flux ratio of various cations in the two segments of Moraine Creek; (b) (U+G)/D flux ratio of the same cations measured both at pH 1 and in filtered water; (c) (U+G)/D ratio normalized to (U+G)/D of lead equals unity. For definition of term see text.

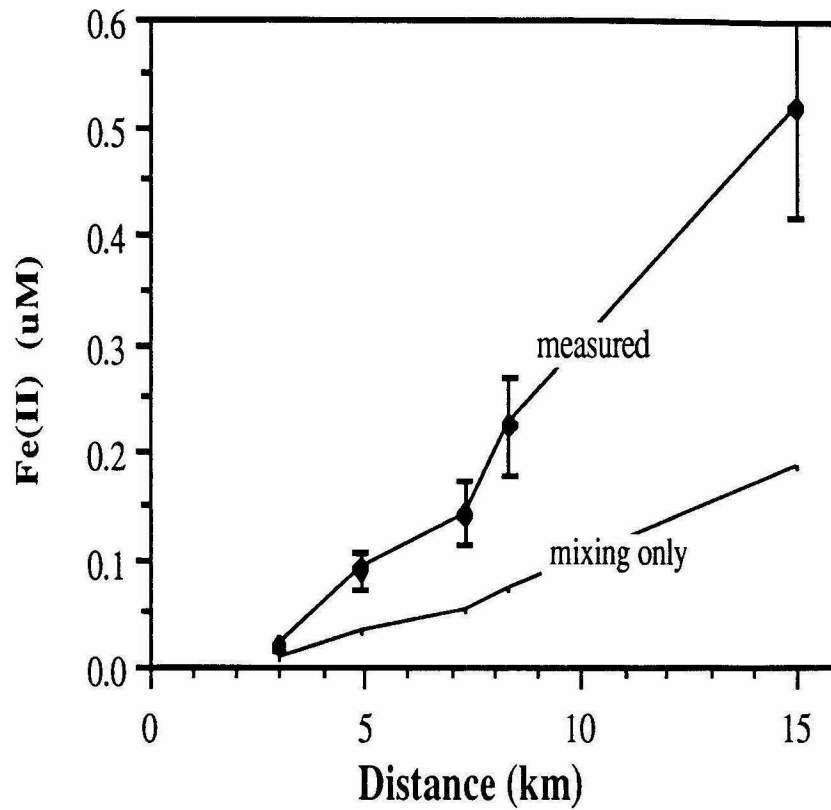


**Figure 3.2.6:** Ferrous iron (Fe(II)) concentration in the stream water as a function of distance. The calculated line is based on simple mixing with ground water, whose Fe(II)/Fe(III) ratio is 0.05.

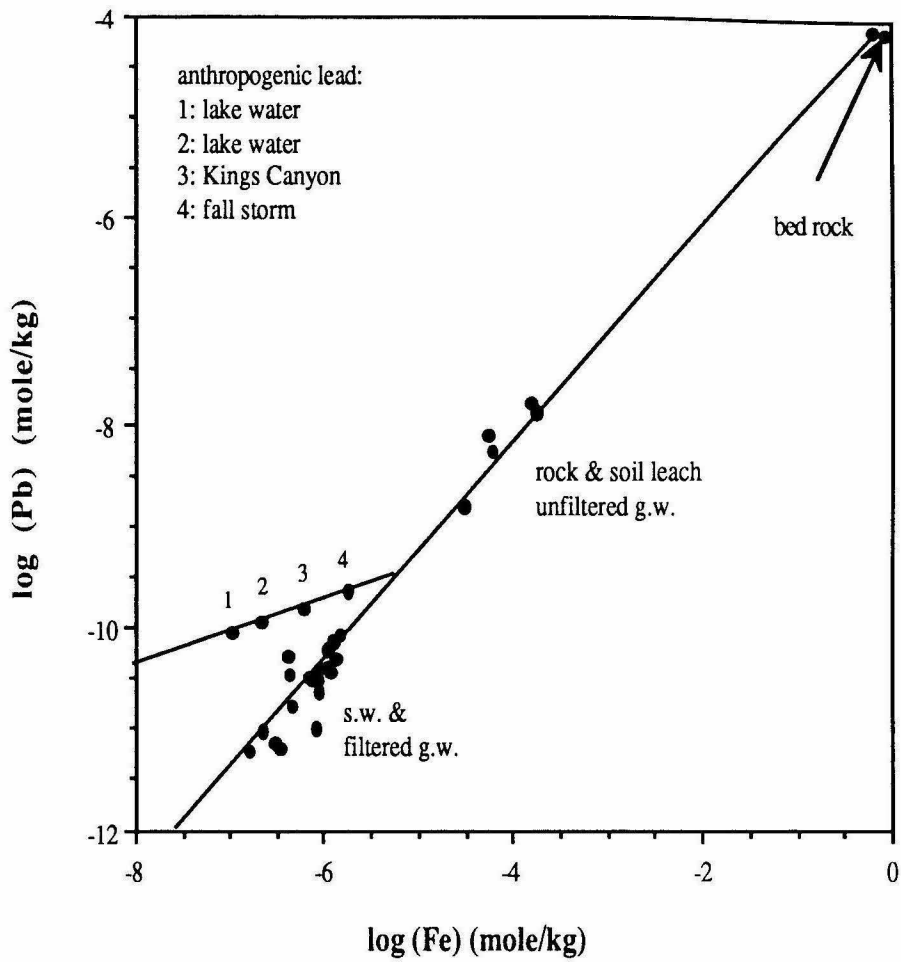


**Figure 3.2.7:** Lead-iron relations in rock, rock and soil leach, stream water, and ground water from Moraine Creek.

## **Chapter 4: Transport of natural lead in rivers: Global flux implications**

This chapter is an attempt to generalize the results from the previous chapter in order to understand the fate of natural lead in rivers. In addition to the work described previously, new data of the concentrations of lead, iron and other elements in rock and unpolluted water samples from granodiorite, basalt, and carbonate terrains are presented and discussed. Samples of granodiorite, basalt and dolomite rocks, as well as biotite and feldspar mineral separates, are used for laboratory leaching and adsorption-desorption experiments. The chapter concludes with an introduction of a new model for the speciation and behavior of trace metals in aquatic systems. The reported concentrations of trace metals in deep-sea water are used in order to test the speciation model.

### **4.1. Introduction**

At present, most of the lead found in the atmosphere and in surface water is introduced directly or indirectly by human activity; therefore its concentrations probably exceed its natural abundance by several orders of magnitude (Patterson, 1965; Murozumi et al., 1969; Boyle et al., 1986; Patterson and Settle, 1987; Shen and Boyle, 1987; Struges and Barrie, 1987; Maring et al., 1989; see section 1.5).

It has been stated repeatedly that lead and other trace metals in rivers are attached to particles (Hem, 1976; Getz et al., 1977; Benes et al., 1985; Sigg et al., 1987; Meybeck and Helmer, 1989; see section 1.3.2). As previously pointed out, using a 0.45  $\mu\text{m}$  pore size filter to separate particulate matter from the solution is an arbitrary, operation-dependent process (Laxen and Chandler, 1983; Morel and Gschwend, 1987; see chapter 3). Therefore, most of the reported "dissolved load" of trace metals in rivers actually contain a substantial particulate (suspended) matter. The suspended ( $< 0.45\mu\text{m}$ )

load of trace metals in rivers is contained in nonlabile and labile reservoirs. The nonlabile reservoir is mostly colloids of crustal minerals which do not undergo exchange reactions with the solution. The particulate matter in the labile reservoir actively interacts with the solution. This labile particulate matter is composed of oxyhydroxides (e.g., Fe-hydroxides, Mn-oxides) and elements attached to particle surfaces (e.g., colloids of crustal minerals, oxyhydroxides, clays, organic colloids, and microorganisms). The adsorption of trace metals on surfaces in general, and iron hydroxides in particular, has been intensively studied, and is believed to be one of the main mechanisms for the attachment of trace metals to particle surfaces in natural-water systems (Benninger et al., 1975; Hem, 1976; Lewis, 1976, 1977; Vuceta and Morgan, 1978; Buffle and Altmann, 1987; Dempsey et al., 1989; see section 1.4.4).

The fraction of lead adsorbed at a certain pH on a given amount of adsorbent is highly dependent on the total concentration of lead (Davis and Leckie, 1978; Benjamin and Leckie, 1980, 1982). Therefore, in order to understand the adsorption of lead in the environment, it is important to study lead adsorption at very low total lead concentrations, similar to natural levels. In addition, it has been pointed out that competition with a major cation (Mg, Ca) may affect the adsorption of trace metals on surfaces (Dempsey and Singer, 1980; Benjamin and Leckie, 1982; Benjamin, 1983; Laxen, 1985), and that a multicomponents oxide system may have different adsorption sites available than a single oxide system (Anderson, 1990; Anderson and Benjamin, 1990a,b).

In Chapter 3, it was found that the molar ratio between natural lead and iron in a mountain stream draining a freshly exposed granodiorite terrain is more than 1:10,000, higher than the relative abundance of these elements in the granodiorite bedrock, approximately 1:8,000. More or less the same ratio between lead and iron is maintained both in the  $>0.45 \mu\text{m}$  and  $<0.45 \mu\text{m}$  fractions of the water. The ratio decreases upon

addition of anthropogenic lead to the system during spring snowmelt runoff and during a fall rain storm.

The reported molar ratios between lead and iron in the  $<0.45 \mu\text{m}$  fraction of water of the major rivers of the world range from 1:150 to 1:1,500 (Taylor and McLennan, 1985; Martin and Meybeck, 1979; Martin and Whitfield, 1983; Salomons and Förstner, 1984; Meybeck and Helmer, 1989). In addition, lead and iron show different profiles in surface ocean water, suggesting different mechanisms of removal by particles and uptake by organisms (Schaule and Patterson, 1981; Martin et al., 1989), and the lead to iron ratio in deep-ocean water is only 1:150 - 300 (Schaule and Patterson, 1981; Martin et al., 1989). Both the major river ratios and the deep-ocean water ratios are much lower than the ratios found in Chapter 3 and the Pb/Fe ratio found in the upper continental crust (1:6,500).

Martin and Meybeck (1979) and Martin and Whitfield (1983) pointed out that lead is 5 to 10 times enriched in river water relative to its crustal abundance, compared with aluminum. Trefry et al. (1985) also used Pb/Al ratios to study lead transport in the Mississippi river sediments, and Li (1981) used this ratio in sea water. The comparison between lead and iron is probably a better tool for studying the fate of lead on its way to the ocean since lead is probably more related to iron than to aluminum in regard to its transport in rivers (Benninger et al., 1975; Hem, 1976; Lewis, 1976, 1977; Buffle and Altmann, 1987; Dzombak and Morel, 1990; see section 3.2.4.5).

In this chapter, laboratory experiments have been combined with field work in order to explain two observations: 1) lead and iron behave in a similar manner in stream water, but have different profiles in the ocean; and 2) the high upper crust Fe/Pb ratio observed in unpolluted streams and fluvial sediments compared to the low Fe/Pb ratios observed in major rivers and in the ocean. The following experiments were undertaken in order to clarify the contrasting behavior of iron and lead in rivers and oceans: 1) leaching experiments of rock and soil samples illustrate the weathering stoichiometry

between iron and lead in different environments; 2) the adsorption behavior of lead to iron hydroxide surfaces was quantified in an experiment which simulates some important natural conditions; 3) the importance of desorption processes in rivers and sea water was assessed in experiments which tested the effect of organic chelators and chloride on adsorption of lead; and 4) chemical speciation calculations were used to extrapolate experimental findings to typical river and sea water environments.

#### 4.2. Results

Lead and iron concentrations in solutions leached from granodiorite, basalt, carbonate, soil, feldspar and biotite, as well as in water samples, are plotted in Figures 4.1a, b, and c. Each sample is compared to the line whose slope has a Pb/Fe ratio equal to that of the upper continental crust (1:6,500: Taylor and McLennan, 1985). The deviation of each sample from the line in Figures 4.1a, b, and c and 4.2 is a measure of its deviation from the upper continental crustal ratio. A more detailed examination of the Fe/Pb ratio in rock, rock and soil leach, stream water, and ground water samples in a granodiorite terrain is plotted in Figure 4.2.

The concentration of major cations and lead in solutions used for the adsorption experiment, the EDTA desorption experiment, the sea water desorption experiment, and the isotopic composition of biotite and spiked lead in solution are given in Table 4.1. Only the particles retrieved from the 100 ml aliquot at pH 8.5 provided an interpretable X-ray diffraction pattern. The particles formed a solid solution between goethite, aluminum, and silica hydroxides with a substantial fraction of amorphous material. The amount of particles collected on filters was not large enough to get a good X-ray diffraction pattern; nevertheless, the main peak (of goethite) appeared in the patterns obtained from the retained particles down to pH 3.5.

The particles remain unaffected by lowering the pH from 8.5 to 6.0; below pH 6.0, however, both the particles and the solution start to change. The particles become

smaller, and show signs of partial dissolution and reprecipitation. The concentrations of aluminum and dissolved silica in solution ( $<0.025 \mu\text{m}$ ) increase continuously until they reach their total concentration at pH 4.5 (Table 4.2). Iron concentration in the  $<0.025 \mu\text{m}$  fraction remains almost unaffected by lowering the pH to pH 4.5; however, at pH 3.5,  $\text{Fe}(\text{OH})_3\text{s}$  approaches its stability edge (Morel, 1983), and is partially dissolved. In addition, some of the iron particles become small enough to pass through the filter pores. The pH-dependence of lead adsorption on particles is plotted in Figure 4.3. There is a substantial difference between biotite lead and the spiked lead at low pH values.

Approximately 24% of the lead is desorbed from the particles in the presence of a  $1.15 \times 10^{-7}\text{M}$  EDTA solution at pH 6.0 (Table 4.1, Fig. 4.4a), and 12% is released in the presence of sea water at pH 7.5 (Table 1). In both cases, the total amount of iron is  $0.7 \mu\text{M}$ , and the total amount of Pb (mostly  $^{208}\text{Pb}$ ) is approximately  $5 \times 10^{-10}\text{M}$  (Table 4.1).

### 4.3. Discussion

#### 4.3.1. The release of lead and iron from rocks and soil

The release of elements during leaching of minerals is a very complex process, involving ion-exchange reactions, hydration and hydrolysis. It is presently believed that hydrolysis controls the rate and the nature of mineral dissolution (Murphy and Helgeson, 1987; Schott and Petit, 1987; Holdren and Speyer, 1987; Bunker and Casey, 1990). Using NMR technique, Bunker and Casey (1990) demonstrate that there are several types of surface hydroxide groups which have different hydrolysis properties. In addition, it has been pointed out that solution composition has a large effect on the relative release of different elements from the mineral surface (Nesbitt and Shoty, 1990; Shoty and Nesbitt, 1990).

Formation of secondary phases on the surface of weathered minerals is a common phenomenon which may alter the relative abundance of various elements in

solution (Stumm and Morgan, 1981; Petit, 1990). Since it is almost impossible to mimic natural dissolution of minerals and rocks in the laboratory, low-pH solutions which eliminate the formation of secondary phases, such as iron hydroxides on the surface of the weathered minerals, have been used. Furthermore, dissolution experiments of muscovite and albite at a wide range of pH values (1.4 -13) indicate congruent dissolution of both minerals under most pH values, with increasing rates at the low-pH range (Knauss and Wolery, 1986, 1989). Therefore, comparing the release of iron and lead at low pH values in the laboratory with their appearance in stream and ground water in catchments of known bedrock composition might provide some insight into the coupled process of iron and lead release from rock.

As mentioned before, the amount of deviation of the Fe/Pb ratio of each sample from the upper continental crustal ratio (Figs. 4.1a,b,c and 4.2) is an indication of different source composition and different release and transport mechanisms. K-feldspar and plagioclase are the main reservoirs of lead in magmatic rocks such as granodiorite, and biotite (as well as magnetite and hornblende) is the main reservoir of iron. Hence, a granodiorite rock and the leaching solution have Fe/Pb values which fall somewhere between the ratios of these minerals (Fig. 4.1a).

The lead and iron leached from the biotite show a very similar ratio as the biotite, suggesting a similar rate of release. In contrast, there is an excess of iron relative to lead in the leached fraction of the feldspars (77% K-feldspar, 19% plagioclase). The higher rate of iron release from the feldspar sample has a two-fold explanation: 1) iron comes mainly from inclusions and impurities in both feldspars, while lead comes from the mineral lattice; and 2) the K-feldspar is more resistant to weathering and releases its lead more slowly than the plagioclase. It has been reported that under normal conditions, the rates of biotite and plagioclase weathering are comparable (Harriss and Adams, 1966; Boettinger, 1988). Since in most rocks the amount of iron coming from weathering of feldspars is negligible, the slow release of

lead from K-feldspar minerals is probably the main source for the relative iron enrichment in weathering products of fresh, unaltered granodiorite.

The concentrations of lead and iron in solutions which leached the basalt are determined by the high Fe/Pb ratio in the rock (Fig. 4.1b). The Fe/Pb ratios in the leached sample and in the ground water sample are almost identical. Similar Fe/Pb ratios can be maintained both in the rock-leach and the ground water only if lead and iron share the same fate after their release from the rock. Both ground water and rock-leach ratios are lower than the bulk rock sample (an excess of lead). The main reservoir of lead in the basalt is the plagioclase, while iron is mainly stored in the olivine, pyroxene and ore minerals. The rate of mineral weathering in basalt rocks is consistent with the susceptibility series: glass > olivine > plagioclase > pyroxene > ore minerals (Eggleton et al., 1987). Hence, the rate of lead and iron release is a complicated interplay involving the relative amount of each phase and its composition. Usually the glass has very low Fe/Pb ratios compared with the whole rock, so that the Fe/Pb ratio is expected to be lower in both the leached phase and in the ground water than in the rock (an excess of lead).

The insoluble residue of the dolomite, mainly composed of clay minerals, has a Fe/Pb ratio very similar to the upper continental crustal ratio (Fig. 4.1c). Since the clay minerals are reworked continental crustal material, whose average composition is granodiorite, similar Fe/Pb ratios in a fresh granodiorite and in reworked crustal material demonstrate the similar behavior of lead and iron throughout the weathering cycle. Moreover, Fe/Pb ratios similar to the upper continental crustal ratio were found in shale and clays collected in a large variety of sites (see Table 1.2).

The soluble (mostly carbonate) part of the rock has a low Fe/Pb ratio compared with the ground water ratio. Therefore, it seems that at high carbonate concentrations, lead speciation is controlled by carbonate rather than by adsorption on iron hydroxides (Stumm and Morgan, 1981; Hem, 1976).

New surfaces of the Sugarloaf granodiorite were exposed in Moraine Creek 10,000 years ago at the end of the Wisconsin Ice Age. A slow release of lead from K-feldspar minerals in the fresh granodiorite probably accounts for the relative enrichment of iron in the leached rock, the stream water, and the ground water samples compared with the bedrock (Fig. 4.2). The soil, which contains more weathered minerals than the rock, has a smaller excess of iron since the K-feldspar minerals are more weathered and release more of their lead. For example, the  $^{206}\text{Pb}/^{207}\text{Pb}$  ratio decreases in the following order (see Table 3.2.5d): leached rock (1.326), leached soil (1.250), whole rock (1.224), and rock feldspar (1.207). Therefore, the soil leach contains more feldspar lead than the rock leach and less than the whole rock sample.

The leached rock has a smaller excess of iron than the stream and ground water, probably because of an experimental artifact (grinding the rock). The K-feldspar and plagioclase which are less ductile and consist of larger minerals, are more affected by grinding than the biotite. Moreover, K-feldspar is more affected by grinding than plagioclase since K-feldspar minerals are weathered mostly along defects associated with exsolution lamella that are exposed by grinding (Holdren and Speyer, 1987). The effect of grinding on Fe/Pb ratio is evident when comparing ground versus unground soil samples; the unground sample has a higher excess of iron compared with the ground sample (Fig. 4.2).

A Fe/Pb ratio similar to the granodiorite ratio reported here is found in soils and sediments from a wide range of environments (see Table 1.2). Brimhall and Dietrich (1987) measured lead and iron profiles in a podzole developed on beach sand overlying graywacke bedrock in northern California and found out that lead and iron have similar profiles in the soil, and that the Pb/Fe ratio is approximately 1:7,500, very close to the upper continental crustal ratio (1:6,500). Knyazev (1986) reports that lead and iron show similar behavior during the process of soil formation on granodiorite bedrock. Scott (1986) suggests that lead is attached to hematite minerals in a sedimentary terrain,

and Laville-Timsit and Wilhelm (1979) and Thornber and Wildman (1984) report a similar transport of lead and iron around sulfide deposits. It seems that the Fe/Pb ratio found in the bedrock is likely to be maintained (with some modifications) during transport in unpolluted rivers.

#### 4.3.2. Adsorption of lead on iron particles

The fraction of lead attached to particles larger than  $0.025\ \mu\text{m}$  as a function of pH is plotted in Figure 4.3. It seems that at a pH value above 4.0, most of the lead is attached to particles. At a pH of 5.2-8.5, the fraction of biotite lead which has been in solution prior to the formation of the particles, and the fraction of spiked lead added after the precipitation of the particles, have an identical adsorption pattern; however, at lower pH values, there is a substantial difference between the amount of particulate spiked lead and the amount of particulate biotite lead (4% difference at pH 4.5, 17% difference at pH 3.5). Less of the biotite lead is released into solution, probably since some of this lead has been coprecipitated with the particles.

The data in Table 4.2 illustrates the contrasting behavior of Si, Al, Fe and Pb: the release of Si to solution starts at pH 8.0 (13%) and the release of Al starts at pH 6.0 (10%), when more than 98% of the Pb and 100% of the Fe are still in particulate form. At pH 5.2, approximately 40% of both Si and Al are already in solution while 95% of the Pb and more than 99% of the Fe are retained by particles. At pH 4.5, both Al and Si are completely dissolved whereas 71-75% of the Pb and 99% of the Fe remain in particulate form. The release of both Al and Si to solution is accompanied by dissolution and reprecipitation of the particles, and a decrease in their grain size. These observations and the fact that the main X-ray diffraction peak of goethite is observed in samples down to pH 3.5 suggest that Pb is mainly adsorbed on iron hydroxide surfaces, and that silica and aluminum hydroxides provide the "cement" which holds the iron particles together at higher pH solution.

The adsorbed fractions of the spiked (surface) lead can be account for by an equilibrium adsorption model which is based on the following measured parameters (Westall, 1980, 1987): 1) total concentration of  $\text{Fe}^{3+}$ ; 2) concentrations of other dissolved major ions (such as calcium, magnesium and bicarbonate); and 3) the measured pH. In addition, the model assumes: 1) a site density of 10 OH groups per  $\text{nm}^2$ ; 2) specific surface area ( $5 \text{ m}^2/\text{g}$ ) based on estimated particle shape and size from SEM pictures, and density of  $2 \text{ g}/\text{cm}^3$ ; 3) the empirical surface equilibrium constant reported by Dzombak (1986); 4) a diffuse layer model; and 5) no competition with other cations on surface sites (Fig. 4.3). Combining the estimated site density with the specific surface area ( $5 \text{ m}^2/\text{g}$ ) and the measured total iron concentration ( $0.052 \text{ g}/\text{l}$ ), a site concentration of about  $4 \text{ }\mu\text{M}$  is obtained. The site concentration is, therefore, 0.4% of the total iron concentration. The model fits well the observed adsorption of spiked lead down to pH 3.5, and the high Mg concentration in solution does not affect the adsorption of lead. The only conclusive result from the experiment at pH 3.5, however, is the large difference between the adsorption of biotite lead and spiked lead, because at pH 3.5 a substantial fraction of the iron particles passes through the filter.

According to Dzombak (1986), the concentration of surface sites available for lead adsorption is approximately 2% of the total ferric iron concentration. The difference in site concentration between the model presented here and the values reported by Dzombak (1986) is a result of the smaller specific surface area of the experiment particles which are larger than common am- $\text{Fe}(\text{OH})_3$  particles ( $100\text{-}300 \text{ m}^2/\text{g}$ ; see Table 1.7). It is important to point out that an estimated fixed surface area is a major simplification since the particles change their size and shape while lowering the pH and, as a result, change their specific surface area.

In conclusion, the experiment demonstrates that at pH values higher than 4.0, lead is likely to be adsorbed on iron hydroxide as soon as iron particles start to form, in spite of high concentrations of other cations and mixed oxide particles. In addition, the

experiment suggests that some fraction of the rock-derived lead actually coprecipitate with iron hydroxides, and is less likely to be released back into solution.

### **4.3.3. Desorption of lead from iron particles**

#### **4.3.3.1. Effect of man-made organic chelators**

During the initial stages of the weathering cycle, lead is likely to be adsorbed and coprecipitate with iron particles; however, several processes might cause a substantial desorption of lead from these surfaces on the way to the ocean. It has been reported that the ratio between dissolved and particulate lead in polluted rivers is higher than in remote streams (Salomons and Förstner, 1984). The higher ratio can be either due to direct discharge of dissolved industrial lead or to transfer of lead from particles to solution. The second process was tested in desorption experiments.

The amount of lead adsorbed on surfaces of iron particles used in the previous experiment decreases from 98% to 76% in the presence of  $1.15 \times 10^{-7} \text{M}$  EDTA (Table 4.1; Fig. 4.4a). The chemical speciation model used for the adsorption experiment predicts that particulate lead will decrease from 98% to 70% under the conditions summarized in Table 4.1. Competition for coordinating trace metals between EDTA and surface sites has been reported by Vuceta (1976) for the system Pb  $\alpha$ -quartz and Cu  $\alpha$ -quartz. Vuceta (1976) observed a decrease in adsorbed lead from 78% to 48% when the concentration of EDTA was equivalent to the concentration of lead in the experiment ( $\text{Pb}_{\text{tot}} = 5 \times 10^{-7} \text{M}$ ).

EDTA is widely used in industry and as a substitute for polyphosphate in detergents, and is not biodegradable. Levels of EDTA between  $3 \times 10^{-8} \text{M}$  and  $1.5 \times 10^{-7} \text{M}$  have been reported recently in many European rivers (AIS, 1987; Frimmel et al., 1989). Furthermore, EDTA represents a wide range of man-made organic chelators released to rivers. Complexation of lead by EDTA and other man-made organic chelators would transfer a substantial fraction of lead from the particulate matter

to solution (Salomons and van Pagee, 1981; Dietz, 1982). In other words, EDTA and other anthropogenic compounds that compete for trace metals with reactive surfaces might cause a secondary pollution effect. The concentrations of dissolved lead in polluted surface water increases regardless of direct emissions of lead, and the association between lead and iron becomes less significant (Gobeil and Silverberg, 1989). Once in solution, lead is transported more efficiently than particulate lead. At the same time, EDTA is also dissolving a small fraction of ferric iron hydroxides (1 to 13% according to the model), which in turn probably releases coprecipitated lead as well.

The effect of EDTA on the speciation of Pb in river water was calculated using the following parameters: major ion concentrations from Meybeck and Helmer (1989),  $Fe_{tot} = 0.7\mu M$  from Taylor and McLennan (1985),  $pH = 7$ , and a natural lead concentration of  $Pb_{tot} = 6.0 \times 10^{-11} M$ . In addition, adsorption site concentration was fixed at 2% of the total iron concentration since natural iron particles are much smaller than the ones used in the experiment (Laxen and Chandler, 1982; see Table 1.7), and in many cases iron provides coatings on other particles, thus increasing its specific surface area (Buckley, 1989). With these parameters, the adsorption model predicts that 95% of the lead in river water will be adsorbed on iron surfaces (Fig. 4.4b). In the presence of  $10^{-8} M$  EDTA, the model predicts a substantial decrease in the amount of lead on the surface (only 35% remains on the surface), and in the presence of  $1.5 \times 10^{-7} M$  EDTA the adsorbed lead fraction will decrease to 4% (Fig. 4.4b).

#### **4.3.3.2. Effect of sea water: A new model for the speciation of trace metals in aquatic systems**

Estimates of the residence time of lead and iron in the deep-ocean water range from 1,100 years for lead and 1,800 years for iron (Martin and Whitfield, 1983) to 45 years for lead and 0.7 year for iron (Taylor and McLennan, 1985). The wide range of

values is attributed to the fact that a variety of methods and assumptions are used for the calculations. While Martin and Whitfield (1983) based their estimate on river flux and assumed relatively high concentrations in sea water, Taylor and McLennan (1985) based their flux estimate on the accumulation rate of lead and iron in deep-ocean clays and assumed lower concentrations in sea water (Li, 1981). All calculations were done under the assumption that the ocean is in steady state with respect to iron and lead. This assumption is questionable, especially for lead (Schaule and Patterson, 1981).

It is believed that the concentrations of trace metals in deep-sea water are largely determined by adsorption/desorption (or precipitation/dissolution) reactions on particle surfaces (Schaule and Patterson, 1981; Whitfield and Turner, 1987). Most elements in sea water can be grouped according to their depth profiles (Whitfield and Turner, 1987). Elements such as Pb, Bi, Co, Hg, and Th have profiles indicative of scavenged elements in sea water and their concentrations drop with depth (Whitfield and Turner, 1987). Lead concentrations decrease 10-fold from surface water to values of approximately 1 ng/l ( $5 \times 10^{-12} \text{M}$ ) in deep Pacific water (3500 m; Schaule and Patterson, 1981). In contrast, elements such as Fe, Cd, Cu, and Zn have profiles indicative of recycled elements, and their concentrations increase with depth (Whitfield and Turner, 1987). Iron levels in the Pacific increase from almost zero at the surface to approximately 50 ng/l ( $10^{-9} \text{M}$ ) in deep water (Martin et al., 1989); however, at depths below 2000 m, most trace metals have relatively constant concentrations (Whitfield and Turner, 1987; Martin et al., 1989).

Although there is a difference in the concentrations of most trace metals between the deep Pacific and the deep Atlantic water, I use the concentrations in the deep Pacific water as a first-order estimate of the elemental abundances in the ocean. Hence, this discussion will focus on greater than 2000 m depth, but not including the water-sediment boundary layer. All the metals mentioned above (and a few others)

have large excesses relative to iron in deep-ocean water compared with shale, clay, soils and lacustrine sediments (see Table 1.2).

The concentration of lead in the surface layer of the ocean is highly affected by human activity (Schaule and Patterson, 1981). On the other hand, it is believed that the  $5 \times 10^{-12}$  M concentration of lead in deep-ocean water is only twice the prehistoric natural concentration (Schaule and Patterson, 1981). A two-fold decrease in lead concentration in mid-ocean water would maintain a Fe/Pb ratio which is more than 10 times lower than the upper continental crustal ratio. Among the trace metals, lead is the element whose anthropogenic emission to the atmosphere is the largest compared with its natural emission (Salomons and Förstner, 1984); however, lead excess in deep-sea water compared with iron is smaller than the excess of copper, cadmium or zinc (see Table 1.2). Therefore, there appears to be a mechanism for the relative enrichment of trace metals in sea water compared to iron which is independent of human activities.

The concentration of iron in deep mid-ocean water ( $10^{-9}$ M) is approximately 800 times less than its concentration in major rivers ( $8 \times 10^{-7}$ M). In pre-industrial time, lead concentrations dropped by a factor of 40 from about  $10^{-10}$ M in unpolluted river water to approximately  $2.5 \times 10^{-12}$ M in deep-ocean water (50% of the lowest values measured by Schaule and Patterson, 1981). Therefore, a release of less than 5% of the lead from riverborne particles in the shelf environment, and airborne and sea-floor recycled particles in the mid-ocean environment is sufficient to lower the Pb/Fe ratio from 1:6,500 to 1:400.

It has been pointed out that remobilization of some trace metals in the estuary environment does occur (Boyle et al., 1982; Elbaz-Poulichet et al., 1984; Salomons and Förstner, 1984; Gobeil et al., 1987). A study by Yeats and Bowers (1982) suggests that while 99.8% of the iron will be retained in the coastal zone, only 69% of the cadmium, 54% of the zinc and 66% of the copper will be retained. Such a difference between the mostly particulate iron and trace metals is best explained by

partial release of trace metals to solution. Unfortunately, there is no reliable data about the partitioning of lead and other trace metals between solution and particulate matter in sea water. The separation scheme proposed by Schaule and Patterson (1981) and Stukas and Wong (1983) distinguishes between labile (both dissolved and adsorbed) lead and non-labile (strongly complexed lead in solution, and coprecipitated lead in minerals). A combination of this separation scheme with ultra filtration techniques is needed in order to examine possible desorption of lead and other metals from particle surfaces.

Laboratory studies indicate that partial desorption of trace metals takes place with increasing chlorinity (Kharkar, 1968; Salomons, 1980). A study by Pucci et al. (1989) correlates elevated lead and cadmium concentrations in ground water with intrusion of saline water, which causes a substantial release of both metals from particles.

I have examined the affinity of trace metals for chloro complexes on one hand, and their tendency to form surface complexes on the other hand, and suggest that these affinities determine the relative abundances of trace metals in deep-sea water. In the following discussion, I use the chloro and surface affinities of transition and post-transition metals, as well as some alkali and alkali earth cations, to explain their average concentrations in deep-ocean water. I have used all the reliable thermodynamic and much of the concentration data available (Smith and Martell, 1976; Turner et al., 1981; Taylor and McLennan, 1985; Whitfield and Turner, 1987; Martin et al., 1989), and have omitted only those elements whose oxidation states in sea water is either unknown or variable.

Many attempts have been made to divide cations present in natural waters into subgroups. I have used a similar approach to the one presented by Turner et al. (1981; see section 1.4.2). Instead of using their definition for  $\Delta\beta$  ( $\Delta\beta = \log[\beta_{MF}^0] - \log[\beta_{MCl}^0]$ ) = the difference between a metal ion's first complexing constant with fluoride and

chloride), I define  $\Delta\beta$  as:  $\Delta\beta = \log[\beta^{\circ}_{\text{MOH}}] - \log[\beta^{\circ}_{\text{MCl}}] =$  the difference between the metal's first hydrolysis constant and its first complexing constant with chloride. It has been shown (Huang and Stumm, 1973; Schindler and Stumm, 1987) that there is a strong correlation between the hydrolysis constant and constants of adsorption on oxide and hydroxide surfaces. I combined my  $\Delta\beta$  with the field strength,  $Z^2/r$  in order to form groups of metals and cations with similar aquatic properties. The result is shown in Figure 4.5.

Figure 4.5 is different from the plot used by Turner et al. (1981; see Fig. 1.3) in several ways. Mercuric ion has a strong affinity to both chloride and hydroxide, and its position near lead and the first-row transition metals represents its behavior in sea water more satisfactorily than the fluoride-chloride parameter. Based on their electrostatic ( $Z^2/r$ ) and covalent ( $\Delta\beta$ ) measures,  $\text{Pb}^{2+}$ ,  $\text{Fe}^{2+}$ ,  $\text{Mn}^{2+}$ ,  $\text{Zn}^{2+}$ ,  $\text{Cu}^{2+}$ ,  $\text{Hg}^{2+}$ , and  $\text{Ni}^{2+}$  fall into one group, while  $\text{Cd}^{2+}$ , which is more strongly complexed by chloride, falls into an adjacent group, together with  $\text{Ba}^{2+}$ . Therefore,  $\text{Cd}^{2+}$ , which has a relatively weak affinity for surfaces and strong affinity for chloride, will be mostly in solution as are the alkali earth metals (except Be).  $\text{Tl}^{+}$  falls in the same group as  $\text{K}^{+}$  (and probably other alkali metals), as would be expected from its behavior in sea water (Flegal and Patterson, 1985).

In order to verify my hypothesis that the difference between chloride affinity and hydroxo surface affinity predicts the relative abundances of metals in the ocean, I plot the change in the ratio of Fe to a trace metal (TM) between the upper crust and the ocean ( $\log\{[\text{Fe}/\text{TM}]_{\text{UC}}/[\text{Fe}/\text{TM}]_{\text{Ocean}}\}$ ) as a function of  $-\Delta\beta$  ( $\log[\beta^{\circ}_{\text{MCl}}] - \log[\beta^{\circ}_{\text{MOH}}]$ ; Fig. 4.6). The result clearly indicates a strong effect of chloride affinity on the concentrations of metals in the ocean. Metals with strong chloride affinities have large excesses in sea water compared with iron. Cadmium, for example, has an excess approaching that of potassium, both being mainly in solution. The slope of the best-fit line on Figure 4.6 is smaller than unity, and the intercept is at -2 since iron hydroxides

are not the only adsorbents in sea water (Morel and Hudson, 1987; Whitfield and Turner, 1987). Following the same argument, chloride is not the only dissolved ligand able to cause desorption of metals from surfaces. Copper, for example, plots above the line on Figure 4.6 and is known to be desorbed from oxide surfaces in the presence of humic acids (Laxen, 1985). Ga, Zr, and Bi are the only elements that do not plot near the best-fit line in Figure 4.6. Recent study by Orians and Bruland (1988) shows that Ga concentrations in deep-Pacific water are more than one order of magnitude lower than previous values, bringing Ga much closer to the best-fit line in Figure 4.6. I believe that reported measured concentrations of Bi and Zr in sea water are either too high or the concentrations of both elements are dominated by nonlabile particulate matter.

The equilibrium constant data base for the formation of surface species is more limited than for dissolved species; however, a rigorous attempt to create a uniform model for the sorption of metals on hydrous ferric oxides has been carried out recently (Dzombak, 1986; Dzombak and Morel, 1990). As shown in Figure 4.7,  $\log[\text{Fe/TM}]_{\text{UC}}/[\text{Fe/TM}]_{\text{Ocean}}$  increases when  $-\Delta\beta'$  ( $\log\beta_{\text{Cl}^-} - \log K_1^{\text{int}}$ ) increases.  $K_1^{\text{int}}$  are the reported values for the adsorption constant of Zn, Cu, Pb and Cd on am- $\text{Fe}(\text{OH})_3$ . The slope of the line in Figure 4.7 is different than the slope of the line in Figure 4.6 because the values of  $K_1^{\text{int}}$  and  $\beta_{\text{MOH}}^0$  are different. The results which involve surface complexation constants, shown in Figure 4.7, further support the results obtained from data of dissolved species only.

The correlation between both  $-\Delta\beta'$  and  $-\Delta\beta$ , and the relative enrichment of trace metals in deep-sea water, suggest that, to a first approximation, the concentrations of many trace metals in deep-sea water are related to adsorption/desorption of metals from particle surfaces due to complexation by chloride. On the other hand, the relative enrichment of the lanthanide group in sea water compared to iron cannot be explained

by the adsorption/desorption model proposed here (Fig. 4.8). It seems that the concentrations of the lanthanides in deep-sea water have a more complex control.

Partial desorption of lead from iron-rich particles in the presence of high chlorinity has been examined experimentally. Mixing the solution used for the adsorption experiment with sea water (pH 7.5) causes a 12% decrease of lead from the particles (Table 4.1). An adsorption model run by Lion and Leckie (1981) predicts that 24% of lead in the presence of sea water will be on iron surfaces, 56% will form chloro complexes and 17% will be in the form of lead carbonate. Such a large difference between model prediction, based on equilibrium speciation, and experimental data can be attributed to changes in the particle properties upon mixing with the high salinity sea water, and is probably in part an experimental bias. Nevertheless, the amount of lead desorbed from the experiment particles (12%) is large enough to explain the observed decrease of Fe/Pb in sea water.

#### 4.4. Conclusions

The fate of lead on its way from the continent to the ocean is initially determined by its coprecipitation and adsorption on particle surfaces, including ferric iron hydroxides. A similar transport mechanism and comparable rates of release from common rock and soil minerals determine a natural ratio between lead and iron in unpolluted rivers, close to their upper continental crustal ratio of 1:6,500. The same Fe/Pb ratio found in fresh granodiorite and its weathering product is also found in clay minerals, reworked crustal material, soil, and river sediments on a global scale.

Competition with major cations on surface sites does not seem to affect the adsorption of lead on surfaces; complexation of lead by man-made organic compounds, however, substantially decreases the amount of lead bound to surface sites. Thus, the natural Fe/Pb ratio may be masked in large rivers due to a secondary pollution effect caused by anthropogenic organic chelators, which transfer lead from particle surfaces to

solution. The desorption of lead from particle surfaces decreases the Fe/Pb ratio in rivers and mobilizes lead, regardless of any direct addition of anthropogenic lead. Such an effect will maintain relatively high values of lead in river water even when emission of lead to the atmosphere and hydrosphere ceases.

Many trace metals maintain their average upper continental crustal ratio with iron in unpolluted river water, river sediments and soils; however, large excesses of most trace metals relative to iron are found in deep-ocean water. At the transition from fresh water to saline ocean water, two processes take place: 1) rapid removal of iron (and other particle-forming elements) from the water column due to coagulation and settling; and 2) partial desorption of trace metals from particle surfaces. While more than 99% of the riverborne iron settles to the sediment within the continental shelf, some of the trace metals are released to solution as dissolved chloro-complexes and are further transported to the open sea. In addition, some of the trace metals attached to airborne and recycled sea-floor particles may desorb when these particles are in contact with sea water.

The adsorption/desorption process in sea water account for the relative abundances of many trace metals in deep-sea water (not including REE). Furthermore, it is suggested that the observed concentrations of these trace metals in deep-ocean water are relatively unaffected by pollution and are largely determined by natural processes.

**Table 4.1:** Composition of the solution leached from Jossi Spring biotite, used for the adsorption-desorption experiments. All values in  $\mu\text{M}$ , except pH, I (ionic strength) and lead (M).

Experiment	Si(OH) <sub>4</sub>	Al	Fe	Mn	Ca	Mg	Na	K
adsorption	1250	926	929	12.7	108	750	13	667
EDTA desorption	1.2	0.9	0.9	0.01	0.1	0.7	0.01	0.7
sea water desorption	1.2	0.9	0.9	0.01	10300	53800	468000	10200

Experiment	biotite Pb	spike Pb	pH	I	% desorbed
adsorption	$5.6 \times 10^{-9}$	$3.3 \times 10^{-8}$	3.5-8.5	.1	-
EDTA desorption	$5.6 \times 10^{-12}$	$5.5 \times 10^{-10}$	6.0	.001	24
sea water desorption	$5.6 \times 10^{-12}$	$5.4 \times 10^{-10}$	7.5	.7	12

	$^{208}\text{Pb}/^{206}\text{Pb}$	$^{208}\text{Pb}/^{207}\text{Pb}$	$^{208}\text{Pb}/^{204}\text{Pb}$
biotite Pb spiked Pb	2.0056 497.2	2.4769 1759	38.31 -

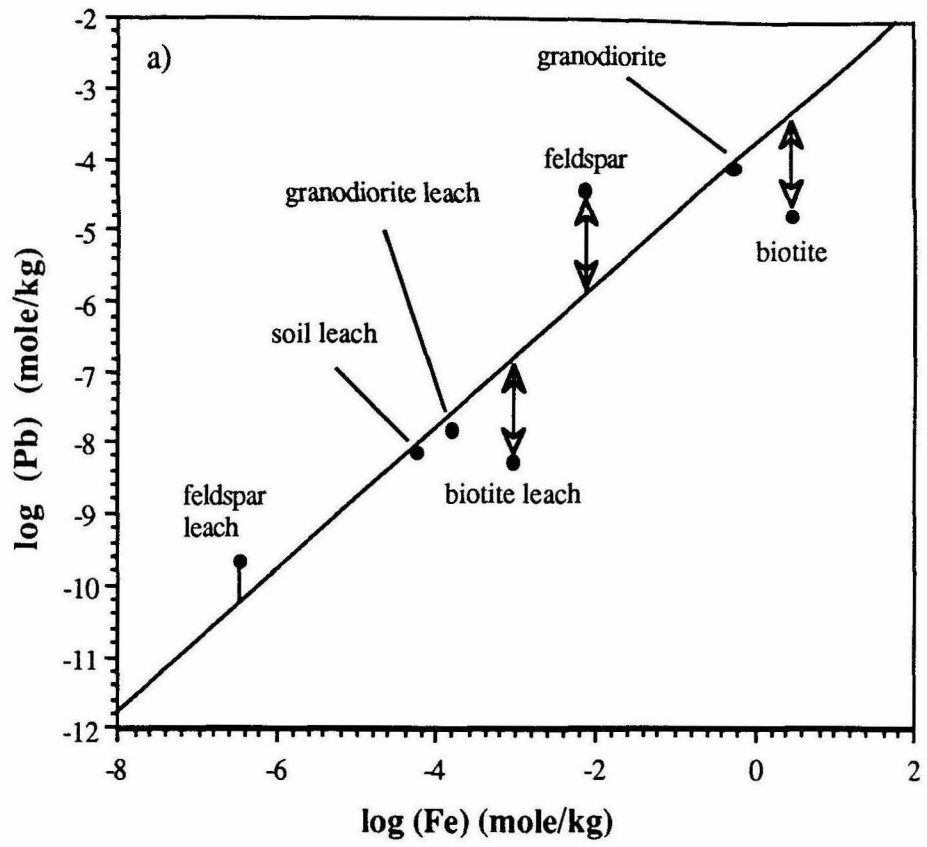
**Table 4.2:** Concentration of major cation of the adsorption experiment solution as a function of pH. The solution (filt) is the fraction which is passed through a 0.025 $\mu$ m pore-size Millipore filter. All concentrations are in  $\mu$ M.

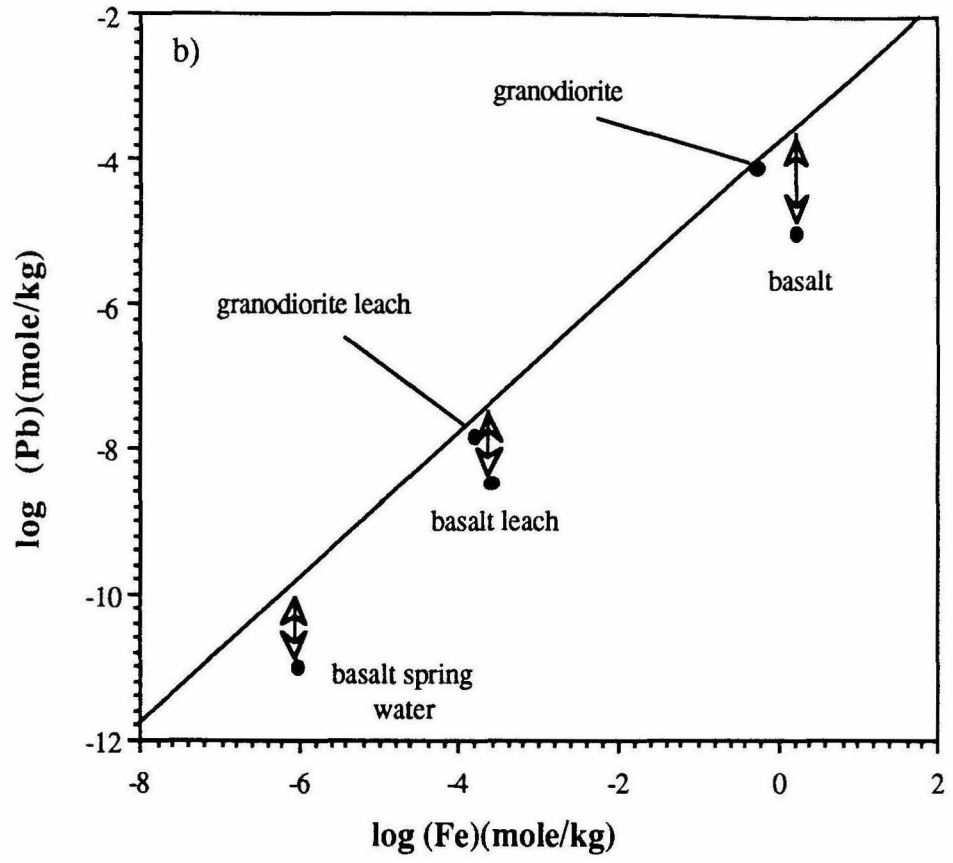
component	total	filt.pH=8	filt.pH=6	filt.pH=5.2	filt.pH=4.5	filt.pH=3.5
Si(OH) <sub>4</sub>	1250	161	500	536	1250	1250
Al(III)	926	7.4	92.6	370	926	926
Fe(III)	929	0	3.6	1.8	5.4	625
Mn(IV)	12.7	3.6	12.7	9.1	12.7	12.7
Ca <sup>2+</sup>	108	108	108	108	108	108
Mg <sup>2+</sup>	750	750	750	750	750	750
Na <sup>+</sup>	13	13	13	13	13	13
K <sup>+</sup>	667	667	667	667	667	667

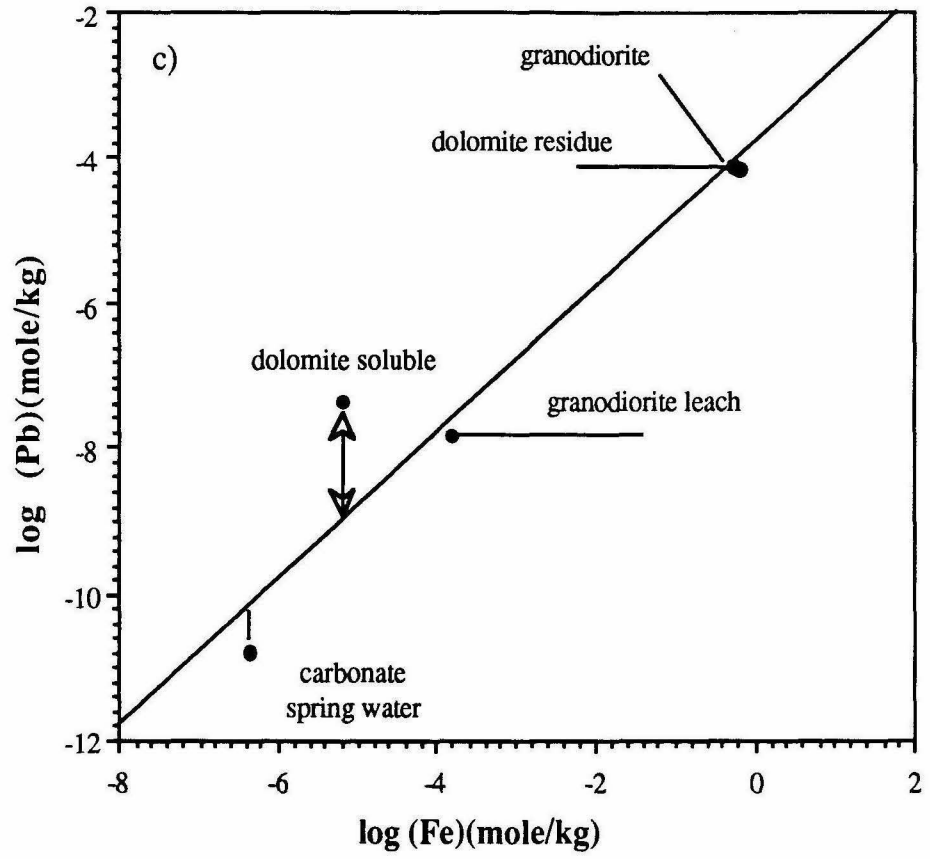
In the following pages:

---

**Figure 4.1:** Concentrations of lead and iron in: a) granodiorite, biotite and feldspar, and their leaching product; b) basalt rock, its leaching product, and a unpolluted basalt spring; and c) the carbonate fraction of a dolomite, the insoluble residue, and an unpolluted carbonate spring water. The diagonal line represents the average upper continental crustal ratio between lead and iron (1:6500).







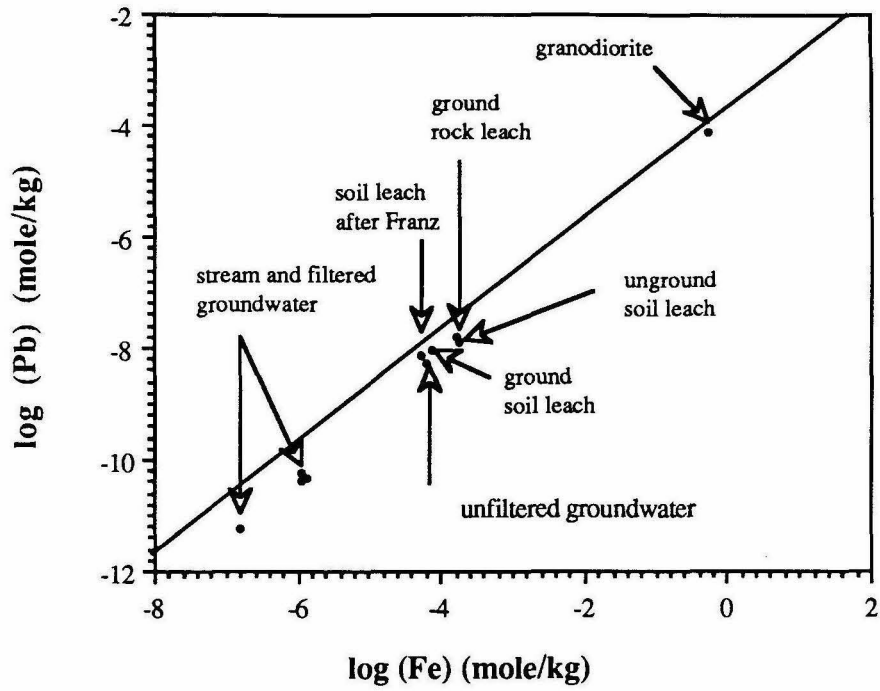


**Figure 4.2:** Concentrations of lead and iron in granodiorite, the leached phase, stream water, and ground water draining the bedrock. The diagonal line represents the average upper continental crustal ratio between lead and iron (1:6500).

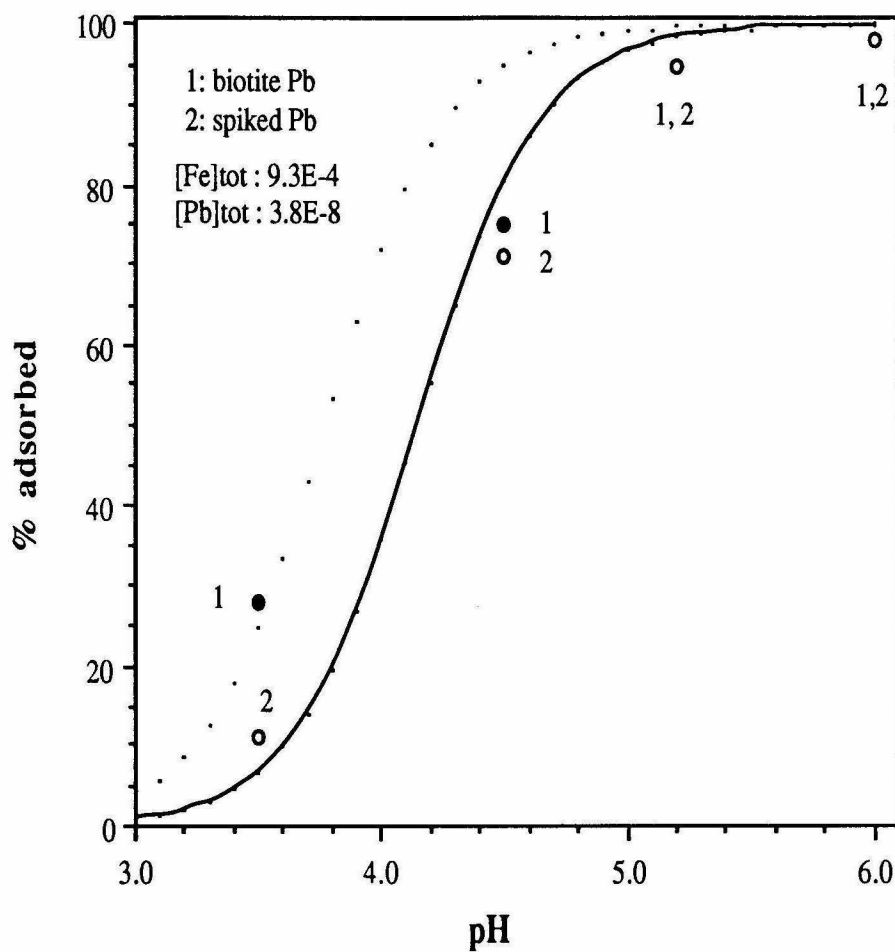


**Figure 4.3:** Lead adsorption on iron-rich particles in the presence of high magnesium concentrations as a function of pH, in a  $NH_4NO_3$  0.1 M solution. The solid line: the adsorption model with  $[>FeOH]=0.004 [Fe]_{total}$ , The dotted line: adsorption model with  $[>FeOH]=0.02 [Fe]_{total}$ . The composition of the solution is summarized in Tables 1 and 2.

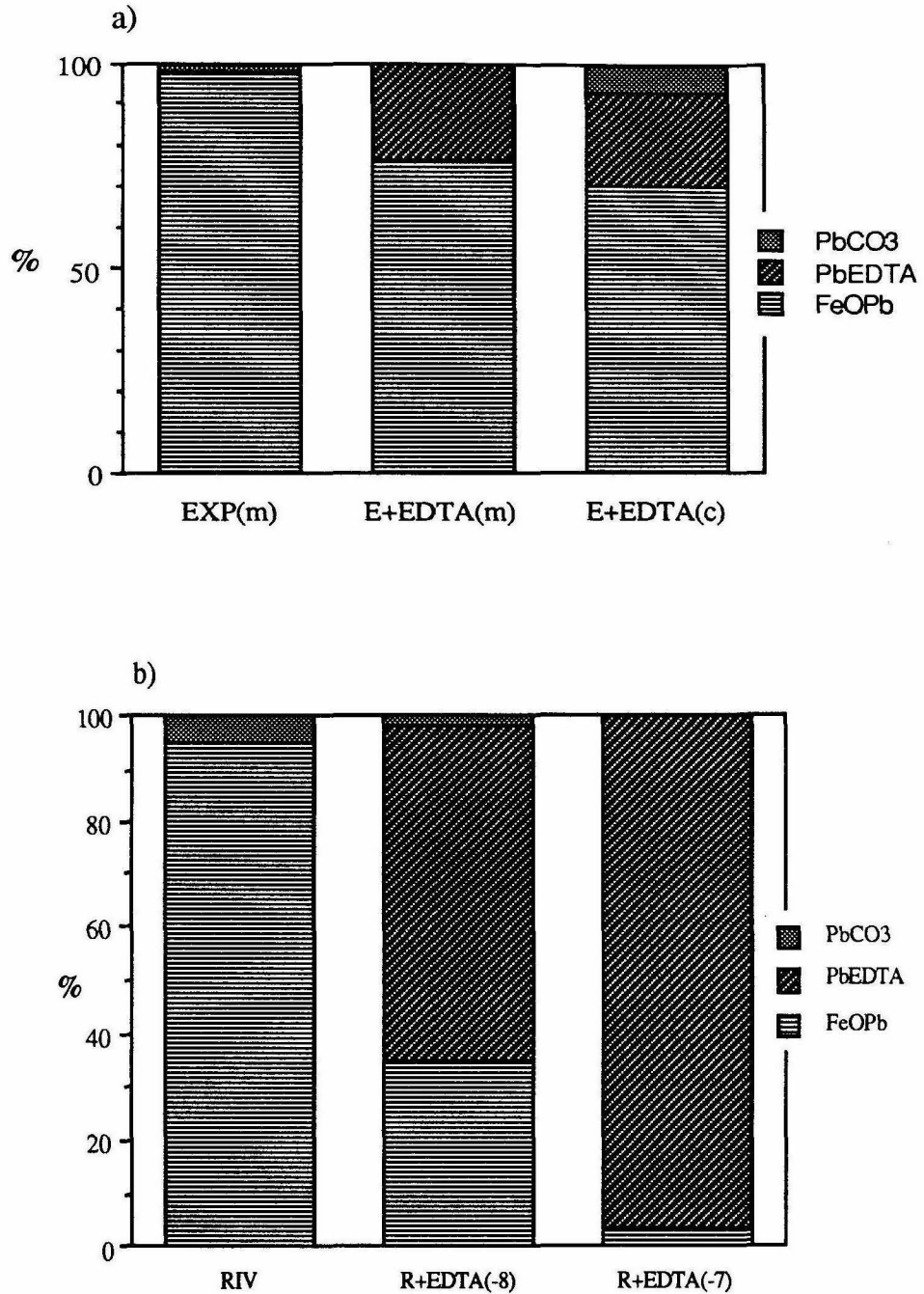


**Figure 4.4:** Desorption of lead from  $\text{Fe}(\text{OH})_3$  surfaces due to complexation by EDTA:

a) experiment versus model prediction: EXP(m) = the measured lead distribution in the experimental solution without EDTA; E+EDTA(m) = the measured lead distribution in the experimental solution with  $0.115 \mu\text{M}$  EDTA; E+EDTA(c) = the model calculation of lead distribution in the experimental solution with  $0.115 \mu\text{M}$  EDTA; and b) model prediction for a typical river composition. See text for values.

		$\Delta\beta$			
		$> -8$	$-8 > \Delta\beta > -11$	$-11 > \Delta\beta > -14$	$< -14$
<b>I</b> $Z^2/r < 2.5$				K, Tl(I)	Ag(I)
<b>II</b> $2.5 < Z^2/r < 7$		Zn, Ni, Co Pb, Fe(II) Hg, Cu(II) Mn(II)		Ba, Cd	
<b>III</b> $7 < Z^2/r < 11$		Y, Ln Tl(III)			
<b>IV</b> $11 < Z^2/r < 23$	Be, Sc, Hf Zr, Fe(III) In, Cr(III) Th(IV), U(IV)				

**Figure 4.5:** Complexation field diagram of cations present in natural water. The cations are divided into four groups both on the horizontal axis ( $\Delta\beta$ ) and on the vertical axis ( $Z^2/r$ ).

$\Delta\beta = \log[\beta^0\text{MOH}] - \log[\beta^0\text{MCl}]$ ; Ln = the rare earth series.

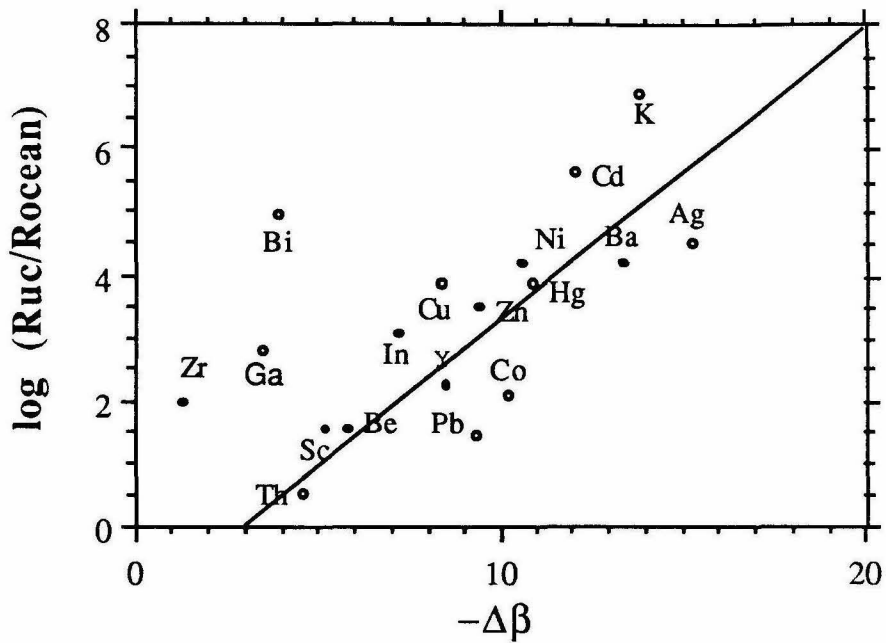


**Figure 4.6:**  $\log[\text{Fe}/\text{TM}]_{\text{uc}}/[\text{Fe}/\text{TM}]_{\text{ocean}}$  as a function of  $-\Delta\beta$ .  $R_{\text{uc}} = [\text{Fe}/\text{TM}]_{\text{uc}}$ ;  $R_{\text{ocean}} = [\text{Fe}/\text{TM}]_{\text{ocean}}$ ;  $-\Delta\beta = \log[\beta^{\circ}\text{MCl}] - \log[\beta^{\circ}\text{MOH}]$ .

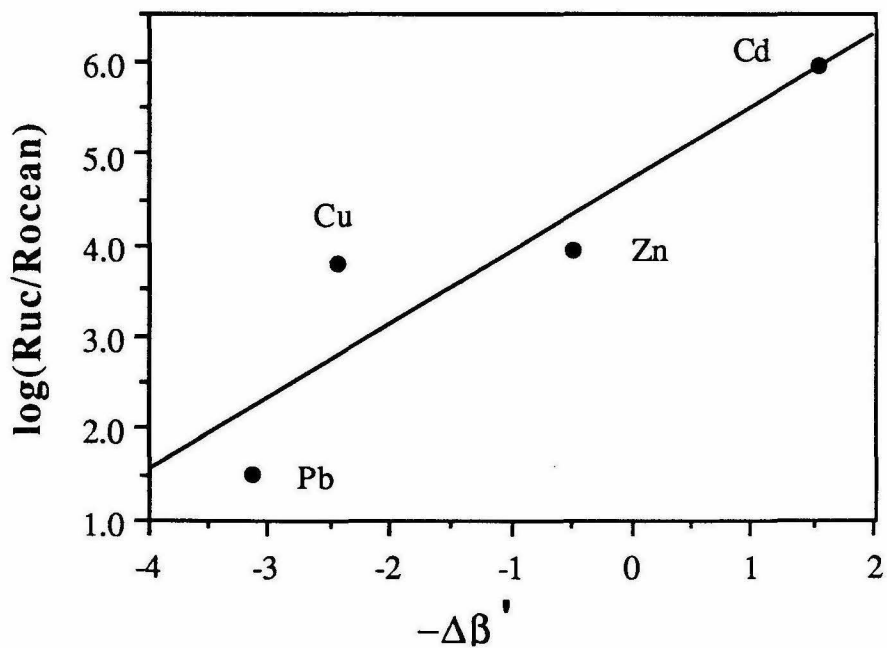


**Figure 4.7:**  $\log[\text{Fe}/\text{TM}]_{\text{uc}}/[\text{Fe}/\text{TM}]_{\text{ocean}}$  as a function of  $-\Delta\beta'$ .  $R_{\text{uc}} = [\text{Fe}/\text{TM}]_{\text{uc}}$ ;  $R_{\text{ocean}} = [\text{Fe}/\text{TM}]_{\text{ocean}}$ ;  $-\Delta\beta' = \log\beta_{\text{Cl}^-} - \log K_1^{\text{int}}$ .

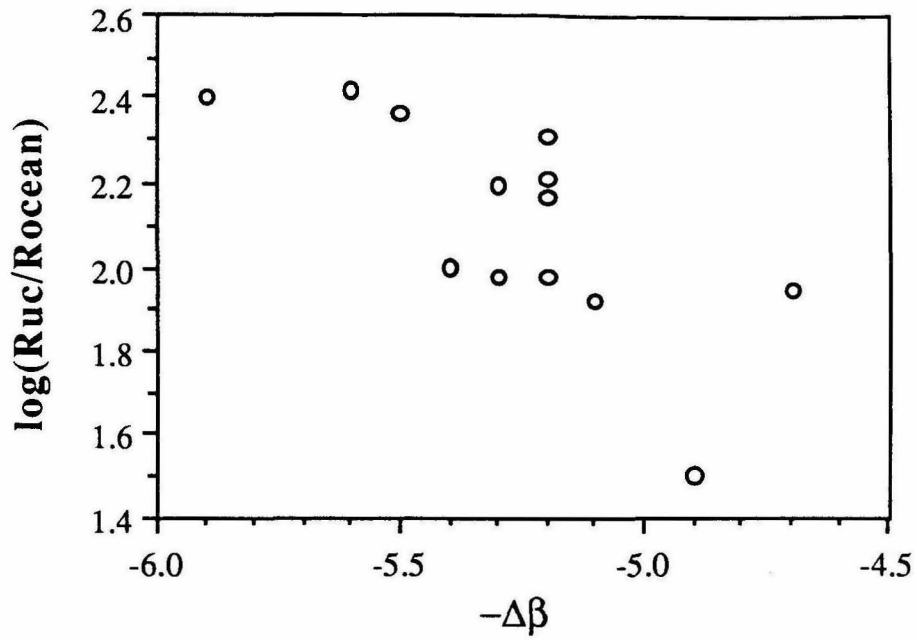


**Figure 4.8:**  $\log[Fe/TM]_{uc}/[Fe/TM]_{ocean}$  of REE as a function of  $-\Delta\beta$ .  $R_{uc} = [Fe/TM]_{uc}$ ;  $R_{ocean} = [Fe/TM]_{ocean}$ ;  $-\Delta\beta = \log[\beta^0_{MCl}] - \log[\beta^0_{MOH}]$ .

## References

- Ahrland S., Chatt J. and Davies N. R. (1958) The relative affinities of ligand atoms for acceptor molecules and ions. *Quart. Rev. Chem. Soc.* **12**, 265-276.
- AIS (1987) *An Assessment of the Implications of the Use of EDTA in Detergent Products*. Environmental Safety Working Group.
- Alexander R. B. and Smith R. A. (1988) Trends in lead concentrations in major U.S. rivers and their relation to the historical changes in gasoline-lead consumption. *Water Res. Bull.* **24**, 557-569.
- Amar P., Fujita E., Tonnessen K., Ahuja M., Westerdahl D., Cabrera H., Ota E., Unger C., Champomier S. and Weir N. (1988) In *Fifth Annual Report to the Governor and the Legislature on the Air Resources Board's Acid Deposition Research and Monitoring Program*. pp. 1-109. California Air Resources Board.
- Anderson P. R. (1990) Modeling adsorption in aluminium-iron oxide suspensions. (*submitted for publication*).
- Anderson P. R. and Benjamin M. M. (1990a) Application of a constant capacitance surface complexation model to describe adsorption in silica-iron binary oxide suspensions. (*submitted for publication*).
- Anderson P. R. and Benjamin M. M. (1990b) Surface and bulk characteristics of binary oxide suspensions. (*submitted for publication*).
- Avotins P. V. (1975) *Adsorption and Coprecipitation Studies of Mercury on Hydrous Iron Oxide*. Ph.D. thesis, Stanford University.
- Baes C. F. and Mesmer R. E. (1976) *The Hydrolysis of Cations*. John Wiley & Sons, New York.
- Basolo F. and Pearson R.G. (1967) *Mechanisms of Inorganic Reactions: A Study of Metal Complexes in Solution*. 2<sup>nd</sup> ed. pp. 124-246. John Wiley & Sons, New York.
- Battelle B. (1986) *Geochemical Behavior of Chromium Species*. Pacific Northwest Laboratories, Electric Power Research Institute, EA 4544 Research project 2485-3.
- Baudo R. (1982) The role of the speciation in the transfer of heavy metals along the aquatic food web. In *Ecological Effects on Heavy Metals Speciation in Aquatic Ecosystems*, (ed., O. Ravera), Unpublished manuscript.
- Benes P., Cejchamova M. and Havlik B. (1985) Migration and speciation of Pb in a river system heavily polluted from a smelter. *Water Res.* **19**, 1-16.

- Benes P. and Steinnes E. (1974) *In situ* dialysis for the determination of the state of trace elements in natural waters. *Water Res.* **8**, 947-953.
- Benjamin M. M. (1983) Adsorption and surface precipitation of metals on amorphous iron oxyhydroxide. *Environ. Sci. Technol.* **17**, 686-692.
- Benjamin M. M. and Leckie J. O. (1980) Adsorption of metals at oxide interfaces: Effects of the concentrations of adsorbate and competing metals. In *Contaminants and Sediments, Vol. 2* (ed., R. A. Baker), pp. 305-322. Ann Arbor Science.
- Benjamin M. M. and Leckie J. O. (1981) Multiple-site adsorption of Cd, Cu, Zn, and Pb on amorphous iron oxyhydroxide. *J. Colloid Interface Sci.* **79**, 209-221.
- Benjamin M. M. and Leckie J. O. (1982) Effects of complexation by Cl, SO<sub>4</sub>, S<sub>2</sub>O<sub>3</sub> on adsorption behavior of Cd on oxide surfaces. *Environ. Sci. Technol.* **16**, 162-170.
- Benninger L. K., Lewis D. M. and Turekian K. K. (1975) The use of natural Pb-210 as a heavymetal tracer in the river estuarine system. In *Marine Chemistry in the Coastal Environment, Vol. 18* (ed., T. M. Church), pp. 202-210. American Chemical Society.
- Boer P. L. and Ingram L. K. (1970) Analysis of coal ash and silicate rock by atomic absorption spectrophotometry by a fusion technique. *Analyst* **95**, 124-130.
- Boettinger J. L. (1988) *Duripan Genesis on Granitic Pediments of the Mojave Desert*. M.A. thesis, University of California, Davis.
- Boyle E. A. (1978) Trace element geochemistry of the Amazon and its tributaries. *EOS* **59**, 276.
- Boyle E. A. (1988) Cadmium: chemical tracer of deep water paleoceanography. *Paleoceanography* **3**, 471-489.
- Boyle E. A., Chapnick S. D. and Shen G. T. (1986) Temporal variability of lead in the western north Atlantic. *J. Geophys. Res.* **91**, 8573-8593.
- Boyle E. A., Huested S. S. and Grant B. (1982) The chemical mass balance of the Amazon Plume-II. Copper, nickel and cadmium. *Deep-Sea Res.* **29**, 1355-1364.
- Bradford G. R., Bair F. L. and Hunsaker V. (1968) Trace and major element content of 170 High Sierra lakes in California. *Limnol. Oceanogr.* **13**, 526-529.
- Brimhall G. H. and Dietrich W. E. (1987) Constitutive mass balance relations between chemical composition, volume, density, porosity, and strain in metasomatic hydrochemical systems: Results on weathering and pedogenesis. *Geochim. Cosmochim. Acta* **51**, 567-587.
- Bruland K. W. (1980) Oceanographic distributions of cadmium, zinc, nickel, and copper in the north Pacific. *Earth Planet. Sci. Lett.* **47**, 176-198.

- Bruland K. W. and Franks R. P. (1983) Mn, Ni, Cu, Zn, and Cd, in the Western North Atlantic. In *Trace Metals in Sea water*, (eds., C. S. Wong, E. Boyle, K. W. Bruland, J. D. Burton and E. D. Goldberg), pp. 395-414. Plenum, New York.
- Bruland K. W., Knauer G. A. and Martin J. H. (1978) Cadmium in northeast Pacific waters. *Limnol. Oceanogr.* **23**, 618-625.
- Buckley A. (1989) An electron microprobe investigation of the chemistry of ferromanganese coatings on fresh water sediments. *Geochim. Cosmochim. Acta* **53**, 115-124.
- Buffle J. and Altmann R. S. (1987) Interpretation of metal complexation by heterogeneous complexants. In *Aquatic Surface Chemistry*, (ed. W. Stumm), pp. 351-382. John Wiley & Sons, New York.
- Bunker B. and Casey W.H. (1990) Hydrolysis mechanisms in oxide dissolution and alteration. In *V.M. Goldschmidt conference*, pp. 33. Symposium Proceedings, The Geochemical Society, Baltimore.
- Butler J. N. (1982) *Carbon dioxide equilibria and their applications*, pp. 44-68. Addison-Wesley, Redwood.
- Bytnerwicz A. and Olszyk D. M. (1988) *Measurement of Atmospheric Dry Deposition at Emerald Lake in Sequoia National Park*. California Air Resources Board, Contract A7-32-039.
- Carter P. (1971) Spectrophotometric determination of serum iron at the submicrogram level with a new reagent (ferrozine). *Anal. Biochem.* **40**, 450-458.
- Chen J. H. and Moore J. G. (1982) Uranium-lead isotopic ages from the Sierra Nevada Batholith, California. *J. Geophys. Res.* **87**, 4761-4784.
- Chen J. H. and Tilton G. R. (1990) Applications of lead and strontium isotopic relations to the petrogenesis of granitoid rocks, central Sierra Nevada Batholith, CA. *Bull. Geol. Soc. Am.* (submitted for publication).
- Chow T. J. (1965) Radiogenic leads of the Canadian and Baltic Shield regions. In *Marine Geochemistry*, Vol. 3, pp. 169-184. Symposium Proceedings, Rhode Island University, Narraganset Marine Lab. Occasional Pub.
- Chow T. J., Bruland K. W., Bertine K. K., Souter A., Koide M. and Goldberg E. D. (1973) Records in Southern California coastal sediments. *Science* **181**, 551-552.
- Clesceri L.S., Greenberg A.E. and Trusell R.R. (1989) *Standard Methods for the Examination of Water and Wastewater*. APHA, AWWA and WPCF.
- Combes J. M., Manceau A., Calas G. and Bottero J. Y. (1989) Formation of ferric oxides from aqueous solutions: a polyhedral approach by X-ray absorption spectroscopy: I. Hydrolysis and formation of ferric gels. *Geochim. Cosmochim. Acta* **53**, 583-594.

- Coombs T.L. (1979) Cadmium in aquatic organisms. In *The Chemistry, Biochemistry and Biology of Cadmium*, Vol. 2 (ed., M. Webb), pp. 93-139. Elsevier, Amsterdam.
- Crecelius E. A. (1982) The significance of atmospheric input on metal concentrations in oceanic surface sea water and suspended matter. In *Paper presented at the NATO Adv. Res. Inst. Symp. Trace Metals in Sea water, Erice, Italy*.
- Dana E. S. and Ford W. E. (1932) *A textbook of mineralogy*. John Wiley & Sons, New York.
- Davies S. H. R. (1985) *Mn (II) Oxidation in the Presence of Metal Oxides*. Ph.D. thesis, California Institute of Technology.
- Davis J. A. (1977) *Adsorption of Trace Metals and Complexing Ligands at the Oxide/Water Interface*. Ph.D. thesis, Stanford University.
- Davis J. A. (1984) Complexion of trace metals by adsorbed natural organic matter. *Geochim. Cosmochim. Acta* **48**, 679-691.
- Davis J. A. and Leckie J. A. (1978) Surface ionization and complexation at the oxide/water interface. *J. Colloid Interface Sci.* **67**, 90-107.
- Dempsey B. A. and Singer P. C. (1980) The effects of calcium on the adsorption of zinc by  $MnO_x(s)$  and  $Fe(OH)_3(am)$ . In *Contaminants and Sediments, Vol. 2* (ed., R. A. Baker), pp. 333-352. Ann Arbor Science, Ann Arbor.
- Dietz F. (1982) Zur Frage der Remobilisierung von Schwermetallen durch Nitritotriessigsäure. *Korresp Abwasser* **29**, 692-693.
- Doe B. R. (1970) *Lead Isotopes*. Springer-Verlag, Berlin.
- Duram W. H. and Haffty J. (1961) Occurrence of minor elements in water. *US Geol. Surv. Circ.* **445**, 11.
- Dzombak D. A. (1986) *Towards a Uniform Model for the Sorption of Inorganic Ions on Hydrous Oxides*. Ph.D thesis, Massachusetts Institute of Technology.
- Dzombak D. A. and Morel F. M. M. (1990) *Surface Complexation Modeling*. John Wiley & Sons, New York.
- Eggleton R.A., Foudoulis C., Varkevisser, D. (1987) Weathering of basalt: Changes in rock chemistry and mineralogy. *Clays Clay Miner.* **35** (3), 161-169.
- Eigen M. and Wilkins R. G. (1965) The kinetics and mechanism of formation of metal complexes. In *Mechanisms of Inorganic Reactions*, (eds., R. K. Murmann, R. T. M. Fraser and J. Bauman), pp. 55-80. ACS Adv. in Chem. Ser. 49.
- Eisenreich S. J., Bannerman R. T. and Armstrong D. E. (1975) A simplified phosphorus analysis technique. *Envir. Lett.* **9**, 43-53.
- Elbaz-Poulichet F. (1988) *Apports Fluviaux et Estuariens de Plomb, Cadmium et Cuivre aux Océans*. Ph.D. thesis, Paris University.

- Elbaz-Poulichet F., Holliger p. and Huang W. W. (1984) Lead cycling in estuaries, illustrated by the Gironde estuary, France. *Nature* **308**, 409-414.
- Elbaz-Poulichet F., Holliger P., Martin J. M. and Petit D. (1986) Stable lead isotopes ratios in major French rivers and estuaries. *Sci. Total Environ.* **54**, 61-76.
- Elias R. W., Hinkley T. K., Hirao Y. and Patterson C. C. (1976) Improved techniques for studies of mass balances and fractionation among families of metals within terrestrial ecosystems. *Geochim. Cosmochim. Acta* **40**, 583-587.
- Elias R. W., Hirao Y. and Patterson C. C. (1982) The circumvention of the natural biopurification of calcium along nutrient pathways by atmospheric inputs of industrial lead. *Geochim. Cosmochim. Acta* **46**, 2561-2581.
- Elliot H. A. and Huang C. P. (1979) The adsorption characteristics of Cu(II) in the presence of chelating agents. *J. Colloid Interface SCI.* **70**, 29-45.
- Feigenson M. D. and Carr M. J. (1985) Determination of major, trace and rare earth elements in rocks by DCP-AES. *Chem. Geol.* **51**, 19-27.
- Flegal A. R., Duda T. F. and Niemeyer S. (1989) High gradients of lead isotopic composition in northeast Pacific upwelling filaments. *Nature* **339**, 458-460.
- Flegal A. R. and Patterson C. C. (1983) Vertical concentration profiles of lead in the Central Pacific at 15° N and 20° S. *Earth Planet. Sci. Lett.* **64**, 19-32.
- Fleischer M. (1976) Lead in igneous and metamorphic rocks and in their rock-forming minerals. In *Lead in the Environment*, (ed., T. G. Lovering), pp. 25-30. U.S. Government Printing Office.
- Fokkink L. G. J., Dekeizer A. and Lyklema J. (1990) Temperature dependence of cadmium adsorption on oxides. *J. Colloid Interface Sci.* **135**, 118-131.
- Förstner U. (1978) Metallanreicherungen in rezenten See-Sedimenten-geochemischer background und zivilisatorische Einflüsse. Internationale Hydrologische Programm der UNESCO, Vol. 2, pp. 66. Koblenz.
- Förstner U. and Müller G. (1974) *Schwermetalle in Flüssen und Seen als Ausdruck der Umweltverschmutzung*. Springer-Verlag, Berlin.
- Fox L. E. (1988) The solubility of colloidal ferric hydroxide and its relevance to iron concentrations in river water. *Geochim. Cosmochim. Acta* **52**, 771-777.
- Frimmel F. H., Grenz R. and Kordik E. (1989) Nitrotriacetate (NTA) and ethylenedinitrilotetraacetate (EDTA) in rivers of the Federal Republic of Germany. *Vom. Wasser* **72**, 175-184.
- Gee G. W. and Bauder J. W. (1986) Particle size analysis. In *Methods of Soil Analysis, Vol. 9, part 1* (ed. A. Klute), pp. 383-411. Amer. Soc. of Agronomy & Soil Sc. Soc. of Am.

- Getz L. L., Haney A. R., Larrimore R. W., Leland H. V., McNurney J. M., Price P. W., Rolfe G. L., Wortman R. H., Hudson J. L. and Solomon R. L. (1977) Transport and distribution in watershed ecosystem. In *Lead in the Environment*, (eds., W. R. Boggess and B. G. Wixson), NSF/RA-770214.
- Gibbs R. J. (1973) Mechanisms of trace metal transportation in rivers. *Science* **180**, 71-73.
- Gobeil C. and N. Silverberg (1989) Early diagenesis of lead in Laurentian Trough sediments. *Geochim. Cosmochim. Acta* **53**, 1889-1895.
- Gobeil C., Silverberg N., Sundby B. and Cossa D. (1987) Cadmium diagenesis in Laurentian Trough sediments. *Geochim. Cosmochim. Acta* **51**, 589-596.
- Grant L. D. (1986) *Air Quality Criteria for Lead*. Environmental Protection Agency, EPA-600/8-83/028aF.
- Groot A. J. de and Allersma E. (1975) Field observations on the transport of heavy metals in sediments. In *Heavy Metals in the Environment* (ed., P. A. Krenkel), pp. 85-97. Symposium Proceedings, International Conference Supplement Progress in Water Technology.
- Gurd F. R. N. (1954) *Chemical Specificity in Biological Interactions*. Academic Press, New York.
- Harriss R. C. and Adams J. A. S. (1966) Geochemical and mineralogical studies on the weathering of granitic rocks. *Am. J. Sci.* **264**, 146-173.
- Hart S. R. and Tilton G. R. (1966) The isotope geochemistry of strontium and lead in Lake Superior sediments and water, pp. 127-137 In *The earth beneath the continents*, Am. Geophys. Union Geophys. Mon. Ser., No. 10.
- Hayes K. F. and Leckie J. O. (1985) Mechanism of lead ion adsorption at the goethite-water interface. In *Geochemical Processes at Mineral Surfaces*, (ed. J. A. Davis and K. F. Hayes), pp. 114-141. American Chemical Society.
- Heinrichs H., Schulz-Dobrick B. and Wedepohl K. H. (1980) Terrestrial geochemistry of Cd, Bi, Tl, Zn, and Rb. *Geochim. Cosmochim. Acta* **44**, 1519-1533.
- Hem J. D. (1976) Geochemical controls on lead concentrations in stream water and sediments. *Geochim. Cosmochim. Acta* **40**, 599-609.
- Hering J. G. and Morel F. M. M. (1988) Kinetics of trace metal complexation: role of alkaline-earth metals. *Environ. Sci. Technol.* **22**, 1469-1478.
- Hingston F. J. (1970) *Specific Adsorption of Anions on Goethite and Gibbsite*. Ph.D. thesis, Univ. of Western Australia.
- Hingston F. J., Posner A. M. and Quirk J. M. (1971) Competitive adsorption of negatively charged ligands on oxide surfaces. *Discuss. Faraday Soc.* **52**, 334-342.
- Hinkley T. K. (1975) *Weathering Mechanisms and Mass Balance in a High Sierra Nevada Watershed Distribution of Alkali and Alkaline Earth Metals in*

*Components of Parent Rocks and Soil, Snow, Soil Moisture, and Stream Outflow.* Ph.D. thesis, California Institute of Technology.

- Hirao Y. and Patterson C. C. (1974) Lead aerosol pollution in the High Sierra overrides natural mechanisms which exclude lead from a food chain. *Science* **184**, 989-992.
- Hohl H., Sigg L. and Stumm W. (1978) Characterization of Surface Chemical Properties of Oxides in Natural Waters. In *Particulates in Water*, (ed., M. C. Kavanaugh and J. O. Leckie), pp. 1-31. American Chemical Society.
- Hohl H. and Stumm W. (1976) Interaction of  $Pb^{2+}$  with hydrous  $\gamma-Al_2O_3$ . *J. Colloid Interface Sci.* **55**, 281-288.
- Holdren G. R. and Speyer P. M. (1987) Reaction rate surface area relations during the early stages of weathering. II. Data on additional feldspars. *Geochim. Cosmochim. Acta* **51**, 2311-2318.
- Huang C. and Stumm W. (1973) Specific adsorption of cations on hydrous  $\gamma-Al_2O_3$ . *J. Colloid Interface Sci.* **43**, 409-420.
- Hunter K. A. (1980) Microelectrophoretic properties of natural surface-active organic matter in coastal sea water. *Limnol. Oceanogr.* **25**, 807-822.
- Hunter K. A. and Liss P. S. (1982) Organic matter and the surface charge of suspended particles in estuarine waters. *Limnol. Oceanogr.* **27**, 322-335.
- Jaworowski Z., Byseik M. and Kownacka L. (1983) Reply to C.C. Patterson's criticism of "Flow of metals into the global atmosphere." *Geochim. Cosmochim. Acta* **47**, 1169-1175.
- Jouanneau J. M. (1982) *Matieres en Suspension et Oligo-Elements Metalliques dans le Systeme Estuarien Girondin: Comportement et Flux.* Ph.D. thesis, l'Universite de Bordeaux.
- Kennedy V. C. and Sebetich M.J. (1976) Trace elements in northern California streams. *Geo. Surv. Res.* 208-209.
- Kennedy V. C., Jackman A. P., Zand S. M., Zellweger G. W. and Avanzino R. J. (1984) Transport and concentration controls for chloride, strontium, potassium and lead in Uvas Creek, a small cobble-bed in Santa Clara County, California. U.S.A. *J. Hydrol.* **75**, 67-110.
- Kerdijk H. N. and Salomons W. (1981) *Heavy Metal Cycling in the Scheldt Estuary* (in dutch). Delft Hydraulics Report.
- Kharkar D.P., Turekian K.K. and Bertine, K.K. (1968) Stream supply of dissolved silver, molybdenum, antimony, selenium, chromium, cobalt rubidium and cesium to the oceans. *Geochim. Cosmochim. Acta* **32**, 285-298.
- Knauss K. G. and Wolery T. J. (1986) Dependence of albite dissolution kinetics on pH and time at 25°C and 70°C. *Geochim. Cosmochim. Acta* **50**, 2481-2497.

- Knauss K. G. and Wolery T. J. (1989) Muscovite dissolution kinetics as a function of pH and time at 70°C. *Geochim. Cosmochim. Acta* **53**, 1493-1501.
- Knyazev S. A. (1986) Distribution of trace elements along the weathering profile of grandiorites of the Vasilkovsk Intrusion (Kokchetov Uplift). (Russ.). *Geol. Geofiz.* **11**, 65-72.
- Kuwabara J. S., Leland H. V. and Bencala K. E. (1984) Copper transport along a Sierra Nevada stream. *J. Environ. Engineer.* **110**, 646-655.
- Laird L. B., Taylor H. E. and Lombard R. E. (1986) Data on snow chemistry of the Cascade-Sierra Nevada mountains. *USGS Open File Report* **86-61**, 1-25.
- Landers D. H., Eilers J. M., Brakke D. F., Overton W. S., Keller P. E., Silverstein M. E., Schonbrod R. D., Crowe R. E., Linthurst R. A., Omernik J. M., Teague S. A. and Meier E. P. (1987) *Western Lake Survey Phase I: Population Descriptions and Physiochemical Relationships*. U.S. Environmental Protection Agency, 600/3-86/054a.
- Laville-Timsit L. and Wilhelm E. (1979) Metal behavior around sulfide deposits of Porte-aux-Moines. *Bull. Bur. Rech. Geol. Min., Sect. 2: Geol. Gites Miner. (Fr)* **2-3**, 195-228.
- Laxen D. P. H. (1985) Trace metals adsorption/coprecipitation on hydrous ferric oxide under realistic conditions. *Water Res.* **19**, 1229-1236.
- Laxen D. P. H. and Chandler I. M. (1982) Comparison of filtration techniques for size distribution in fresh waters. *Analyt. Chem.* **54**, 1350-1355.
- Leckie J. O., Benjamin M. M., Hayes K. F., Kaufman G. and Atlmann S. (1980) *Adsorption/Coprecipitation of Trace Metals from Water with Iron Oxyhydroxide*. Electric Power Research Institute, Palo Alto, Ca., EPRI RP-910-1.
- Lewis D. M. (1976) *The Geochemistry of Manganese, Iron, Uranium, Lead-210 and Major Ions in the Susquehanna River*. Ph.D. thesis, Yale University.
- Lewis D. M. (1977) The use of  $^{210}\text{Pb}$  as a heavy metal tracer in the Susquehanna river system. *Geochim. Cosmochim. Acta* **40**, 164-167.
- Li Y. H. (1981) Geochemical cycles of elements and human perturbation. *Geochim. Cosmochim. Acta* **45**, 2073-2084.
- Liang L. (1988) *Effects of Surface Chemistry on Kinetics of Coagulation of Submicron Iron Oxide Particles ( $\alpha\text{-Fe}_2\text{O}_3$ ) in Water*. Ph.D. thesis, California Institute of Technology.
- Lion L. W., Altman R. S. and Leckie J. O. (1982) Trace-metal adsorption characteristics of estuarine particulate matter: evaluation of contribution of Fe/Mn oxide and organic surface coating. *Environ. Sci. Technol.* **16**, 660-666.

- Lion L. W. and Leckie J. O. (1981) Chemical speciation of trace metals at the air-sea interface: The application of an equilibrium model. *Environ. Geol.* **3**, 293-314.
- Livingstone D. A. (1963) Chemical composition of rivers and lakes. In *Data of Geochemistry. Geol. Surv. Prof. Pap 440-G*, (ed., M. Fleischer). pp. 64.
- Lund L. J., Brown A. D., Lueking M. A., Nodvin S. C., Page A. L. and Sposito G. (1987) *Soil Processes at Emerald Lake Watershed*. California Air Resources Board, A3-105-32.
- Maring H., Patterson C. and Settle D. (1989) Atmospheric input fluxes of industrial and natural Pb from the westerlies to the Mid-North Pacific. In *Chemical Oceanography*, (eds., J. P. Riley and R. Chester), pp. 84-105. Academic Press, New York.
- Maring H., Settle D. M., Baut-M'enard P., Dulac F. and Patterson C. C. (1987) Stable lead isotope tracers of air mass trajectories in the Mediterranean region. *Nature* **330**, 154-155.
- Martin J. H., Gordon R. M., Fitzwater S. and Broenkow W. W. (1989) Vertex: phytoplankton/iron studies in the Gulf of Alaska. *Deep-Sea Res.* **36**, 649-680.
- Martin J. M. and Meybeck N. (1979) Elemental mass balance of material carried by major world rivers. *Mar. Chem.* **7**, 173-206.
- Martin J. M. and Whitfield M. (1983) The significance of the river input of chemical elements to the ocean. In *Trace Metals in Sea Water*, (ed., C. S. Wong, E. Boyle, K. W. Bruland, J. D. Burton and E. D. Goldberg), pp. 265-296. Plenum Press, New York.
- McKenzie R. M. (1971) The synthesis of birnessite, cryptomelane, and some other oxides and hydroxides of manganese. *Miner. Mag.* **38**, 493-502.
- McKnight D. M. and Bencala K. E. (1989) Reactive iron transport in an acid mountain stream in Summit County, Colorado: a hydrologic perspective. *Geochim. Cosmochim. Acta* **53**, 2225-2234.
- McQuaker N. R., Kluckner P. D. and Chang G. N. (1979) Calibration of an inductively coupled plasma-atomic emission spectrometer for the analysis of environmental materials. *Anal. Chem.* **51**, 888-895.
- Mehra O. P. and Jackson M. L. (1960) Iron oxide removal from soils and clays by a dithionite-citrate system buffered with sodium bicarbonate. In *Clays and Clay minerals*, (ed., A. Swineford), Proc. 7th Natl. Conf., Washington D.C., Pergamon Press, New York.
- Meixner G. D. (1988) *Water Conditions in California*. CA Dept. of Water Resources.
- Melack J. M., Copper S. D., Holmes R. W., Sickman J. O., Kratz K., Hopkins P., Hardenbergh H., Thieme M. and Meeker L. (1987) *Chemical and Biological Survey of Lakes and Streams Located in the Emerald Lake Watershed, Sequoia National Park*. California Air Resources Board, A3-096-32.

- Meybeck M. and Helmer R. (1989) The quality of rivers: From pristine stage to global pollution. *Paleoclimatol., Palaeoecol. (Global Planet. Change Sect.)* **75**, 283-309.
- Moore J. G. and Sisson T. M. (1987) *Geological Map of the Tiple Divide Peak Quadrangle, Tulare County, California*. USGS Report .
- Morel F. M. M. (1983) *Principles of Aquatic Chemistry*. John Wiley & Sons,
- Morel F. M. M. and Gschwend P. M. (1987) The role of Colloids in the partitioning of solutes in natural waters. In *Aquatic Surface Chemistry*, (ed., W. Stumm), pp. 405-421. John Wiley & Sons, New York.
- Morel F. M. M. and Hudson R. J. M. (1987) The geobiological cycle of trace elements in aquatic systems: Redfield revisited. In *Chemical Processes in lakes*, (ed., W. Stumm), pp. 251-281. John Wiley & Sons, New York.
- Morel F. M. M., Westall J. C. and Yeasted J. G. (1981) Adsorption models: a mathematical analysis in the framework of general equilibrium calculations. In *Adsorption of Inorganics at Solid-Liquid Interfaces*, (eds., M. A. Anderson and A. J. Rubins), pp. 263-294. Ann Arbor Science, Ann Arbor.
- Mouvet C. and Bourg A. C. M. (1983) Speciation (including adsorbed species) of copper, lead, nickel and zinc in the Meuse river. *Water Res.* **17**, 641-649.
- Murozumi M., Chow T. J. and Patterson C. (1969) Chemical concentrations of pollutant lead aerosols, terrestrial dusts and sea salts in Greenland and Antarctic snow strata. *Geochim. Cosmochim. Acta* **33**, 1247-1294.
- Murphey W. M. and Helgeson H. C. (1987) Thermodynamic and kinetic constraints on reaction rates among minerals and aqueous solutions. III. Activated complexes and the pH-dependence of the rates of feldspar, pyroxene, wollastonite, and olivine hydrolysis. *Geochim. Cosmochim. Acta* **51**, 3137-3154.
- Neiboer E. and Richardson D. H. S. (1980) The replacement of the nondescript term "heavy metals" by a biologically and chemically significant classification of metal ions. *Environ. Pollut.* **B1**, 3-26.
- Nelson D. W. and Sommers L. E. (1982) Total carbon organic carbon and organic matter. In *Methods of Soil Analysis, Vol. 9 (2)* (ed., A. L. Page), pp. 539-579. American Society of Agronomy & Soil Science of America.
- Nelson P.O., Chung A.K., and Hudson M.C. (1981) Factors affecting the fate of heavy metals in the activated sludge process. *J. Water Pollut. Control Fed.* **53**, 1323-1333.
- Nesbitt H. W. and Shotyk W. (1990) Congruent incongruent dissolution in labradorite in HCl solutions containing Na, Ca, Al, and Si. In *V.M. Goldschmidt conference*, pp. 69. Symposium Proceedings, The Geochemical Society, Baltimore.
- Ng A. and Patterson C. C. (1982) Changes of lead and barium with time in California off-shore basin sediments. *Geochim. Cosmochim. Acta* **46**, 2307-2321.

- Ng A. C. and Patterson C. C. (1979) Chronological variations in barium concentrations, lead concentrations, and lead isotopic composition in sediments of four Southern California offshore basins. Southern California Baseline Study: Benthic, Year 2, Vol. 11. Bureau of Land Management, Dept. of Interior Contract AA550-CT6-40, 14.
- Ng A. C. and Patterson C. C. (1981) Natural concentrations of lead in ancient Arctic and Antarctic ice. *Geochim. Cosmochim. Acta* **45**, 2109-2121.
- Nowlen G. A. (1976) Genesis of manganese-iron oxides in stream sediments of Maine. *USGS Open File Report 76-878*, 1-50.
- Nriagu J. O. (1978) *The Biochemistry of Lead in the Environment*. Elsevier, Amsterdam.
- Nriagu J. O. (1989) A global assessment of natural sources of atmospheric trace metals. *Nature* **338**, 47-49.
- Oppenheim M. (1959) *The Volcanic Occurrences in the Southeast Lower Galilee, Israel* (Heb.). Ph.D. thesis, Hebrew University.
- Orians K. J. and Bruland K. W. (1988) Dissolved gallium in the open ocean. *Nature* **332**, 717-719.
- Oscarson D. W., Huang P. M., Liaw W. K. and Hammer U. T. (1983) Kinetics of oxidation of arsenite by various manganese dioxides. *Soil Sci. Soc. Am. J.* **47**, 644-648.
- Patterson C. C. (1965) Contaminated and natural lead environments of man. *Arch. Env. Health* **11**, 344-460.
- Patterson C. C. (1972) Silver stocks and losses in ancient and medieval times. *Econ. Hist. Rev.* **25**, 205-235.
- Patterson C. C., Hinkley T. K., Hirao Y. and Settle D. M. (1973) *Determination of Biological Discrimination Factors for Metals Within Natural Ecosystems*. GB31038, California Institute of Technology.
- Patterson C. C. and Settle D. M. (1976) The reduction of orders of magnitude errors in lead analysis of biological materials and natural waters by evaluating and controlling the extent and sources of industrial lead contamination introduced during sampling collecting, handling and analysis. *National Bureau of Standards, Special Publication 422*, 321-351.
- Patterson C. C. and Settle D. M. (1987) Review of data on eolin fluxes of industrial and natural lead to the lands and seas in remote regions on a global scale. *Mar. Chem.* **22**, 137-162.
- Paulson A. J., Feeley R. A., Curl H. C., Crecelius E. A. and Geiselman T. (1988) The impact of scavenging on trace metal budgets in Puget Sound. *Geochim. Cosmochim. Acta* **52**, 1765-1780.

- Petit J. C. (1990) Application of energetic-ion beam techniques to kinetic geochemistry. In *V.M. Goldschmidt conference*, pp. 73. Symposium Proceedings, The Geochemical Society, Baltimore.
- Pucci A. A., Harriman D. A., Ervin E. M., Bratton L. and Gordon A. (1989) Lead and cadmium associated with saltwater intrusion in a New Jersey aquifer system. *Water Res. Bull.* **25**, 1267-1272.
- Richards L. A. (1954) *Diagnosis and Improvement of Saline and Alkali Suits*. U.S. Department of Agriculture.
- Salomons W. (1980) Adsorption processes and hydrodynamic conditions in estuaries. *Environ. Technol. Lett.* **1**, 356-365.
- Salomons W. and Förstner U. (1984) *Metals in the Hydrocycle*. Springer-Verlag, Berlin.
- Salomons W. and van Pagee J. A. (1981) Prediction of NTA levels in river systems and their effects on metal concentration. In *Heavy metals in the environment*, pp. 694-697. Int. Conf., Amsterdam.
- Sandler A. (1981) *The Geochemistry of Ground water from Basaltic Aquifers in the Golan and the Lower Galilee, Israel* (Heb.). M. Sc. thesis, Hebrew University.
- Sass E. and Katz A. (1982) The origin of platform dolomites: New evidence. *Am.J. Sci.* **282**, 1184-1213.
- Schaule B. K. and Patterson C. C. (1981) Lead concentrations in the northeast Pacific: Evidence for global anthropogenic perturbations. *Earth Planet Sci. Lett.* **54**, 97-116.
- Schell W. R. and Nevissi A. (1977) Heavy metals from waste disposal in Central Puget Sound. *Environ. Sci. Technol.* **11**, 887-893.
- Schindler P. W. (1981) Surface complexes at oxide-water interfaces. In *Adsorption of Inorganics at Solid-Liquid Interfaces*, (ed. M. A. Anderson and A. Rubin), pp. 1-50. Ann Arbor Science, Ann Arbor.
- Schindler P. W., Fürst B., Dick R. and Wolf P. U. (1976) Ligand Properties with  $\text{Fe}^{3+}$ ,  $\text{Cu}^{2+}$ , and  $\text{Pb}^{2+}$ . *J. Colloid Interface Sci.* **55**, 469-475.
- Schindler P. W. and Stumm W. (1987) The Surface Chemistry of Oxides, Hydroxides and Oxide Minerals. In *Aquatic Surface Chemistry*, (ed., W. Stumm), pp. 83-107. John Wiley & Sons, New York.
- Schott J. and Petit J. (1987) New evidence for the mechanisms of dissolution of silicate minerals. In *Aquatic Surface Chemistry*, (ed. W. Stumm), pp. 293-312. John Wiley & Sons.
- Schultz M. F., Benjamine M. M. and Ferguson J. F. (1987) Adsorption and desorption of metals on ferrihydrite: reversibility of the reaction and sorption properties of the regenerated solid. *Environ. Sci. Technol.* **21**, 863-869.

- Scott K.M. (1986) Elemental partitioning into manganese- and iron-oxides derived from dolomitic shale-hosted lead-zinc deposits, northwest Queensland, Australia. *Chem. Geol.* **57**, 395-414.
- Scott M. J. (1990) *Dynamics of Arsenic and Selenium in Aqueous Systems of Iron and Manganese oxides*. Ph.D. thesis, California Institute of Technology. In preparation.
- Settle D. M. and Patterson C. C. (1980) Lead in albacore: Guide to lead pollution in Americans. *Science* **207**, 1167-1176.
- Settle D. M. and Patterson C. C. (1982) Magnitudes and sources of precipitation and dry deposition fluxes of industrial and natural leads to the north Pacific at Enewetak. *J. Geophys. Res.* **87**, 8857-8869.
- Shen G. T. and Boyle E. A. (1987) Lead in corals: reconstruction of historical industrial fluxes to the surface ocean. *Earth Planet. Sci. Lett.* **82**, 289-304.
- Shirahata H., Elias R. W. and Patterson C. C. (1980) Chronological variations in concentrations and isotopic compositions of anthropogenic atmospheric lead in sediments of a remote subalpine pond. *Geochim. Cosmochim. Acta* **49**, 149-162.
- Shotyk W. and Nesbitt H. W. (1990) Direct evidence of ligand-promoted dissolution from sims analysis of feldspar surfaces. In *V.M. Goldschmidt conference*, pp. 81. Symposium Proceedings, The Geochemical Society, Baltimore.
- Sigg L. (1987) Surface chemical aspects of the distribution and fate of metal ions in lakes. In *Aquatic Surface Chemistry*, (ed., W. Stumm), pp. 319-346. John Wiley & Sons, New York.
- Silver L. T., Woodhead J. A. and Williams I. S. (1982) Primary mineral distribution and secondary mobilization of uranium and thorium in radioactive granites. In *Uranium Exploration Methods*, pp. 355-366. Symposium Proceedings, OECD Nuclear Energy Agency, Paris.
- Silver L. T., Woodhead J. A., Williams I. S. and Chappell B. W. (1984) *Uranium in Granites from the Southwestern United States: Actinide Parent-Daughter Systems, Sites and Mobilization*. Dept. of Energy, DE-AC13-76GI01664.
- Solorzano L. (1967) Determination of ammonia in natural waters by the phenol-hypochlorite method. *Limnol. Oceanogr.* **14**, 799-801.
- Smith R.M. and Martell A.E. (1976) *Critical Stability Constants. Vol. 4.* Plenum Press, New York.
- Stookey L. L. (1970) Ferrozine: a new spectrophotometric reagent for iron. *Anal. Chem.* **42**, 119-121.
- Stukas V. J. and Wong C. S. (1983) Accurate and precise analysis of trace levels of Cu, Cd, Pb, Zn, Fe, and Ni in sea water by isotope dilution mass spectrometry. In *Trace Metals in Sea water*, (eds., C. S. Wong, E. Boyle, K. W. Bruland, J. D. Burton and E. D. Goldberg), pp. 395-414. Plenum, New York.

- Stumm W., Huang C. P. and Jenkins S. R. (1970) Specific chemical interaction affecting the stability of dispersed systems. *Croat. Chem. Acta* **42**, 223-245.
- Stumm W. and Morgan J. J. (1981) *Aquatic Chemistry*. John Wiley & Sons, New York.
- Sturchio N. C., Muehlenbachs K. and Seitz M. G. (1986) Element redistribution during hydrothermal alteration of rhyolite in an active geothermal system: Yellowstone drill cores Y-7 and Y-8. *Geochim. Cosmochim. Acta* **50**, 1619-1631.
- Sturges W. T. and Barrie L. A. (1987) Lead 206/207 isotope ratios in the atmosphere of North America as tracers of U.S and Canadian emission. *Nature* **239**, 144-146.
- Tatsumoto M. and Patterson C. C. (1963) The concentration of common lead in sea water. In *Earth Science and Meteorics*, pp. 74-89. North-Holland Publ. Co.
- Taylor S. R. and McLennan S. M. (1985) *The Continental Crust: its Composition and Evolution*. pp. 9-52. Blackwell Scientific Publications.
- Tessier A., Campbell P. G. C. and Bisson M. (1979) Sequential extraction procedure for the speciation of particulate trace metals. *Anal. Chem.* **51**, 844-851.
- Thomas G.W. (1982) Exchangeable cations. In *Methods of Soil Analysis, Vol. 9, part 2* (eds., A.L. Page, R.H. Miller and D.R. Keeney), pp. 159-165. Amer. Soc. of Agronomy & Soil Science. Soc. of Amer.
- Thornber M. R. and Wildman J. E. (1984) Supergene alteration of the sulfides, VI. The binding of copper, nickel, zinc, cobalt, and lead with gossan (iron-bearing) minerals. *Chem. Geol.* **44**, 399-434.
- Trefry J. H., Metz S., Trocine R. P. and Nelson T. A. (1985) A decline in lead transport by the Mississippi river. *Science* **230**, 439-441.
- Trefry J. H. and Presley B. J. (1976) Heavy metal transport from the Mississippi River to the Gulf of Mexico. In *Marine pollution transfer*, (eds., H. L. Windom and R. A. Duce), pp. 39-76. Heath & Co.
- Troup B.N. and Bricker O. P. (1975) Processes affecting the transport of materials from continents to oceans. In *Marine Chemistry in Coastal Environment*, (ed., T. M. Church), Vol. 18, pp. 135-151. Symposium Proceedings, American Chemical Society.
- Truitt R.E. and Weber J.H. (1981) Determination of complexing capacity of fulvic acid for copper(II) and cadmium(II) by dialysis titration. *Anal. Chemistry* **53**, 337-342.
- Turekian K. K. (1971) River tributaries and estuaries. In *Impingment of Man on the Oceans*, (ed. D. W. Hood), pp. 9-73. John Wiley & Sons.
- Turekian K. K. (1977) The fate of metals in the ocean. *Geochim. Cosmochim. Acta* **41**, 1139-1144.

- Turekian K. K. and Wedepohl K. H. (1961) Distribution of the elements in some major units of the earth's crust. *Bull. Geol. Soc. Am.* **72**, 175-192.
- Turner D. R., Whitfield M. and Dickson A. G. (1981) The equilibrium speciation of dissolved components in freshwater and sea water at 25 °C and 1 atm pressure. *Geochim. Cosmochim. Acta* **45**, 855-881.
- Turner R.R., Lindberg, S.E. and Coe J.E. (1985) Comparative analysis of trace metal accumulation in forest ecosystems. In *Heavy Metals in the Environment*. International conference, Athens, Greece.
- Ure A. M. and Berrow M. L. (1982) The chemical constituents of soils. In *Environmental Chemistry. R. Soc. Chem.* (ed., H. J. M. Bowen), pp. 94-202. Burlington House.
- Vuceta J. (1976) *Adsorption of Pb(II) and Cu(II) on  $\alpha$ -quartz from Aqueous Solutions: Influence of pH, Ionic Strength, and Complexing Ligands*. Ph.D. thesis, California Institute of Technology.
- Vuceta J. and Morgan J. J. (1978) Chemical modeling of trace metals in fresh waters: Role of complexation and adsorption. *Environ. Sci. Technol.* **21**, 863-869.
- Weast R. C. (1986) *CRC Handbook of Chemistry and Physics*. CRC Press, Boca Raton.
- Wehrli B. (1987) *Vanadium in the Hydrosphere: Surface Chemistry and Oxidation Kinetics*. Ph.D. thesis, ETA, Zurich, Switzerland.
- Westall J. (1980) Chemical Equilibrium including adsorption on charged surfaces. In *Particulates in Water*, (ed., M. C. Kavanaugh and J. O. Leckie), pp. 33-44. American Chemical Society.
- Westall J. C. (1987) Adsorption Mechanisms in Aquatic Surface Chemistry. In *Aquatic Surface Chemistry*, (ed., W. Stumm). pp. 3-31. John Wiley & Sons, New York.
- Westall J. C. and Hohl H. (1980) A comparison of electrostatic models for the oxide/solution interface. *Adv. Colloid Interface Sci.* **12**, 265-294.
- Whitfield M. (1981) The world ocean. Mechanisms or machination. *Interdis. Sci. Rev.* **6**, 12-35.
- Whitfield M. and Turner D.R. (1987) The role of particles in regulating the composition of sea water. In *Aquatic Surface Chemistry*, (ed., W. Stumm), pp. 457-493. John Wiley & Sons, New York.
- Wong P.T.S. (1987) Toxicity of cadmium to fresh water microorganisms, phytoplankton and invertebrates. In *Cadmium in the aquatic environment* (ed., J.O. Nriagu and J.B. Sprague). pp 117-139. John Wiley & Sons, New York.
- Yates D. E. (1975) *The Structure of the Oxide-Aqueous Electrolyte Interface*. Ph.D thesis, University of Melbourne.

- Yeats P. A. and Bowers J. M. (1982) Discharge of metals from the St. Lawrence River. *Can. J. Earth Sci.* **19**, 982-992.
- Yeats P.A. and Bowers J.M. (1987) Evidence for anthropogenic modification of global transport of cadmium. In *Cadmium in the aquatic environment* (ed., J.O. Nriagu and J.B. Sprague).pp 19-34. John Wiley & Sons, New York.
- Young J. R. (1982) *A Study of Adsorption onto an Anamorphous Silicon Surface by Chemical and NMR Methods*. Ph.D. thesis, California Institute of Technology.
- Zielinski R. A., Peterman Z. E., Stuckless J. S., Rosholt J. N. and Nkomo I. T. (1981) The chemical and isotopic record of rock-water interaction in the Sherman granite, Wyoming and Colorado. *Contrib. Mineral. Petrol.* **78**, 209-219.